

Integrated Ocean Drilling Program Expedition 320T Preliminary Report

USIO Sea Trials and Assessment of Readiness Transit (START): Ontong Java Plateau

25 January–5 March 2009

Expedition 320T Scientists



Published by
Integrated Ocean Drilling Program Management International, Inc.,
for the Integrated Ocean Drilling Program

Publisher's notes

Material in this publication may be copied without restraint for library, abstract service, educational, or personal research purposes; however, this source should be appropriately acknowledged.

Citation:

Expedition 320T Scientists, 2009. USIO Sea Trials and Assessment of Readiness Transit (START): Ontong Java Plateau. *IODP Prel. Rept.*, 320T. doi:10.2204/iodp.pr.320T.2009

Distribution:

Electronic copies of this series may be obtained from the Integrated Ocean Drilling Program (IODP) Scientific Publications homepage on the World Wide Web at www.iodp.org/scientific-publications/.

This publication was prepared by the Integrated Ocean Drilling Program U.S. Implementing Organization (IODP-USIO); Consortium for Ocean Leadership, Lamont Doherty Earth Observatory of Columbia University, and Texas A&M University, as an account of work performed under the international Integrated Ocean Drilling Program, which is managed by IODP Management International (IODP-MI), Inc. Funding for the program is provided by the following agencies:

National Science Foundation (NSF), United States

Ministry of Education, Culture, Sports, Science and Technology (MEXT), Japan

European Consortium for Ocean Research Drilling (ECORD)

Ministry of Science and Technology (MOST), People's Republic of China

Korea Institute of Geoscience and Mineral Resources (KIGAM)

Australian Research Council (ARC) and New Zealand Institute for Geological and Nuclear Sciences (GNS), Australian/New Zealand Consortium

Ministry of Earth Sciences (MoES), India

Disclaimer

Any opinions, findings, and conclusions or recommendations expressed in this publication are those of the author(s) and do not necessarily reflect the views of the participating agencies, IODP Management International, Inc., Consortium for Ocean Leadership, Lamont-Doherty Earth Observatory of Columbia University, Texas A&M University, or Texas A&M Research Foundation.

Expedition 320T participants*

Jay Miller (transit/sea trials)
SODV Project Manager
Integrated Ocean Drilling Program
Texas A&M University
1000 Discovery Drive
College Station TX 77845-9547
USA
miller@iodp.tamu.edu

Readiness Assessment Team

Sean Higgins (transit/sea trials)
Oversight
Consortium for Ocean Leadership
1201 New York Avenue NW, Fourth Floor
Washington DC 20005
USA
shiggins@oceanleadership.org

Gary D. Acton (sea trials)
Paleomagnetist
Department of Geology
University of California, Davis
One Shields Avenue
Davis CA 95616
USA
gdacton@ucdavis.edu

Mark Leckie (sea trials)
Paleontologist
Department of Geosciences
University of Massachusetts
611 North Pleasant Street
Amherst MA 01003-5820
USA
mleckie@geo.umass.edu

Kathleen Marsaglia (sea trials)
Sedimentologist
Department of Geological Science
California State University, Northridge
18111 Nordhoff Street
Northridge CA 91330-8266
USA
kathie.marsaglia@csun.edu

Kitty Milliken (sea trials)
Sedimentologist/Geochemist
Department of Geological Sciences
University of Texas at Austin
1 University Station C 1100
Austin TX 78712
USA
kittym@mail.utexas.edu

Clive Neal (sea trials)
Geochemist/Petrologist
Department of Civil Engineering and
Geological Sciences
University of Notre Dame
156 Fitzpatrick Hall
Notre Dame IN 46556
USA
neal.1@nd.edu

Kristen St. John (sea trials)
Sedimentologist
Department of Geology and Environmental
Science
James Madison University
7125 Memorial Hall
Harrisonburg VA 22807
USA
stjohnke@jmu.edu

Roy Wilkens (sea trials)
**Physical Properties/Stratigraphic
Correlation/Downhole Logging Specialist**
Hawaii Institute of Geophysics and
Planetology
1680 East West Road
Honolulu HI 96822
USA
rwilkens@hawaii.edu

*Transit 25 January–6 February 2009; sea trials 6 February–5 March 2009

IODP-USIO scientific staff

Carlos Alvarez-Zarikian (transit/sea trials)
Expedition Project Manager
Integrated Ocean Drilling Program
Texas A&M University
College Station TX 77845-9547
USA
zarikian@iodp.tamu.edu

Kusali Gamage (transit/sea trials)
Expedition Project Manager
Integrated Ocean Drilling Program
Texas A&M University
College Station TX 77845-9547
USA
gamage@iodp.tamu.edu

Joerg Geldmacher (transit/sea trials)
Expedition Project Manager
Integrated Ocean Drilling Program
Texas A&M University
College Station TX 77845-9547
USA
geldmacher@iodp.tamu.edu

Louise Anderson (sea trials)
Logging Staff Scientist
Borehole Research Group
Department of Geology
University of Leicester
Leicester LE1 7RH
United Kingdom
lma9@le.ac.uk

Annick Fehr (sea trials)
Logging Staff Scientist
University of Aachen
Angewandte Geophysik
Lochnerstrasse 4-20
D-52064 Aachen
Germany
afehr@eonerc.rwth-aachen.de

Gilles Guerin (transit/sea trials)
Logging Staff Scientist
Borehole Research Group
Lamont-Doherty Earth Observatory
of Columbia University
Palisades NY 10964
USA
guerin@ldeo.columbia.edu

Jenny Inwood (sea trials)
Logging Staff Scientist
Borehole Research Group
Department of Geology
University of Leicester
Leicester LE1 7RH
United Kingdom
ji18@le.ac.uk

Eric Meissner (transit/sea trials)
LDEO Project Lead
Borehole Research Group
Lamont-Doherty Earth Observatory
of Columbia University
Palisades NY 10964
USA
meissner@ldeo.columbia.edu

Angela Slagle (sea trials)
Logging Staff Scientist
Borehole Research Group
Lamont-Doherty Earth Observatory
of Columbia University
Palisades NY 10964
USA
aslagle@ldeo.columbia.edu

IODP-USIO technical staff

Michael Storms (transit/sea trials)
Operations Superintendent

Kevin Grigar (transit/sea trials)
Drilling Engineer

Liping Chen (sea trials)
Engineer

Stefan Mrozewski (transit/sea trials)
Engineer

Kerry Swain (transit/sea trials)
Schlumberger Engineer

Brad Julson (transit/sea trials)
Laboratory Officer

Chieh Peng (transit/sea trials)
Assistant Laboratory Officer

Steve Prinz (transit/sea trials)
Assistant Laboratory Officer

Heather Barnes (transit/sea trials)
X-Ray/Microbiology Laboratory

Eric Jackson (transit/sea trials)
X-Ray/Microbiology Laboratory

Ted (Gus) Gustafson (transit/sea trials)
Downhole Tools/Thin Section Laboratory

Peter Blum (transit)
Manager of Tools and Analytical Services

David Houpt (transit/sea trials)
Supervisor of Analytical Systems

Chris Bennight (transit/sea trials)
Chemistry Laboratory

Lisa Brandt (transit/sea trials)
Chemistry Laboratory

Kazuho Fujine (transit/sea trials)
Chemistry Laboratory

Margaret Hastedt (transit/sea trials)
Petrophysics Laboratory

Maxim Vasilyev (transit/sea trials)
Petrophysics Laboratory

Zenon Mateo (transit/sea trials)
Core Description Laboratory

Etienne Claassen (transit/sea trials)
Marine Instrumentation Specialist

Jurie Kotze (transit/sea trials)
Marine Instrumentation Specialist

Paul Foster (transit/sea trials)
Supervisor of Applications Development

David Fackler (transit/sea trials)
Applications Developer

Algie Morgan (transit/sea trials)
Applications Developer

Stephanie Zeliadt (sea trials)
Applications Developer

Hai (James) Zhao (transit/sea trials)
Applications Developer

Rakesh Mithal (transit/sea trials)
Supervisor of Databases and Archives

John Beck (transit)
Imaging Specialist

Tim Fulton (transit/sea trials)
Imaging Specialist

Philip Gates (transit)
Supervisor of Information Technology and Support

Jennifer Hutchinson (transit/sea trials)
Systems Administrator

Matthew Nobles (transit/sea trials)
Marine Computer Specialist

Andrew Trefethen (transit/sea trials)
Marine Computer Specialist

Chad Broyles (transit/sea trials)
Curator

Debbie Partain (transit/sea trials)
Publications Specialist

Karen Graber (transit/sea trials)
Staff Researcher

Tanzhuo Liu (sea trials)
Senior Log Analyst

Kristin Hillis (transit/sea trials)
Property Specialist

Doug Conroy (sea trials)
Vendor

Saravanan Nagarajan (sea trials)
Vendor

Abstract

The Sea Trials and Assessment of Readiness Transit (START), or Integrated Ocean Drilling Program (IODP) Expedition 320T, was planned as a shakedown of the R/V *JOIDES Resolution*. The ship, operated under the auspices of the United States Implementing Organization (USIO) as part of IODP, has just completed an extensive 115+ million dollar refit in Jurong Shipyard, Singapore. The scientific research vessel spent 29 months (September 2006–January 2009) in Singapore, where the ship's hotel and laboratory structure was replaced and the marine and drilling systems were completely refurbished. The overall objectives of Expedition 320T included a shakedown of the ship's drilling, coring, and downhole logging capabilities, in particular the testing of the new wireline heave compensator. Additionally, all the scientific laboratory analytical systems, computer applications, and data uploading/storage capabilities were assessed. Lastly, this expedition served to relocate the ship from Southeast Asia to Hawaii for the start of IODP-USIO Phase 2 science operations in the equatorial Pacific (Expeditions 320 and 321).

Introduction and background

The revitalized and modernized R/V *JOIDES Resolution* left Singapore for sea trials and assessment of readiness on 25 January 2009 after extensive reconstruction over the last 2.5 years. This reconstruction project, known as United States Implementing Organization (USIO) Scientific Ocean Drilling Vessel (SODV), was funded by a grant from the National Science Foundation (NSF) Major Research Equipment and Facilities Construction (MREFC) account. Integrated Ocean Drilling Program (IODP) Expedition 320T marks the final phase of SODV before rejoining IODP-USIO and full international science operations.

The SODV construction project replaced nearly everything inside the hull on the ship from the derrick forward, including all new laboratories, accommodations, and bridge. Other vessel and drilling systems throughout the *JOIDES Resolution* were also overhauled and refurbished, notably the top drive and passive heave systems and the propeller shafts, screws, and thrusters. Downhole logging operations were completely made over as well, including a new wireline heave compensator (WHC) and support systems. In tandem with construction work in Singapore was complete redesign of all the science laboratories with many new and redesigned analytical systems, as well as extensive new software, databases, and information technology (IT) infrastructure.

In order to gauge the overall readiness of the research vessel prior to the beginning of Expedition 320 in March 2009 in Honolulu, Hawaii, the USIO planned a ~6 week transit expedition. During this transit expedition, Expedition 320T, the ship covered almost 6000 nmi in its voyage from Singapore to Honolulu (Fig. F1). The transit included a stopover in Guam to pick up additional technical staff and a group of seven scientists that served as an external Readiness Assessment Team (RAT). A U.S. Coast Guard (USCG) inspection was also carried out in Guam. Sea trials were conducted at Ontong Java Plateau during transit to Honolulu.

Objectives

Expedition 320T was planned to achieve several important goals including testing the operational readiness, the drilling and coring systems, and the performance of the new WHC and logging tools at sea. Given that the ship and vital systems were operational, an additional goal of the transit expedition was to assess the overall readiness of the science systems, accommodations, and IT system for carrying out full IODP expeditions.

To accomplish all these goals during the transit, Ocean Drilling Program (ODP) Site 807, on the Ontong Java Plateau at ~2800 m water depth, was chosen as a location to revisit and test drilling, coring, and logging systems. A key element in choosing Site 807 was the existence of a reentry cone in Hole 807C, a 1500 m hole into basement that would potentially be a safe and appropriate location for testing not only the WHC and tool responses but also the ship's dynamic positioning (DP) system, Global Positioning System (GPS), vibration isolated television (VIT) camera frame, beacons, and thrusters. Although not the key objective of testing drilling systems, the collection of new cores and testing of some new downhole tools while drilling at a new site (U1330) would provide the assessment team an opportunity to evaluate almost all the science and IT systems. This fresh core material also allowed for new rig floor crew and technical staff to organize collecting, curating, and evaluating core flow through the new laboratories.

Operations

Singapore Loyang port call

Once the shipyard and harbor trials testing of the ship's systems were completed, the ship docked at the Loyang Offshore Supply Base in Singapore for final loading and mobilization activities. Besides completing all last-minute loading aboard of supplies and equipment, the ship was bunkered, taking on 2700 metric tons of marine gas oil. Bulk products were also loaded, including 74 metric tons of cement and 103 metric tons of barite. The ship passed her final American Bureau of Shipping (ABS) audit and received her Liberian certification; both were required before the ship was cleared to leave port. The ship departed Singapore on schedule with the last line away Loyang Offshore Supply Base at 0811 h on 25 January 2009 (Fig. F1).

Transit to Guam

With so many remnant ship issues to deal with, plus the routine challenges associated with the first extended sea transit after a lengthy shipyard period, Overseas Drilling Limited (ODL) resources (engineers, rig mechanics, electronics technicians [ETs], and electricians) were focused according to priority. In general, the priority was

1. Ship's propulsion, power plant, safety, and ABS requirements;
2. Drilling package readiness (primarily top drive, core winch, subsea television capability, and so on);

3. Automatic station keeping (ASK) system/positioning beacons, and so on; and
4. Laboratory stack elevator operation.

Work on air conditioning units and toilets were continually recurring (daily) tasks. Of major importance was the resolution of all International Safety Management (ISM) audit and safety issues identified throughout ship. It was an ABS requirement that these be rectified before arriving in Guam.

The ship continued to transit at full speed to Guam to pick up the assessment team scientists. The ship's speed was impacted by a strong head current of ~1.0 kt, variable headwinds that on some days attained 25 kt sustained with gusts up to 40 kt, and problems early on with the propulsion electrical system. Initial problems were related to inadequate ventilation causing overheating and subsequent failures in the aft thy-rig room transformers. Those were overcome once the new heating, ventilation, and air conditioning (HVAC) system was better understood/adjusted and vents to the outside were opened. In addition, the new breakers installed continually tripped when turns on the main screws were increased from 120 rpm to the desired 130 rpm. This caused propulsion motors to kick off-line. The old breakers did not trip as early as the new ones, requiring troubleshooting by the ship's engineers. During the last 2 days of the transit, the problems appeared to be resolved because of the diligent efforts of on-board engineers, ETs, and electricians. Another primary issue was the elevator system, which was inoperable for an entire week. Elevator and HVAC technicians were requested for the Guam port call. Toilet functionality continued to be an issue until personnel learned the idiosyncrasies of the new vacuum system. Drilling package readiness efforts also continued throughout the transit, as well as preparations for laboratory acceptance and the RAT review. The 2638 nmi transit to Guam required 12.3 days at an average speed of 8.9 kt. The first line was ashore pier F-3 in Apra, Guam, at 1830 h on 6 February 2009, ending the transit (Fig. F1).

Guam port call

The *JOIDES Resolution* spent 2.8 days in Guam, which was nearly 2 days longer than originally planned. During that time seven RAT scientists joined the ship, as well as six additional Lamont-Doherty Earth Observatory (LDEO) loggers (including a wire-line compensator vendor representative from Deep Down, Inc.) and three Texas A&M University (TAMU) personnel (including an Asset Management System [AMS; India] vendor representative). TAMU also had three personnel depart the ship. Port call activities included service work on the elevator by a vendor representative and service

work on freezers by a local refrigeration company. HVAC work also continued with a vendor representative. Additional vendor work on the elevator and HVAC was scheduled for the port call in Honolulu. A USGC annual inspection was conducted. The ship passed with no deficiencies cited and complimentary comments from the USCG about the ship's condition. The last line away pier F-3 was at 1354 h on 9 February 2009, and the *JOIDES Resolution* headed for Site 807 located on the Ontong Java Plateau.

Transit to Sites 807 and U1330

The 943 nmi transit to Site 807 (Fig. F1) was completed in 4 days at an average speed of 9.8 kt. Speed was impacted by the strong but highly variable Northern Equatorial Current and erratic headwinds. The RAT scientists spent their initial few days attending briefings on the status of systems aboard the *JOIDES Resolution*. During the transit the USIO development, technical, and science teams worked on assessment and acceptance testing activities. Transocean personnel continued to troubleshoot and correct remnant shipyard deficiencies, as well as prepared the drilling package and subsea television/sonar systems for operations. The ship arrived on location at Hole 807C (published coordinates: 3°36.42'N, 156°37.49'E) at 1440 h on 13 February 2009.

Operations at Sites 807 and U1330

Thrusters and hydrophones were lowered, and after maneuvering the ship to the exact coordinates of Site 807 (Fig. F2), the ship was switched over to DP control. A new Falmouth Scientific positioning beacon was deployed at 1950 h on 13 February 2009; however, during initial use of the ASK system the electrical supervisors and DP operators discovered that the ship's response did not appear to match the commands given. It was ultimately determined that two thrusters (Numbers 8 and 9) were turning in the wrong direction. This was soon corrected by adjusting the wiring, and the drill crew went to work detorquing the coaxial subsea television cable, picking up drill collars, and spacing out core barrels.

Hole 807C

Final location coordinates: 3°36.3529'N, 156°37.4469'E

Established water depth: 2816.0 meters below rig floor (mbrf)

Total penetration depth: not applicable

Coring system: not applicable (reentry only)

During the pipe trip to the seafloor, the VIT camera was deployed, and after tagging bottom to verify the water depth for determining reentry space out, the ship was maneuvered over the Hole 807C reentry cone. Reentry required a mere 13 min from the time maneuvering was initiated until the bit was in the cone. Unfortunately, the euphoria of the outstanding ASK and subsea television/sonar system performance was short-lived when the bit would not advance further into the casing string. After unsuccessful deliberate attempts to entice the bit further into the casing, it became obvious to the operations and drill crews that the 11-7/16 inch advanced piston corer (APC)/extended core barrel (XCB) bit was too big to fit inside the 11-3/4 inch casing string with an inside diameter of 10.99 inches. This important nuance was completely overlooked by all involved. The drill string was recovered and the bottom-hole assembly (BHA) was visually inspected. To everyone's relief, no damage was identified other than to the used APC/XCB bit. The unforeseen pipe round trip and the inability to marry APC coring with the logging tests in Hole 807C on a single pipe trip necessitated changing the operational approach for the remainder of on-site operations.

Hole U1330A

Final location coordinates: 3°36.3349'N, 156°37.4478'E

Established water depth: 2816.0 mbrf (2805 meters below seal level [mbsl])

Total penetration depth: 553.8 meters below seafloor (mbsf)

Coring system: rotary core barrel (RCB)/RCB center bit

The BHA was changed to a RCB variety and tripped to the seafloor in preparation for drilling a dedicated wireline logging hole. Hole U1330A was spudded at 1355 h on 15 February 2009. This hole was offset 30 m due south of Hole 807C and was drilled to 103.6 mbsf with an RCB wash barrel (1W) in place. A wash barrel has the check valve at the top removed to allow circulation down the inner diameter of the barrel to flush away any material that might get in. It is occasionally used in lieu of a center bit and by definition is designed not to intentionally recover core. Despite this configuration, the core catcher retrieved 7 cm of sediment. This sample was curated as 320T-U1330A-1W-CC. Two RCB cores (2R and 3R) were then cut from a 103.6 to 122.8 mbsf, recovering 84.2% of the formation penetrated. These cores were processed through the laboratories, allowing continued readiness assessment and evaluation of core flow through the laboratories by the RAT (Tables [T1](#), [T2](#)).

An RCB center bit was used to deepen the hole to 553.8 mbsf for WHC and logging tools evaluation. A wiper trip was made to condition the hole for logging, the bit was released, the hole displaced with 190 bbl of heavy 10.5 pound per gallon (ppg) mud,

and the end of the pipe was placed at 96.7 mbsf. Logging system testing required 48.25 h, with initial testing taking place inside the drill pipe followed by open-hole testing. A total of three logging runs were made using three separate tool strings. The first tool string, consisting of the Hostile Environment Gamma Ray Sonde (HNGS), Hostile Environment Litho-Density Sonde (HLDS), General Purpose Inclinometer Tool (GPIT), and Phasor Dual Induction and Spherically Focused Resistivity Tool (DIT-E), reached to within 1 m of bottom. The second tool string, with the Formation MicroScanner (FMS), reached 524 mbsf or ~30 m off bottom. The third tool string, consisting of the HNGS, HLDS, DIT-E, GPIT, and Magnetic Susceptibility Sonde (MSS), reached 469 mbsf (~85 m off bottom). Preliminary results indicated that although the new Schlumberger WHC was performing at an acceptable level, LDEO and Schlumberger personnel felt that the system ultimately would be capable of exceeding performance levels achieved with the LDEO WHC used previously during IODP Phase 1. Logging activities encompassed general maintenance of the WHC, performance documentation, and analysis of the suite of logging data collected in Hole U1330A.

Logging operations

Hole U1330A was completed to 3369.8 meters drilling depth below rig floor (DRF) (553.8 meters drilling depth below seafloor [DSF]) at 1330 h on 16 February 2009. Conditioning of the hole included several mud sweeps and a complete wiper trip. After the RCB bit was released at the bottom, the hole was swept with 190 bbl of heavy mud (barite) and the pipe was lifted to the logging depth of 96.7 DSF at 0230 on 17 February. This allowed the ~20 m interval (103.6–122.7 m DSF) that was cored in Hole U1330A to be included in the logging program.

A critical component of logging operations during this expedition was testing of the WHC, both in the drill pipe in the water column and below the seafloor, as well as in open hole. Acceleration data were collected on the ship (using the MRU) and down-hole (using the GPIT). The heave compensation system was tested at static stations (300, 600, 1200, 2800, and 3000 meters wireline log depth below rig floor [WRF]) and during dynamic logging runs of all three tool strings.

The first logging tool string composed of the HNGS, HLDS, GPIT, and DIT-E was built and lowered into the hole at 0415 h on 17 February. The first pass started at 3369 m WRF (542 meters wireline log depth below seafloor [WSF]) and continued to 3275 m WRF (448 m WSF). During this pass, the winch experienced some difficulty in pulling, leading to some concern about the caliper. The second pass logged the entire hole from 3369 m WRF (542 m WSF) to the mudline (2815 m WRF, 0 m WSF). Because of

concern for the caliper, this pass was logged at 1800 ft/h, with the caliper closed for the deepest ~50 m of the section. At the completion of this run, the tool string was brought back on deck and it was confirmed that the caliper was undamaged.

The FMS tool string (HNCS/GPIT/FMS) was then rigged up and lowered into the hole. The FMS tool experienced some bridging at ~3343 m WRF (~25 m of hole fill from the base) and did not descend all the way to total depth. The first pass was run from 3342 mbrf (515 m WSF) to 2938 m WRF (111 m WSF). The second pass started at 3331 m WRF (504 m WSF) and ended at 2938 m WRF (111 m WSF) when the tool arms were closed. Both runs were made with a logging speed of 1800 ft/h.

The final logging run utilized the new MSS accompanied by the HNCS/HLDS/GPIT/MSS tool string. The tool string was rigged up and lowered into the hole, and three passes were made, logging at 1800 ft/h except over three intervals (3280–3250, 3220–3190, and 3150–3120 m WRF), which were logged at 900 ft/h. The first pass was logged from 3284 to 3080 m WRF with the HLDS caliper open. The second pass, from 3286 to 3097 m WRF, was logged with the caliper closed in order to test the influence of the caliper in assisting the MSS bowsprings as they push the tool against the borehole wall. A bridge was met at ~3280 m WRF on the way down for the final pass, indicating deteriorating hole conditions. The third and final pass, from 3280 to 2888 m WRF, was logged with the caliper open all the way into the pipe.

Hole U1330B

Final location coordinates: 3°36.3213'N, 156°37.4467'E

Established water depth: 2814.8 mbrf (2802.2 mbsl)

Total penetration depth: 92.2 mbsf

With time running out, the drill string was tripped back to bottom with an APC/XCB BHA and Hole U1330B was spudded at 1945 h on 19 February 2009. This hole was continuously APC cored to 92.2 mbsf. Ten APC cores were recovered with an overall average recovery of 94.6% (Table T2). The relatively low recovery for APC coring resulted from Core 320T-U1330B-4H losing 76% of its material when the flapper core catcher stuck in the open position. The other nine cores achieved more respectable recovery rates of 101.1% to 105.4%. The new FlexIt core orientation tool (replacement for the Tensor tool) was successfully deployed on all 10 APC cores. The APC temperature tool (APCT-3) was successfully deployed on Cores 320T-U1330B-5H, 7H, and 9H at depths of 44.7, 63.7, and 82.7 mbsf, respectively. The drill string acceleration (DSA) tool was deployed for Cores 320T-U1330B-5H through 8H (35.2–73.2

mbsf), recovering just under 6 h of motion data. These data coupled with LDEO Motion Reference Unit (MRU) data from the WHC should allow later evaluation of passive heave compensator (PHC) performance. All rig floor drilling equipment and all downhole tools/coring systems performed well and are considered operational for science operations. The upgraded Falmouth Scientific positioning beacon also performed well, including the wide-angle transducer (shallow water) version mounted on the subsea television frame. The beacon was successfully recovered at the conclusion of drilling operations. The drill string was recovered, the drilling assembly laid out, and the rig floor secured for transit. Per schedule, the vessel departed Site U1330 bound for Honolulu at 1645 h on 20 February 2009.

Transit to Honolulu

The transit to Honolulu was marked by periods of excellent speed (≥ 11.5 kt) intermixed with periods where slower speeds (~ 6 kt) prevailed. Variations in speed were due to a highly variable Northern Equatorial Pacific Current and associated counter-currents, as well as variable winds taken on or just off the bow. In general the transit was marked by extended periods of overcast skies, cloudy/overcast days, and either rain or intermittent drizzles. Effort continued in commissioning laboratory equipment and software applications, as well as support of the RAT scientists as they continued with their SODV and vessel readiness assessment tasks and reports. The 2901 nmi transit to Honolulu, Hawaii, required 13 days at an average speed of 8.9 kt. The first line was ashore Pier 29, Honolulu, at 1042 h on 5 March 2009, ending the transit and officially ending Expedition 320T.

Methods

We have included a brief methodology section in the *Preliminary Report* because a *Proceedings* volume will not be produced for Expedition 320T.

Lithostratigraphy

This section outlines the procedures used to document the lithology of the sediment material recovered during Expedition 320T, including visual core description, smear slide description, digital color imaging, and color spectrophotometry. It is modeled after the Methods chapter for IODP Expedition 306 Sites U1312 and U1313 (Expedi-

tion 306 Scientists, 2006) with only general procedures outlined, highlighting new systems and equipment used and evaluated during the transit.

Overview of new core description process and integration of databases

A new core description process was implemented and assessed during Expedition 320T using the DESClogik application. The use of visual core description forms (VCDs) for hand-written descriptions has been supplanted by direct entry of descriptive and interpretive information into the DESClogik program through the Tabular Data Capture (TDC) mode. Prior to core description, a spreadsheet template was constructed in TDC (Fig. F3). Tabs and columns established within this program were customized to include many of the former VCD form information categories (e.g., lithology, drilling disturbance, and bioturbation), as well as other information that allows for complete documentation of the observations made during core description in the new database format. A second template was developed specifically for recording smear slide data (Fig. F4), which contains category columns similar to the former smear slide forms to record texture and relative abundance of biogenic and minerals components.

Visual core description

Lithology

Sediments recovered during Expedition 320T are composed of >60% pelagic components and described as pelagic sediments using the classification scheme of Mazzullo et al. (1988). These sediments comprise the skeletal debris of open-marine calcareous and siliceous microfauna (e.g., foraminifers and radiolarians, respectively) and microflora (e.g., calcareous nannofossils and diatoms, respectively) and associated organisms. The lithologic names assigned to these sediments consist of a principal name based on composition, degree of lithification, and/or texture as determined from visual description of the cores and from smear slide observations. For sediment that is a mixture of components, the principal name is preceded by major modifiers (in order of increasing abundance) that refer to components making up $\geq 25\%$ of the sediment. Minor components that represent between 10% and 25% of the sediment follow the principal name (after a “with”) in order of increasing abundance. In the Expedition 320T classification of biogenic carbonate oozes, only one category was used: nannofossil ooze (content of nannofossils = >50%). The term ooze (rather than chalk) was applied because all the sediment lithification was soft (i.e., could be easily deformed by touch).

Sediment color was determined qualitatively for core intervals using Munsell Color Charts (Munsell Color Company, Inc., 1991, 1994). Toothpick samples were taken at selected intervals in the core and used to create smear slides according to the method outlined in Mazzullo et al. (1988). Note that owing to the absence of a reticulated eyepiece on the microscope in the core description area during core description, no determinations of texture were made (4 μm silt/clay boundary was difficult to estimate). The petrographic determinations of the proportion of sediment components as tabulated in DESClogik were used along with visual descriptions to determine sediment lithology. The DESClogik database included percentages of biogenic and mineral components, as well as whether the sample represents a major or a minor lithology in the core.

Sedimentary structures and diagenetic and other features

The locations and types of bedding features, bedding styles, and other sedimentary structures, as well as diagenetic features, visible on the prepared surfaces of the split cores were recorded by core interval in the DESClogik spreadsheet. Those observed in the Expedition 320T cores are listed in Figure F5, along with the symbol used to depict them in the summary (barrel) sheets created using the Strater application (see “**Summary (barrel) sheets**”).

The bioturbation classification scheme employed during Expedition 320T defined three levels (moderate, slight, and absent) of bioturbation intensity modified from Mazzullo et al. (1988). Note, however, that in a homogeneous uniformly colored sediment section it may not be possible to differentiate “absent” from “homogenized” by bioturbation.

Intervals of core ~10 cm or more exhibiting drilling-related sediment disturbance were recorded in the DESClogik spreadsheet with the type and degree of disturbance described using the following categories (modified from Mazzullo et al., 1988): biscuited, slight, moderate, mousseliike, very disturbed, soupy, and fractured.

Summary (barrel) sheets

DESClogik includes a graphic display (GD) mode for core data (e.g., digital images of section halves and measurement data) that can be used to augment core description. The end product of DESClogik, a data spreadsheet, must be manipulated using the LIMS2Excel application before importing the data into another program, Strater, to produce a publication-quality, simplified, annotated standard graphic report of the core, similar to the “barrel sheets” created by AppleCORE on prior expeditions/legs.

During Expedition 320T, Strater reports were created at the core level and included descriptive, graphical interpretation, core image, and biostratigraphic zone data. Lithologies and sedimentary structures of the core intervals recovered are represented on barrel sheets by graphic patterns in the Graphic Lithology column using the symbols illustrated in Figure F5.

Digital color imaging

The Section-Half Imaging Logger (SHIL) captures continuous high-resolution images of section-half surfaces for analysis, description, and reporting of recovered core material. The system uses a commercial line scan camera, a specially assembled light emitting diode (LED)-based illumination subsystem for maximum image quality, and an optical bar code scanner to identify the section halves from the physical label on the core liner. Capturing images is made very simple for the user. With minimum user interaction, the image logger control software saves the original high-resolution image with gray scale and ruler as well as a cropped and reduced image for easy handling and display in many applications.

Spectrophotometry (color reflectance)

The Section-Half Multisensor Logger (SHMSL) integrates multiple sensors for the measurement of bulk physical properties in a motorized and computer-controlled core section logging machine. The sensors included in the SHMSL are reflectance spectroscopy and colorimetry (RSC) and magnetic susceptibility. We attempted to use this equipment, but technical issues prevented us from collecting meaningful data. We were, however, able to assess its use in the context of core flow.

Sampling plan

The sampling plan for cores from Hole U1330A was to take two interstitial water samples and two moisture and density (MAD) samples per core. Samples for whole-rock analysis were taken on an as-needed basis (i.e., to determine chemical variations within and between cores). Headspace gas analysis was conducted on each core. The sampling plan for Hole U1330B was similar, except we took one interstitial water and MAD sample per core.

X-ray diffraction analysis

No X-ray diffraction analyses were conducted during the expedition owing to equipment nonfunction.

Biostratigraphy

A standard, simplified process for micropaleontological analyses was carried out during Expedition 320T. Core catcher (CC) samples were soaked in water and briefly placed on a hot plate with a small volume of hydrogen peroxide added to disaggregate the nannofossil ooze. Samples were then washed over a 63 μm sieve and dried in a warm oven. Washed residues from all core catchers were examined by stereo binocular microscopy. The relative abundances of most taxa present in the assemblages of planktonic foraminifers were estimated and tabulated using the DESClogik application. Relative abundance values are as follows:

- A = abundant (>25%).
- C = common (11%–25%).
- F = few (6%–10%).
- R = rare (1%–5%).
- VR = very rare (<1%).

The planktonic foraminifer biostratigraphy and zonal scheme are based on Berggren et al. (1995) and the astrochronologically tuned datums of Chaisson and Pearson (1997). FO = first occurrence datum, and LO = last occurrence datum.

Geochemistry

During Expedition 320T, the following geochemical analyses were performed on cores taken from Holes U1330A and U1330B:

- Alkalinity on interstitial waters,
- Elemental concentrations of interstitial water samples,
- Headspace gas composition, and
- Elemental whole-rock compositions.

Methods for each of these analyses are given below. The analytical methods followed the procedures outlined in the user guides for the various pieces of analytical equipment. Carbonate content was not determined because of a lack of silver nitrate reagent on board.

Interstitial water analysis

Interstitial water samples were obtained by sampling whole-round pieces (~10 cm long) of the core and taking them immediately to the Chemistry Laboratory for processing. Processing involved scraping away the outer few centimeters of the core using a plastic spatula (to remove any smeared sediment and contamination). From both APC and RCB cores, sediment was removed until the core consistency appeared to be firm, or at least significantly firmer than the outside. After removing the potentially contaminated material, the remaining sediment was placed into a sediment squeezer with a titanium case/pressure plate/mesh with a stainless piston and base, modified after the stainless steel squeezer of Manheim and Sayles (1974). In most cases, gauge pressures up to 20 MPa were applied using a laboratory hydraulic press to extract interstitial water. The interstitial water was filtered through a prewashed Whatman Number 1 filter fitted above a titanium screen, filtered through a 0.45 μm Whatman polyethersulfone disposable filter, and subsequently extruded into a pre-cleaned (10% HCl) 100 mL plastic syringe attached to the bottom of the squeezer assembly.

Interstitial water samples were analyzed for alkalinity, pH, and elemental composition. Alkalinity and pH were measured by Gran titration with a Brinkman pH electrode and a Metrohm 702 SM autotitrator using 0.1 N HCl. The alkalinity analysis is a measure of how much acid it takes to lower the pH of the water sample enough to convert all bicarbonate (HCO_3^-) and carbonate (CO_3^{2-}) to carbonic acid (H_2CO_3), given that almost all alkalinity (~97%) in seawater is due to carbonate. The electrode was calibrated at pH 4, 7, and 10 prior to the expedition.

For inductively coupled plasma–atomic emission spectroscopy (ICP-AES) analyses, interstitial water samples were immediately acidified using clean (trace metal grade) concentrated nitric acid (10 μL of acid per 1 mL of sample) to prevent Fe precipitation. Samples were diluted to 1:10 (1 mL sample + 9 mL nanopure water) immediately prior to being analyzed and placed in scintillation vials reserved for ICP pore water analysis. Samples were run on a Leeman Teledyne Labs Prodigy high-efficiency ICP-AES that allowed simultaneous detection of different wavelengths and detection in both axial and radial positions. Samples were run in two batches: major elements (Na, K, Mg, and Ca), where the samples underwent a 100-fold dilution, and minor elements (Li, B, Sr, Mn, and Fe), where the samples underwent a 25-fold dilution. All analyses were conducted in 5% HNO_3 acid. Major elements were standardized using International Association for the Physical Sciences of the Ocean (IAPSO) seawater (at

dilutions of 0, 1, 3, 5, 50, 100, and 120). Minor elements in interstitial water samples were only run in test mode and are not reported here.

Whole rock analyses

ICP-AES analysis of whole rock samples quantified the major (Al, Ca, Fe, K, Mg, Mn, Na, P, Si, and Ti) and trace (Ba, Cr, Ni, Sc, Sr, V, Y, and Zr) elements. Samples were prepared by flux-fusion using a lithium metaborate flux (from rock to bead) and then dissolution of the bead (from bead to solution). An aliquot of 100 mg of the ignited sample powder was weighed and added to a vial containing lithium metaborate flux that was preweighed on shore to 400 mg. The combination of sample powder and flux was then fused to make a glass bead that was dissolved in nitric acid (via a bench-top hand shaker). The resulting fluid was analyzed by ICP. Weighing the ignited sample is a fairly critical step. The weight should be as close to 100 mg as possible. Inaccuracies in the weight will affect the analytical results. The sample bead was dissolved in 50 g (50 mL) of nitric acid to yield a dilution factor of 100 for the sample plus flux and a dilution factor of 500 for the sample. This solution was further diluted in a 2.5 mL sample (17.5 mL 10% HNO₃).

Headspace gas

Concentrations of methane through propane hydrocarbon gases were monitored at intervals of one sample per core. The standard gas analysis program for safety and pollution prevention purposes was conducted (Kvenvolden and McDonald, 1986). Samples for headspace analysis were collected with interstitial water samples to integrate the interstitial water and gas data sets. For the required safety analysis, a 3 cm³ bulk sediment sample from a freshly exposed end of a core section was collected upon core removal using a brass boring tool or plastic syringe and then extruded into a 20 mL headspace vial and immediately capped with a silicone/polytetrafluoroethylene (PTFE) septum, which was sealed with an aluminum crimp cap. The vial was then heated to 80°C for ~30 min prior to analysis.

Gas chromatography (GC) analyses of headspace samples was performed in the following way. A 5 mL volume of headspace gas was extracted from the sealed sample vial using a standard gas syringe and directly injected into the GC. The headspace gas samples were analyzed using the GC3 chromatograph, an Agilent 6890 GC equipped with an 8 ft × 1/8 inch stainless steel column packed with HayeSep R (80–100 mesh) and a flame ionization detector (FID). Some samples were analyzed for higher molecular weight hydrocarbons by injection into the natural gas analyzer, a modified Hewl-

ett Packard 5890 II Plus GC with an FID and a thermal conductivity detector. Concentrations of methane, ethane, ethene, propane, and propene were obtained. The carrier gas was helium, and the GC oven was programmed from 100°C (5.5 min hold) to 140°C (4 min hold) at a rate of 50°C/min. Data were processed using Agilent Chemstation software.

The concentration of dissolved methane, both in the safety and refined protocols, was derived from the headspace concentration by the following equation:

$$\text{CH}_4 = [(\chi_M - \chi_{\text{bkg}})^\circ - P_{\text{atm}}^\circ - V_H] / (R^\circ - T^\circ - \phi^\circ - V_S) \quad (1)$$

where

V_H = volume of the sample vial headspace,

V_S = volume of the whole sediment sample,

χ_M = molar fraction of methane in the headspace gas (obtained from GC analysis),

χ_{bkg} = molar fraction of methane in headspace gas because of background,

P_{atm} = pressure in the vial headspace (assumed to be the measured atmospheric pressure when the vials were sealed),

R = the universal gas constant,

T = temperature of the vial headspace in degrees Kelvin, and

ϕ = sediment porosity (determined either from MAD measurements on adjacent samples or from porosity estimates derived from gamma ray attenuation [GRA] data representative of the sampled interval).

Physical properties

Physical properties were measured on core material recovered during Expedition 320T to test the new installation of the shipboard measurement systems and the ability of the users to upload and retrieve data from the Laboratory Information Management System (LIMS).

Magnetic susceptibility, GRA bulk density, compressional wave velocity (V_p), and natural gamma ray activity were measured on the whole-core samples. Thermal conductivity was not measured because of problems with the new system (see “**Thermal conductivity**”). Split-core measurements on the working half of the core included V_p with the IODP P -wave sensor system (PWS-3; three measurement directions in soft sediment), sediment strength with the automated vane shear (AVS) system, and MAD.

A comprehensive description of the methodologies and calculations used in the *JOIDES Resolution* physical properties laboratory can be found in Blum (1997). Manuals and quick start guides are available upon request from the USIO.

Multisensor track sampling strategy

Magnetic susceptibility, compressional wave velocity, and GRA bulk density were measured nondestructively with the Whole-Round Multisensor Logger (WRMSL) on all whole-round core sections. To optimize WRMSL performance, sampling intervals and measurement residence times were the same for all sensors for any one core. Sampling intervals were therefore set at 5 cm so that a 9.5 m long core would take ~1 h to pass through the WRMSL with a residence time of 3 s for each measurement. These sampling intervals are common denominators of the distances between the sensors installed on the WRMSL (30–50 cm) and allow truly simultaneous measurements and optimal use of total measurement times.

Magnetic susceptibility

Magnetic susceptibility is a measure of the degree to which a material can be magnetized by an external magnetic field. It provides information on the magnetic composition of the sediments that often can be related to mineralogical composition (e.g., terrigenous versus biogenic materials) and/or diagenetic overprinting. Magnetite and a few other iron oxides with ferromagnetic characteristics have a specific magnetic susceptibility several orders of magnitude higher than clay, which has paramagnetic properties. Carbonate, silica, water, and plastics (core liner) have small negative values of magnetic susceptibility. Sediments rich in biogenic carbonate and opal therefore have generally low magnetic susceptibility, even negative values, if practically no clay or magnetite is present. In such cases, measured values approach the detection limit of magnetic susceptibility meters.

Magnetic susceptibility was measured with the Bartington Instruments MS2C system on the WRMSL. The output of the magnetic susceptibility sensors can be set to centimeter-gram-second (cgs) units or SI units. The IODP standard is the SI setting. However, to actually obtain the dimensionless SI volume-specific magnetic susceptibility values, the instrument units stored in the IODP database must be multiplied by a correction factor to compensate for instrument scaling and the geometric ratio between core and loop dimensions, as described above.

Gamma ray attenuation bulk density

Bulk density reflects the combined effect of variations in porosity, grain density (dominant mineralogy), and coring disturbance. Porosity is mainly controlled by lithology and texture, compaction, and cementation (controlled by both mechanical and chemical processes).

The GRA densitometer uses a 10 mCi ^{137}Cs capsule as the gamma ray source (with the principal energy peak at 0.662 MeV) and a scintillation detector. The narrow collimated peak is attenuated as it passes through the center of the core. Incident photons are scattered by the electrons of the sediment material by Compton scattering.

The attenuation of the incident intensity (I_0) is directly related to the electron density in the sediment core of diameter (D), which can be related to bulk density given the average attenuation coefficient (in micrometers) of the sediment (Evans, 1965; Harms and Choquette, 1965). Because the attenuation coefficient is similar for most common minerals and aluminum, bulk density is obtained through direct calibration of the densitometer using aluminum rods of different diameters mounted in a core liner that is filled with distilled water. The GRA densitometer has a spatial resolution of <1 cm.

Natural gamma radiation

The Natural Gamma Radiation Multisensor Logger (NGRL) was designed and built at the Texas A&M University IODP facility from 2006 to 2008. The NGRL measures gamma rays emitted from whole-round core sections, which arise primarily because of the decay of uranium, thorium, and potassium isotopes. Data generated from this instrument are used to augment geologic interpretations.

The main NGRL detector unit consists of 8 sodium iodide (NaI) scintillator detectors, 7 plastic scintillator detectors, 22 photomultipliers, and passive lead shielding. The NaI detectors are covered by at least 8 cm of lead shielding. In addition, lead separators (~7 cm of low-background lead) are positioned between the NaI detectors. Half of the lead shielding closest to the NaI detectors is composed of low-background lead, and the outer half is composed of regular (virgin) lead. In addition to this passive lead shielding, the NGRL employs a plastic scintillator to suppress the high-energy gamma and muon components of cosmic radiation by producing a veto signal when charged particles from cosmic radiation pass through the plastic scintillator.

A core section measurement run consists of two positions on each core section counted for at least 5 min each for a total of 16 measurements per section. Complete spectra for each measurement are uploaded to the LIMS.

Thermal conductivity

Thermal conductivity was not measured at Site U1330. We tried to use the Teka TK04 measurement system, which employs the transient linear heat source method with a needle probe that is inserted into the soft sediment. The TK04 uses an automated routine to find the conductivity by least-squares fitting to the measured temperature time series. No calibration is required for this system because each probe is calibrated prior to leaving the factory. The heating curves displayed on the computer screen while being collected appeared reasonable, but the software failed to calculate a value of thermal conductivity. We suspect that the parameters set to accept a measurement are perhaps set too narrowly. Measurements on a standard were satisfactory, so the system seems to be functioning.

P-wave velocity

P-wave velocity in marine sediments varies with lithology, porosity, and bulk density, state of stress (such as lithostatic pressure), fabric or degree of fracturing, degree of consolidation and lithification, occurrence and abundance of free gas and gas hydrate, and other properties. *P*-wave velocity was measured with two systems during Expedition 320T: the WRMSL-mounted *P*-wave logger (PWL) on whole-round cores and the PWS3 on every section of the split cores. All IODP *P*-wave piezoelectric transducers transmit a 500 kHz compressional wave pulse through the core at a repetition rate of 1 kHz.

Traveltime is determined by the software, which automatically picks the arrival of the first wavelet to a precision of 50 ns. It is a challenge for an automated routine to pick the first arrival of a potentially weak signal with significant background noise. The search method skips the first positive amplitude and finds the second positive amplitude using a detection threshold limit, typically set to 30% of the maximum amplitude of the signal. Then it finds the preceding zero crossing and subtracts one period to determine the first arrival. To avoid extremely weak signals, minimum signal strength can be set (typically to 0.02 V) and weaker signals ignored. To avoid cross-talk signals at the beginning of the record from the receiver, a delay (typically set to 0.01 ms) can be set to force the amplitude search to begin in the quiet interval preceding the first arrival. In addition, a trigger (typically 4 V) is selected to initiate the

arrival search process, and the number of waveforms to be stacked (typically 5) can also be set. Linear voltage differential transducers determine length of the travel path.

The *P*-wave velocity systems require two types of calibration, one for the displacement of the transducers and one for the time offset. For the displacement calibration, five acrylic standards of different thickness are measured and the linear voltage-distance relationship determined using least-squares analyses. For the time offset calibration, room temperature water in a plastic bag is measured multiple times with different transducer displacements. The inverse of the regression slope is equal to the velocity of sound in water, and the intercept represents the delay in the transducers.

Moisture content and density

Samples of 10 cm³ were taken from the working-half sections with a piston minicorer and transferred into previously calibrated 10 mL glass vials. Usually one sample from the middle of Section 3 or 4 was taken. Wet and dry weights were determined with twin Mettler Toledo electronic balances, which compensate for the effect of the ship's motion on the balance and give a precision better than 1%. Samples were dried in a convection oven at a temperature of 105° ± 5°C for a period of 24 h.

Dry volume was measured in a helium-displacement penta-pycnometer with an uncertainty of 0.02 cm³. This equipment allowed the simultaneous analysis of four different samples and a calibration sphere and took ~15–20 min. Three measurements were averaged per sample. The calibration sphere was cycled from cell to cell of the pycnometer during each batch so that all cells could be checked for accuracy at least once every five runs.

Automated vane shear test

The Giesa Automated Vane System (AVS) consists of a controller and a gantry for shear vane insertion. A four-bladed vane is inserted into the split core and rotated at a constant rate (determined by the user) to determine the torque required to cause a cylindrical surface (having a diameter equal to the overall width of the vane) to be sheared by the vane. This destructive measurement is done in the working half, with the rotation axis parallel to the bedding plane. The torque required to shear the sediment along the vertical and horizontal edges of the vane is a relatively direct measure of the shear strength. Typical sampling rates are one per core section until the sediment becomes too firm for insertion of the vane.

Downhole measurements

The downhole logging program during Expedition 320T was specifically designed to determine the efficiency of the new WHC system on the *JOIDES Resolution* by using uphole (surface) and downhole acceleration data to evaluate the efficiency of the heave compensation and by comparing logging data collected on Leg 130 from Site 807 to data collected onboard. In addition the MSS, a new third-party LDEO tool, needed testing in readiness for deployment during Expedition 320. Several wireline logging tools were deployed as described below.

Wireline logging tools and tool strings

Individual logging tools were joined together into tool strings so that several measurements could be made during each logging run. Tool strings were lowered to the bottom of the borehole and data were logged as the tool string was pulled back up the hole. Repeat runs were made to confirm the accuracy of log data. The following tool strings were deployed in Hole U1330A (Fig. F6):

1. The trial combination string (gamma ray, acceleration, and resistivity measurements), which consisted of the HNGS, HLDS (without radioactive source, used for caliper measurement only), GPIT, and DIT-E.
2. The FMS tool string, composed of the HNGS and FMS with the GPIT.
3. The MSS tool string, made of the HNGS, HLDS (without source, used for caliper measurement only), GPIT, and MSS.

Principles and uses of the wireline logging tools

The properties measured by each tool, sampling intervals, and vertical resolutions are summarized in Table T3. Explanations of tool name acronyms and their measurement units are summarized in Table T4. More detailed descriptions of individual logging tools and their geological applications can be found in Ellis (1987), Goldberg (1997), Rider (1996), Schlumberger (1989, 1994), Serra (1984, 1986, 1989), and the LDEO-Borehole Research Group (BRG) Logging Services Manual (LSM) (2001).

Hostile Environment Gamma Ray Sonde

The HNGS measures natural gamma radiation from isotopes of potassium, thorium, and uranium and uses a five-window spectroscopic analysis to determine concentrations of radioactive potassium (in weight percent), thorium (in parts per million), and uranium (in parts per million). The HNGS uses two bismuth germanate scintillation detectors for gamma ray detection with full spectral processing. The HNGS also pro-

vides a measure of the total gamma ray emission and uranium-free or computed gamma ray (CGR) emission that are measured in American Petroleum Institute units (gAPI). The HNGS response is influenced by the borehole diameter. HNGS data are corrected for borehole diameter variations during acquisition.

Hostile Environment Litho-Density Sonde

The HLDS normally consists of a radioactive cesium (^{137}Cs) gamma ray source (622 keV) and far- and near-gamma ray detectors mounted on a shielded skid, which is pressed against the borehole wall by a hydraulically activated eccentricizing arm. Radioactive sources were not used on this expedition, but the tool was used for its eccentricizing arm (or caliper) to measure the diameter of the borehole and to aid with pressing the MSS tool sensor against the borehole wall. In standard deployment, gamma rays emitted by the source experience both Compton scattering and photoelectric absorption. The number of scattered gamma rays that reach the detectors is directly related to the number of electrons in the formation, which is related to bulk density. Porosity may also be derived from this bulk density if the matrix density is known. The HLDS also measures the photoelectric effect factor (PEF) caused by absorption of low-energy gamma rays. Photoelectric absorption occurs when gamma rays reach <150 keV after being repeatedly scattered by electrons in the formation. PEF depends on the atomic number of the elements in the formation; thus, the PEF varies according to the chemical composition of the formation. Coupling between the tool and borehole wall is essential for high-quality HLDS logs. Poor contact results in underestimation of density values. Both density correction and caliper measurement of the hole are used to check the contact quality.

Phasor Dual Induction Spherically Focused Resistivity Tool

The DIT-E provides three different measurements of electrical resistivity, each with a different depth of penetration into the formation. Two induction devices (deep and medium resistivity) transmit high-frequency alternating currents through transmitter coils, creating magnetic fields that induce secondary (Foucault) currents in the formation. These ground-loop currents produce new inductive signals, proportional to the conductivity of the formation, which are measured by the receiving coils. The measured conductivities are then converted to resistivity. A third device, a spherically focused resistivity instrument, gives higher vertical resolution, as it measures the current necessary to maintain a constant voltage drop across a fixed interval.

Formation MicroScanner

The FMS produces high-resolution images of borehole wall microresistivity that can be used for detailed lithostratigraphic or structural interpretation. This tool has four orthogonally oriented pads, each with 16 button electrodes that are pressed against the borehole walls. Good contact with the borehole wall is necessary for acquiring good-quality data. Approximately 30% of a borehole with a diameter of 25 cm is imaged during a single pass. Coverage may be increased by a second run. The vertical resolution of FMS images is ~5 mm. Resistivity measurements are converted to color or gray-scale images for display. Local contrast in FMS images was improved by applying dynamic normalization to the FMS data. A linear gain is applied, which keeps a constant mean and standard deviation within a sliding window of 2 m. FMS images are oriented to magnetic north using the GPIT, assuming that the GPIT can locate magnetic north in magnetite-rich environments (see “**General Purpose Inclinometer Tool**” for more details). This method allows the dip and strike of interpreted geological features intersecting the hole to be measured from processed FMS images.

General Purpose Inclinometer Tool

The GPIT is included in the FMS and MSS tool strings to calculate tool acceleration and orientation during logging. Tool orientation is defined by three parameters: tool deviation, tool azimuth, and relative bearing. The GPIT utilizes a three-axis inclinometer and a three-axis fluxgate magnetometer to record the orientation of the FMS images as the magnetometer records the magnetic field components (F_x , F_y , and F_z). Corrections for cable stretching and/or ship heave using acceleration data (A_x , A_y , and A_z) allow precise determinations of log depths. A hydraulic WHC designed to adjust for rig motion during logging operations minimizes ship heave.

Magnetic Susceptibility Sonde

The MSS, a new wireline tool designed by LDEO, measures the ease with which particular formations are magnetized when subjected to a magnetic field (in this case that of Earth). The ease of magnetization is ultimately related to the concentration and composition (size, shape, and mineralogy) of magnetizable material within the formation. These measurements provide one of the best methods for investigating stratigraphic changes in mineralogy and lithology because the measurement is quick, repeatable, and nondestructive and because different lithologies often have strongly contrasting susceptibilities. High-resolution susceptibility measurements aid significantly in paleoclimatic and paleoceanographic studies, where construction of an accurate and complete stratigraphic framework is critical to observe past climatic

changes but core recovery is often imperfect. The MSS measures at two vertical resolutions and depths of investigation. A single-coil sensor provides high-resolution measurements (~10 cm) but is shallow-reading; therefore, bowsprings are used to eccentricize the tool (additionally the HLDS caliper arm can aid with forcing the tool against the borehole wall). A dual-coil sensor provides low-resolution (~40 cm), deeper-reading measurements, and because of its more robust nature acts as a quality control for the high-resolution readings. The MSS can be run as a component of a Schlumberger tool string, using a specially developed data translation cartridge, saving hours of operation time. For quality control and environmental correction, the MSS also measures internal temperature, z-axis acceleration, and low-resolution borehole conductivity. In future expeditions, the MSS may be run as part of the “Paleo-combo” tool string with the Multi-Sensor Spectral Gamma Ray Tool (MGT) and the HLDS.

Wireline Heave Compensator

Expedition 320T was the first time the new passive WHC system was used on the *JOIDES Resolution*. Using measurements made by a MRU (located under the rig floor near the center of gravity of the ship), it is designed to adjust the length of the wireline with its vertically moving flying head to compensate for the vertical motion of the ship. Real-time measurements of uphole (surface) and downhole acceleration are made simultaneously by the MRU and GPIT, respectively. A LDEO-developed software package allows these data to be analyzed and compared in real time, displaying the actual motion of the logging tool string and enabling the efficiency of the compensator to be evaluated. In addition to an improved design and smaller footprint compared to the previous system, its location, together with the winch unit, on the starboard side of the derrick contributed to a significant reduction in the time necessary to prepare for logging operations.

Logging data flow and processing

Data for each wireline logging run were recorded and stored digitally and monitored in real time using the Schlumberger MAXIS 500 system. After logging was completed, preliminary processing was performed by the shipboard logging team so that data could be utilized almost immediately by the science party. Standardized data processing took place onshore at LDEO, and the data were made available (in ASCII and DLIS formats) through the shipboard IODP logging database ~1 week after collection.

Wireline log data quality

Logging data quality may be seriously degraded by changes in hole diameter and in sections where the borehole diameter greatly decreases or is washed out. Deep-investigation measurements such as resistivity are the least sensitive to borehole conditions; however, measurements such as density and neutron porosity (not measured here) are more sensitive because of a shallower depth of investigation and the effect of drilling fluid volume on neutron and gamma ray attenuation. Corrections can be applied to the original data in order to reduce these effects. Gamma ray logs (e.g., HNGS) are generally used for depth correlations between logging runs. Logs from different tool strings may, however, still have depth mismatches caused by either cable stretch or ship heave during recording.

Lithostratigraphy

Two holes were drilled at Site U1330 (Fig. F2). Hole U1330A was drilled without coring (washed) to ~100 mbsf where two RCB cores were recovered from the interval of ~103 to 123 mbsf. Hole U1330B was cored continuously to a maximum depth of 91.2 mbsf. Sediments at Site U1330 are characterized by varying proportions of calcareous nanofossils and planktonic foraminifers with minor amounts of siliceous microfossils (Table T5). The stratigraphy recovered from both holes can be described as a single lithostratigraphic unit (Fig. F7). Note that Core 320T-U1330B-10H was not cut during Expedition 320T but was reserved for core flow demonstration for Expedition 320 scientists. From visual inspection of the whole-round sections and comparison with Site 807 results (Kroenke, Berger, Janecek, et al., 1991), this core is assumed to be part of the same lithostratigraphic unit as the preceding nine cores.

Description of Unit 1

Intervals: Cores 320T-U1330A-1W, 2R, and 3R (0–122.7 mbsf) and 320T-U1330B-1H through 10H (0–91.2 mbsf)

Age: Pleistocene–early Pliocene

Depth: 0–122.7 mbsf

Unit 1 consists predominantly of light gray to white nanofossil ooze with foraminifers, locally grading to foraminifer nanofossil ooze. The latter lithology dominates the uppermost core (320T-U1330B-1H), which is noticeably more brownish in color, perhaps owing to the presence of terrigenous material and organic matter. Traces of

siliceous microfossils (radiolarians, silicoflagellates, and diatoms) are present throughout. The entire unit is characterized by moderate to slight burrowing with common darker burrow-mottled horizons.

Prominent diagenetic features include color banding and burrow halos in shades of green and purple. Locally burrows are partly pyritized, forming hard “bits” in the otherwise soft ooze. Black burrow features without visible framboidal pyrite in smear slide may contain submicroscopic sulfides such as greigite (see Musgrave et al., 1993).

Interpretation

Site U1330 is a reoccupation of ODP Leg 130, Site 807, which is situated near the Equator (~3°N) in a basement graben feature of the Ontong Java Plateau, a location thought to have protected it from bottom current activity as pelagic sediment accumulated (Kroenke, Berger, Janecek, et al., 1991). The single unit designation (Unit 1) for Expedition 320T core is consistent with that of Site 807 (Kroenke et al., 1991) where Unit IA extended from Holocene/Late Pleistocene calcareous ooze at the sediment/water interface to the ooze–chalk transition in Miocene (~10.4 Ma) sediments at 293 mbsf. This transition is approximately the timeframe (~10–12 Ma) when the site crossed the equator (Kroenke, Berger, Janecek, et al., 1991).

As at Site 807, pelagic sediment cored at Site U1330 contains very little terrigenous input except perhaps in the uppermost few meters of the section. No pyroclastic debris was observed. Sediment was deposited above the lysocline (Kroenke, Berger, Janecek, et al., 1991) in a zone of perhaps lower than expected organic carbon content suggesting low surface water productivity compared to other equatorial sites (Stax and Stein, 1993).

The color bands are fairly early diagenetic (redox) features in that they are present ~10 m below the sediment/water interface. According to Lind et al. (1993), the purplish bands reflect the distribution of disseminated fine-grained iron sulfide and the green bands are enriched in Fe- and Al-bearing silicates. The latter may be clays derived from volcanic ash as suggested by Lind et al. (1993); however, we saw no evidence for this in smear slides of these laminae. Furthermore, Kroenke et al. (1993) only noted distinct ash layers at Site 807 below the section cored at Site U1330.

Planktonic foraminifer biostratigraphy and sedimentation rates

Core catcher samples were examined for planktonic foraminifers from Holes U1330A and U1330B. The oldest sediments cored at this site are lower Pliocene (Zone N18–N19). Key planktonic foraminifer FO and LO datums are used to estimate sedimentation rate based on the low-resolution sampling conducted here.

Hole U1330A

The wash core (320T-U1330A-1W) and the core catchers from the two RCB cores (320T-U1330A-2R and 3R) all yield an early Pliocene age based on the presence of *Globobulimina nepenthes* (LO = 4.37 Ma) and *Globobulimina tumida* (FO = 5.82 Ma). The FO of *Sphaeroidinella dehiscens* (5.54 Ma) is a reliable proxy for some tropical regions, but earlier work on Ontong Java Plateau demonstrated that this is not a reliable datum in this area (Chaisson and Leckie, 1993). Comparison with Hole 807A indicates that the Miocene/Pliocene boundary was expected at a depth of ~125 mbsf (Kroenke, Berger, Janecek, et al., 1991).

Hole U1330B

Chronostratigraphy for Hole U1330B is tentative because of the coarse 9.5 m resolution of the core catcher samples examined here, as well as the use of a single microfossil group and lack of paleomagnetic data. The Pliocene/Pleistocene boundary is tentatively placed near the LO of *Globigerinoides fistulosus* (1.88 Ma) at ~27 mbsf. The lower/upper Pliocene boundary is placed near the LO of *Globobulimina margaritae* (3.85 Ma) at ~59 mbsf. Hole U1330B bottomed out in the lower Pliocene (>4.37 Ma) based on the presence of both *G. nepenthes* and *G. tumida*.

Sedimentation rates

Sediments accumulated at an average rate of ~26.5 m/m.y. during the Pliocene and slowed to ~16 m/m.y. during the Pleistocene based on a coarse resolution study of core catcher samples (Table T6; Fig. F8). These estimates are very similar to the rates calculated based on several microfossil groups and paleomagnetic polarity data from nearby Site 807 (Kroenke, Berger, Janecek, et al., 1991).

Geochemistry

The geochemical methods and sampling plan have been outlined in “[Methods](#).” Here we report the data obtained from the analyses. It should be remembered that the cores from Hole U1330A were taken from a greater depth than those for Hole U1330B (102.5–122.5 meters core depth below seafloor [CSF]-A and 0–92.1 m CSF-B, respectively).

Interstitial water samples

A total of 14 interstitial water samples were analyzed for pH, alkalinity, and elemental composition. Figures [F9](#) and [F10](#) show alkalinity and pH, major elements, and minor elements. Only three of the four samples taken for interstitial water pH and alkalinity tests gave reliable results from Hole U1330A. Alkalinity increases downhole in Hole U1330B and appears to slightly decrease with depth in the Hole U1330A interval, whereas pH exhibits a slight decrease downhole in Hole U1330B and is higher and variable in Hole U1330A (Fig. [F9](#); Table [T7](#)).

In terms of the major elemental abundances (Fig. [F10](#); Table [T8](#)), Na and K are quite variable and do not exhibit a consistent trend. Average abundances for Na in Holes U1330A and U1330B are same (462 mM in each hole), whereas Hole U1330B has a slightly higher average K content than Hole U1330A (9.8 versus 9.7 mM). The trends for Ca and Mg are complementary, with Ca increasing downhole in Hole U1330B to Hole U1330A and Mg decreasing. For Ca, Hole U1330A data appear more variable.

Whole-rock samples

Six whole-rock samples were analyzed using ICP-AES from Section 320T-U1330A-3R-2 to investigate the nature of the color banding observed in this core (Fig. [F11](#)). Data are reported in Table [T9](#). On the basis of these preliminary data, there does not appear to be any correlation between geochemistry and color banding.

Headspace gas samples

A total of 14 samples were analyzed for hydrocarbons. The results for methane are presented in Figure [F12](#) and Table [T10](#). Abundances are between 1.5 and 2.0 ppmv methane at the top of Hole U1330B between 3 and 19.1 mbsf. Below this point methane increases to 4.3 ppmv at 47.6 mbsf followed by a decrease to 1.8 ppmv at 66.5

mbsf. Methane abundances in Hole U1330A are higher (6.6–13.9 ppmv), but no systematic variations are apparent in the four data points from this core.

Quality assurance/Quality control

No quality assurance/quality control (QA/QC) data were available to judge the alkalinity and pH data other than the calibration of the electrode prior to the expedition. Normally, the IAPSO seawater standard is tested as an unknown, but this was not done during Expedition 320T.

QA/QC data were taken from the ICP-AES analyses through the analysis of standards and the peak heights and shapes of the wavelengths used to quantify each element. However, extracting these data to be able to judge the data quality is a labor-intensive task. Scripts must be written in order to automate this process, but these were not available for Expedition 320T.

For the whole-rock analyses, reference materials were analyzed as unknowns and demonstrated a glitch in the Teledyne Leeman Labs data reduction software. All data should be taken as preliminary while these glitches are fixed and the Expedition 320T data are recalibrated.

For methane analyses, four standards were analyzed as unknowns on the GC3:

1. Standard A (15 ppmv) yielded 4.19 ppmv methane,
2. Standard B (100 ppmv) yielded 95.3 ppmv methane,
3. Standard C (1,000 ppmv) yielded 750.0 ppmv methane, and
4. Standard D (10,000 ppmv) yielded 10,140 ppmv methane.

Physical properties

Physical properties were measured on core material recovered during Expedition 320T to test the new installation of the shipboard measurement systems and the users' ability to upload and retrieve data from the LIMS. Magnetic susceptibility, GRA bulk density, and compressional wave velocity were measured on the whole-core sections with the WRMSL. Magnetic susceptibility data collected on the WRMSL are discussed along with magnetic susceptibility data collected on the Special Task Multisensor Logger (STMSL) and the SHMSL in "**Paleomagnetism.**" Natural gamma ray (NGR) activity was measured on a new separate track. Thermal conductivity was measured only

on several sections of Core 320T-U1330B-10H because of problems with the new system (likely user error). Split-core measurements on the working half of the core included V_p and MAD. A single test of the AVS sediment strength system was also performed, resulting in a satisfactory measurement.

Profiles of whole-core bulk density and V_p as well as split-core V_p are shown in Figure **F13**. Bulk density initially increases from a value near 1.40 g/cm^3 at the seafloor to $\sim 1.65 \text{ g/cm}^3$ at 15 mbsf. Thereafter, bulk density is generally variable between 1.60 and 1.65 g/cm^3 to the bottom of the cored interval at 92 mbsf. In the density data plotted in Figure **F13** a tendency can be seen in each individual core to have low-to-high density gradient from top to bottom. This has been observed before in soft sediments and is probably an artifact produced by pullout of the piston core.

Compressional wave velocity measured with the WRMSL generally stays close to that of water at $\sim 1440 \text{ m/s}$. There is a systematic difference of $\sim 150 \text{ m/s}$ (10%) between the measurements of V_p made on the whole-round core and those made on the split core. The cause for this variation was not determined. In either case velocity does not vary appreciably with depth.

Bulk density, grain density, and porosity as determined from discrete samples using the MAD system are illustrated in Figure **F14**. Bulk density values generally agree with those measured by the WRMSL and are reasonably constant with depth. Of the eight determinations of grain density, three are anomalous, exhibiting values $>3 \text{ g/cm}^3$ rather than the expected range of 2.20 g/cm^3 (biogenic silica) to 2.72 g/cm^3 (calcium carbonate). The addition of $\sim 15\%$ pyrite (grain density = 5 g/cm^3) could account for the high values, but there was no indication of that much pyrite in the samples. Sampling for MAD specifically avoided the pyrite-rich burrows observed locally throughout the cores. Unfortunately, the dried samples whose weights and volumes were used to calculate grain density were already destroyed in the chemistry laboratory during the carbonate analysis process by the time the anomalies were discovered. Future expeditions will have to monitor these measurements to assess whether there is a real problem. There was no MAD sampling of Core 320T-U1330B-10H because the whole-round sections were left intact for training purposes. Porosity is $\sim 75\%$ in the upper 20 m and decreases as the sediment compacts to $<70\%$ by 80 mbsf (Fig. **F14**).

NGR data were successfully measured from the core sections. Data from Hole U1330B are shown in Figure **F15**. All of the count levels are low, reflecting the mainly biogenic nature of the sediment. The relatively higher readings in the upper 5 m and the de-

cline to near background levels below that depth may be the result of a postglacial increase in the dust component of the sediment and/or some function of biological and geochemical influences.

The thermal conductivity measurement system collects data (time-temperature curves during heating cycles) but routinely fails to derive a thermal conductivity value from those data. Postmeasurement processing of the data files offline resulted in reasonable thermal conductivity values of ~ 1.2 W/(m·K) in Core 320T-U1330B-10H.

Downhole measurements

The FlexIt and APCT-3 downhole tools were tested during coring operations in Hole U1330B. The FlexIt tool is used for core orientation and was run in all cores. The APCT-3 tool provides the temperature of the formation and was run on Cores 320T-U1330B-5H, 7H, and 9H. The Sediment Temperature Tool (SET) tool was not run because of time constraints.

During each run of the three APCT-3 tools, mudline temperatures were taken for 5 min both before and after shooting the APC core. Each tool was left in the sediment for 10 min to allow the temperature to equalize prior to pulling out the tool (Fig. F16).

The tools measured a mudline temperature of $\sim 2^\circ\text{C}$ and a sediment temperature ranging from 4.57°C at 45 mbsf to 6.25°C at ~ 83 mbsf (Fig. F17).

The FlexIt tool was purchased as an APC core orientation tool to replace the aging Tensor tools used during ODP and Phase 1 of IODP. The same type of tool has been run successfully on the D/V *Chikyu* during expeditions in 2008. The FlexIt tool is run in the sinker bar assembly of the APC tool. The FlexIt is lowered through the drill string until the APC lands in place. The string is then held steady for 5 min while the FlexIt orients prior to shooting the APC core. Data collected from the FlexIt tools are still being processed.

Downhole logging

Data quality and comparison with Hole 807A logs

Hole U1330A was cored between 103.6 and 122.8 m DSF but was primarily drilled for logging and testing of the new WHC. Multiple passes were made with each of the three tool strings over a maximum depth range of 424 m (106–530 m WSF) in Hole U1330A. The HLDS caliper log (Fig. F18A) shows that borehole diameter was generally constrained and the borehole wall relatively smooth. The caliper arm maintained good contact with the borehole wall, with the exception of an interval between ~160 and 260 m wireline log matched depth (below seafloor) (WMSF), suggesting that the data are of good quality. Even in the interval with poor contact, resistivity data continue to show amplitudes similar to those within the narrower portion of the hole, indicating that the data reflect real variations in the formation. The caliper logs from the FMS (two per pass) provided another means for assessing borehole condition (diameter and rugosity) (Fig. F19). FMS caliper logs indicated that borehole conditions for the majority of the logged section were good. However, between ~290 m WSF and the top of the logged section, two of the four caliper arms of the FMS were not touching the borehole wall, degrading the quality of the logs.

Logs from Hole U1330A compare well with the data recorded ~150 m away in Hole 807A during Leg 130 (Fig. F18). Comparison between the two HLDS caliper logs in Figure F18A shows that hole conditions were better in Hole U1330A. Hole 807A was cored before logging, resulting in a larger hole, whereas Hole U1330A was drilled as a logging-dedicated hole. Accurate caliper data were not collected during the main pass of the lower ~80 m of Hole U1330A, where the caliper arm was closed because of winch problems. Figure F18B shows that gamma ray values from the first pass with the first tool string were very low in Hole U1330A, particularly in the upper section. The low values are due, in part, to the low natural radioactivity of the nannofossil ooze that constitutes the bulk of the formation. When comparing the holes, one can observe similar features between the two curves. The difference is mainly in amplitude, although below ~500 m WMSF, gamma ray data from Hole U1330A do approach values similar to those from Hole 807A. Gamma ray data were collected using two different tools (the Natural Gamma Ray Spectrometry Tool [NGT] in Hole 807A and the HNGS in Hole U1330A), but both were operating at the lower limits of their sensitivity. The apparent discrepancy may be due to the fact that the HNGS was not calibrated for several months prior to Expedition 320T. The gamma ray data from Hole U1330A will be corrected as soon as the tool is recalibrated for future expeditions. Resistivity

logs show good agreement between Holes U1330A and 807A (Fig. **F18C**), exhibiting an almost perfect match in the common interval.

Logging stratigraphy

At Site 807, the upper 950+ m of sediments was placed in a single lithostratigraphic unit (nannofossil ooze and chalk), with a subdivision at ~290 m CSF identified as the ooze–chalk transition (Kroenke, Berger, Janecek, et al., 1991). Site U1330 sediments can generally be described by low natural radioactivity and resistivity. Although there is some variation in the resistivity log, there are no common events in the limited data collected to clearly define distinct logging units. The lack of distinctive character in the logs reflects the relatively uniform composition of the sediments. Sediments at this site are defined as a single logging unit, and the subunits shown in Figure **F18** are predominantly based on changes in resistivity values.

Logging Subunit 1A is characterized by relatively constant low resistivity and gamma ray values. Minor peaks in resistivity in this subunit may correspond to more competent chalk intervals in the surrounding ooze. Logging Subunit 1B displays an increasing trend with depth in resistivity and gamma ray values, starting at ~290 m WMSF. The top of this subunit corresponds to the base of lithostratigraphic Subunit 1A at Site 807, which is characterized by increasing induration (Kroenke, Berger, Janecek, et al., 1991). Logging Subunit 1C is characterized by a decrease with depth in resistivity and gamma ray values. There is a local increase in gamma ray values in Hole U1330A but no corresponding change in resistivity.

FMS images

FMS imagery (Fig. **F20**) captures the banded and laminated nature of the formation(s) in the borehole wall. When compared with core taken from Hole 807A, features such as bioturbation (Fig. **F20B**), bedding/laminations (Fig. **F20B**), and wispy structures (observed as braided color bands, Fig. **F20C**) can be picked out from the images (Kroenke, Berger, Janecek, et al., 1991). The good correlation between the features seen in the Hole 807A core and the FMS images collected ~150 m south of Hole 807A attest to the lateral extent of the formations. However, sinusoidal features seen in FMS images (Fig. **F20A**) indicating dipping structures are not apparent in the corresponding core section, likely because of the steep nature of these features (25°–30°) and the large offset between the holes. These features may be due to local sediment instabilities or local tectonic influences, such as microfaulting.

Paleomagnetism

Paleomagnetic analyses during Expedition 320T consisted of long-core measurements of the natural remanent magnetization (NRM) of split-core sections from Site U1330 before and after alternating-field (AF) demagnetization. During the expedition, the superconducting rock magnetometer (SRM), which is used to make these measurements, was being evaluated for its readiness following refurbishment of the *JOIDES Resolution* (see “[New shipboard Paleomagnetism Laboratory](#),” below). Initial measurements indicated that a significant source of magnetic field noise existed in the laboratory. The first 3 weeks of the 4 week expedition were mainly spent determining the origin of this noise and attempting to abate its impact on measurement quality. Once we reduced the magnetic noise to acceptable levels, the last week of the expedition was used to further test the SRM (track positioning and sample measurement accuracy and precision) and to measure a few but not all of the split-core sections. In this section, we highlight paleomagnetic results from one short interval. Additional data collected the last few days of the expedition are available in the LIMS database.

We also obtain rock magnetic information from susceptibility data and from coercivity and magnetic concentration constraints derived from NRM data. Susceptibility data were collected on the WRMSL, STMSL, and SHMSL.

Because Site U1330 is at the same location as Site 807, the paleomagnetism and rock magnetism results from sediments collected during Leg 130 (e.g., Kroenke, Berger, Janecek, et al., 1991; Musgrave et al., 1993; Kok and Tauxe, 1999) provide details beyond the shipboard measurements presented here, such as a magnetostratigraphy, a relative paleointensity record, and details on reduction diagenesis. They also provided us with background information that helped guide coring and measurement strategies as we tested the SRM and extracted new paleomagnetic information from the core.

Paleomagnetic results

Much of the paleomagnetic data from the expedition was collected while the SRM software was in a constant state of change. Units were being recorded in cgs rather than SI units until 2 March 2009, the sign of the y -axis moment was inverted for some measurements, and declination data were therefore in error for most of the data collected before 2 March. On 2 March, we measured Cores 320T-U1330B-1H and 2H after

the software had matured sufficiently that all computations done internally were correct and all data were output in SI units.

We also used the raw moment data from Section 320T-U1330B-8H-7 to calculate the paleomagnetic direction in order to illustrate the capability of the magnetometer independent of the software. Progressive AF demagnetization of this section shows a smooth decrease in magnetization with an associated migration of the direction from a steep drill string overprint direction to a shallow direction, presumably related to the depositional remanent magnetization (Figs. F21, F22). The declination points fairly consistently to the north, which may be caused by a radial drilling overprint. Given the very weak magnetization of these sediments, the results illustrate that the magnetometer is capable of making accurate and precise measurements.

Kok and Tauxe (1999) observed the Brunhes/Matuyama reversal at 12.19 m depth in Hole 807A. Based on this information, we examined paleomagnetic data from this interval in Hole U1330B. The Brunhes/Matuyama is recorded by a change in declination of $\sim 180^\circ$ between 11.7 and 12.2 m depth, giving a mean depth of 11.95 m, which is very consistent with the Hole 807A Brunhes/Matuyama (Fig. F23).

Magnetic susceptibility

Raw susceptibility data from the three multisensor loggers contain several artifacts caused by drilling contamination (rust), drilling disturbance, and measurement practices. These dominate the susceptibility record available from the LIMS database (Fig. F24).

Drilling contamination appears to be a problem in the upper ~ 2 m of all cores from Hole U1330A and in the upper ~ 2 m of Cores 320T-U1330B-5H through 10H. The largest signal is very likely caused by rust from the pipe. Pyrite pieces that are not as easily washed out of the hole during drilling also accumulate at the top of each core. The top of Core 320T-U1330A-3R is particularly contaminated, with susceptibilities exceeding 400×10^{-5} SI. We confirmed that this was not an artifact of the WRMSL measurement for Section 320T-U1330A-3R-1 by repeating the measurement on the STMSL. The results were virtually identical.

Exceptionally low (negative) susceptibility values are observed for all data at the ends of each core owing to the WRMSL measurement practice in which the density standard is measured directly after the last section of each core. The density standard is

made of aluminum and has a minimum (peak negative) value of about -8000×10^{-5} SI. This standard needs to be measured at least 40 cm below the last section to avoid this artifact. Similarly, the susceptibility values from the STMSL are shifted by about -14×10^{-5} to -20×10^{-5} SI (Fig. F25). This is related to the plastic bars on which the split-core sections sit and the braces on which the plastic bars sit. This problem could be easily overcome by measuring the susceptibility of the track without a sample present and then using this “track signal” from each measurement as a background correction.

Once these artifacts are removed, the magnetic susceptibility measurements give low but positive values ($\sim 3 \times 10^{-5}$ to 10×10^{-5} SI) for the upper four cores from Hole U1330B (above 32 m depth) (Figs. F26, F27). Given these low susceptibilities, measurement precision could have been improved by taking more than one measurement at each depth. By only taking one measurement, which was recorded as an integer raw meter value, the data plot with steplike precision from one observation to the next (e.g., the WRMSL data in Fig. F25). Below Core 320T-U1330B-4H the sediment is diamagnetic, resulting in slightly negative susceptibility values (about -1×10^{-5} SI). This pattern mimics that observed for Site 807, with the drop to negative susceptibility occurring at ~ 32 m depth (Kroenke, Berger, Janecek, et al., 1991), which is in the coring gap between Cores 320T-U1330B-4H and 5H.

New shipboard Paleomagnetism Laboratory

As part of getting the new Paleomagnetism Laboratory ready for future expeditions, we conducted a variety of tests of the paleomagnetism equipment and did magnetic field surveys of the laboratory and inside the instruments. This included testing and calibrating the KappaBridge (KLY 4S) susceptibility meter using vendor-supplied standards and testing the Schonstedt TSD-1 shielded oven, DTECH AF demagnetizer, portable fluxgate magnetometer, and ASC IM-10 impulse magnetizer for general functionality. All of these instruments were functional, as was the SRM, by the end of the expedition.

Software issues aside, the SRM functioned poorly during the first 3 weeks of the expedition owing mainly to magnetic noise. Initial measurements of the carbonate ooze split-core samples were plagued by large flux counts on the y -axis of the magnetometer, which could occur abruptly even when the sample was not moving nor even fully in the SRM sensor region. Given the relatively weak magnetizations of carbonate

ooze sediments, these large flux counts were unexpected even when the sample was in the sensor region.

The rapid flux counts, which were clearly unrelated to the magnetic remanence of the carbonate ooze samples, have been observed before on past expeditions and in shore-based laboratories but have not been well explained. They are commonly referred to as flux jumps and are suspected to arise from a number of factors. Most commonly flux jumps are associated with the inability of the superconducting quantum interference device (SQUID) sensors to count (i.e., measure) the number of flux quanta associated with highly magnetized materials as the material moves through the sensor region. For example, mafic igneous rocks are notoriously difficult to measure accurately in SRMs owing to their high magnetizations. Similarly, flux jumps occur frequently when large gradients occur along a long-core sample, as would be the case when a weakly magnetized carbonate is juxtaposed against a highly magnetized ash or clay layer. Flux jumps may also be caused by random power surges that generate radio-frequency (RF) magnetic fields (generally those magnetic fields with frequencies from a few hundred kilohertz to a few gigahertz). RF magnetic field surges are usually relatively rare and can often be traced to specific equipment, like the saws used in the core splitting room and arc welders used during ship maintenance. As noted in the 2G Enterprises guidebook (Applied Physics Systems, 1995), SQUID sensors are very sensitive to RF interference.

In order to track down the source of the magnetic noise, we conducted a number of tests and measurements. First we mapped the static (long wavelength) magnetic field in the laboratory and within the SRM by doing magnetic surveys with a three-axis fluxgate magnetometer. The frequency response of the fluxgate magnetometer is flat from direct current to 250 Hz (Applied Physics Systems, 2003).

The magnetic field in the laboratory met with expectations, with field values generally comparable within a factor of 2–3 to Earth's magnetic field (Fig. [F27](#); Tables [T11](#), [T12](#), [T13](#), [T14](#)). Highs (80,000–130,000 nT) were associated with some of the air-conditioning vents, the corner of a wall near the elevator, the SRM cold head, and the region near the forward wall, which has the air-conditioning unit behind it. The two support columns produced lows near the ceiling of ~20,000 nT. The position and size of the magnetic anomalies are, of course, dependent on geographic position, ship orientation, and the relative positions of electronic equipment and metallic objects. Mainly, the survey showed that there are no anomalously high magnetic fields within the Paleomagnetism Laboratory.

Magnetic surveys along the SRM track inside the shielded region (Fig. F28) indicate that a very low null field (1 nT while the ship was stationary in Guam and 7 nT while transiting toward Hawaii) had been trapped by the marine technician (M. Hastedt) during the Guam port call. This is comparable to the field trapped within the SRM that resides inside a shielded room on the *Chikyu*. This is also the lowest field region within any of the shielded instruments on the *JOIDES Resolution* (SRM, Schonstedt oven, or D-Tech AF demagnetizer). Elsewhere within the SRM shield, the field is <400 nT, which is ~2–4 times higher than similar regions in the *Chikyu's* SRM. Exceptionally high fields occur within the shielded region of SRM at the joints in the magnetic shield, on either side of the in-line AFd magnetometer. This is true for the SRM on both the *JOIDES Resolution* and the *Chikyu*. The maximum field is ~1400 nT for the *JOIDES Resolution* and is <500 nT for the *Chikyu*. During the expedition, we took the three main sections (the main SRM section, the in-line AF unit, and the back slim-diameter shielded region) apart and attempted to reinstall them with tighter connections between sections. A much tighter connection was established, shortening the track by ~2.5 cm. Unfortunately, the magnitude of the magnetic field at these joints did not change appreciably.

We next ran a series of samples consisting of split-core sections from Hole U1330B, a concrete split-core sample (153 cm long), and empty tray samples. Flux jumps were absent when measuring the concrete sample or empty tray but occurred on virtually all of the Hole U1330B carbonate ooze sections. We noted that the flux jumps were common when the back of the 150 cm long sample spanned the two joints in the shield and the front of the sample was near or in the sensor region. The number of flux jumps increased significantly when the servo motor that drives the track was engaged and were notably higher when the power supply was plugged into the ship's unregulated power versus the regulated power. The power supply for the servo motor was near one of the shield joints and had a power cable that was not magnetically shielded. With the help of the ET (J. Kotze), we rectified this by moving the power supply to the very front of the magnetometer and by shielding its cables and any other cables in the vicinity of the magnetometer. This reduced the RF magnetic field significantly but not completely.

We continue to track the origin of the remaining RF magnetic fields and to understand why the position and type of sample controlled the occurrence of flux jumps. The best two indicators of when flux jumps were prone to occur or were occurring were to watch the digital readout on the SQUID electronics (in count mode rather than analog mode) or to watch the oscilloscope for degradation of the tuned SQUID

signal. The SQUID electronics digital readout (SEDR) allows for all three axes to be monitored, whereas the oscilloscope monitors only one axis at a time. We connected the oscilloscope to the y -axis because it was the most prone to extraneous flux counts. An antennae was constructed by the ET that would receive or transmit RF magnetic fields of a few gigahertz. Stray RF magnetic fields were noted when the antennae was in receiver mode and moved around the laboratory, but no clear new sources of RF magnetic fields were identified.

In contrast, thousands of flux counts were measured by the SQUID when the antennae was in transmit mode and a carbonate ooze sample was in the magnetometer, in a position as described above, or when it was basically anywhere near the SQUID sensors. No flux counts were noted when the sample was removed. With the sample in the magnetometer, the number of flux counts increased dramatically when the antennae was pointed at the joints in the shield.

This is very conclusive evidence that the RF magnetic fields are being transmitted through the poorly shielded joints. Furthermore, the sample is acting like an antennae or wire in that it is transmitting the RF magnetic fields along its length from the joints in the shield up to the SQUID sensors, in a process called RF magnetic induction (e.g., see Wikipedia).

We worked diligently the rest of the expedition to track down other sources. A significant source arose when the new 220 V outlet was installed at the fore end of the laboratory. When the crest amplifier was plugged into this outlet, the SRM recorded a large number of flux jumps during measurements. This problem was solved by plugging the amplifier into a transformer, which was then plugged into the ship's regulated 110 V power. With these changes, we managed to reduce flux jumps that occur during measurements to a manageable level.

Discussion and conclusions

The main objectives of Expedition 320T were testing the WHC and the refurbished drilling and coring systems. In addition, the expedition provided an opportunity for assessing the overall readiness of all science systems before the start of international scientific operations. Many of the instruments and applications are entirely new or upgraded, and all of them are newly installed in the renovated ship's laboratories. The cores recovered during this expedition are allocated as USIO cores (rather than IODP) and will be used primarily for education and training.

All routine shipboard analytical measurements and descriptive observations made on the recovered core material and the corresponding data were uploaded to the new LIMS. Litho- and biostratigraphic observations are essentially consistent with findings previously reported for Site 807 (Kroenke, Berger, Janecek, et al., 1991). A Holocene/upper Pleistocene calcareous ooze extends from the sediment/water interface to the ooze–chalk transition at 293 mbsf, about three times deeper than the cored depth of the two holes drilled during this expedition. Coarse examination of the planktonic foraminifer assemblages recovered from core catcher samples yielded average sediment accumulation rates that are very similar to the rates calculated based on several microfossil groups and paleomagnetic polarity data for Site 807.

The downhole logging program during Expedition 320T was specifically designed to determine the efficiency of the new WHC system by using uphole (surface) and downhole acceleration data to evaluate the efficiency of the heave compensation and by comparing the new logging data with the data collected from Site 807. As with the core data, the new logging results correspond well with the previously reported data. As expected, the sediment section logged in Hole U1330A is characterized by generally low natural radioactivity and resistivity. The relatively uniform composition and the limited data collected did not allow the definition of distinct logging units. However, the three defined subunits, based on slight variations in resistivity and gamma ray values, correspond to the lithostratigraphic subunits defined by the Leg 130 scientific party (Kroenke, Berger, Janecek, et al., 1991). Performance testing of the WHC both in pipe and in open hole in Hole U1330A proved satisfactory. This is also confirmed by the high-resolution FMS images (sensitive to heave conditions) that showed excellent agreement of layering and sedimentary features recorded during different runs. However, further fine-tuning and testing of the WHC will need to continue over the next few years to evaluate the system's response under varying heave conditions.

In conclusion, the successful deployment of the APC and RCB coring systems and the retrieval of ~103 m of drill core (with an average recovery rate of 93%), the full on-board processing of the cored material and subsequent scientific examination (largely confirming the results reported for Site 807), and the successful runs of new and standard logging tools using the new WHC during Expedition 320T have proven the operational readiness of the drillship and its analytical systems. The crew and IODP personnel are looking forward to the beginning of international operations on 5 March 2009.

References

- Applied Physics Systems, 1995. *Electronics Operating Manual and Technical Reference*: Mountain View, CA (2G Enterprises).
- Berggren, F.C., Kent, D.V., Swisher, C.C., III, and Aubry, M.-P., 1995. A revised Cenozoic geochronology and chronostratigraphy. In Berggren, W.A., Kent, D.V., Aubry, M.-P., and Hardenbol, J. (Eds.), *Geochronology, Time Scales and Global Stratigraphic Correlation*. Spec. Publ.—SEPM (Soc. Sediment. Geol.), 54:129–212.
- Blum, P., 1997. Physical properties handbook. *ODP Tech. Note*, 26. doi:10.2973/odp.tn.26.1997
- Chaisson, W.P., and Leckie, R.M., 1993. High-resolution Neogene planktonic foraminifer biostratigraphy of Site 806, Ontong Java Plateau (western equatorial Pacific). In Berger, W.H., Kroenke, L.W., Mayer, L.A., et al., *Proc. ODP, Sci. Results*, 130: College Station, TX (Ocean Drilling Program), 137–178. doi:10.2973/odp.proc.sr.130.010.1993
- Chaisson, W.P., and Pearson, P.N., 1997. Planktonic foraminifer biostratigraphy at Site 925: middle Miocene–Pleistocene. In Shackleton, N.J., Curry, W.B., Richter, C., and Bralower, T.J. (Eds.), *Proc. ODP, Sci. Results*, 154: College Station, TX (Ocean Drilling Program), 3–31. doi:10.2973/odp.proc.sr.154.104.1997
- Ellis, D.V., 1987. *Well Logging for Earth Scientists*: New York (Elsevier).
- Evans, H.B., 1965. GRAPE—a device for continuous determination of material density and porosity. *Trans. SPWLA 6th Ann. Logging Symp.*: Dallas, 2:B1–B25.
- Expedition 306 Scientists, 2006. Site U1312–U1315 methods. In Channell, J.E.T., Kanamatsu, T., Sato, T., Stein, R., Alvarez Zarikian, C.A., Malone, M.J., and the Expedition 303/306 Scientists, *Proc. IODP*, 303/306: College Station, TX (Integrated Ocean Drilling Program Management International, Inc.). doi:10.2204/iodp.proc.303306.110.2006
- Goldberg, D., 1997. The role of downhole measurements in marine geology and geophysics. *Rev. Geophys.*, 35(3):315–342. doi:10.1029/97RG00221
- Harms, J.C., and Choquette, P.W., 1965. Geologic evaluation of a gamma-ray porosity device. *Trans. SPWLA 6th Ann. Logging Symp.*: Dallas, C1–C37.
- Kok, Y.S., and Tauxe, L., 1999. A relative geomagnetic paleointensity stack from Ontong-Java Plateau sediments for the Matuyama. *J. Geophys. Res., [Solid Earth]*, 104(B11):25410–25413. doi:10.1029/1999JB900186
- Kroenke, L.W., Berger, W.H., Janecek, T.R., et al., 1991. *Proc. ODP, Init. Repts.*, 130: College Station, TX (Ocean Drilling Program). doi:10.2973/odp.proc.ir.130.1991
- Kroenke, L.W., Resig, J.M., and Leckie, R.M., 1993. Hiatus and tephrochronology of the Ontong Java Plateau: correlation with regional tectono-volcanic events. In Berger, W.H., Kroenke, L.W., Mayer, L.A., et al., *Proc. ODP, Sci. Results*, 130: College Station, TX (Ocean Drilling Program), 423–444. doi:10.2973/odp.proc.sr.130.050.1993
- Kvenvolden, K.A., and McDonald, T.J., 1986. Organic geochemistry on the *JOIDES Resolution*—an assay. *ODP Tech. Note*, 6. doi:10.2973/odp.tn.6.1986
- Lamont-Doherty Earth Observatory–Borehole Research Group, 2001. *Guide to ODP Wireline Logging Services CD*: Palisades, NY (Lamont-Doherty Earth Observatory, Columbia Univ.).
- Lind, I.L., Janecek, T.R., Krissek, L.A., Prentice, M.L., and Stax, R., 1993. Color bands in Ontong Java Plateau carbonate oozes and chalks. In Berger, W.H., Kroenke, L.W., Mayer, L.A., et al., *Proc. ODP, Sci. Results*, 130: College Station, TX (Ocean Drilling Program), 453–470. doi:10.2973/odp.proc.sr.130.007.1993

- Manheim, F.T., and Sayles, F.L., 1974. Composition and origin of interstitial waters of marine sediments, based on deep sea drill cores. *In* Goldberg, E.D. (Ed.), *The Sea* (Vol. 5): *Marine Chemistry: The Sedimentary Cycle*: New York (Wiley), 527–568.
- Mazzullo, J.M., Meyer, A., and Kidd, R.B., 1988. New sediment classification scheme for the Ocean Drilling Program. *In* Mazzullo, J.M., and Graham, A.G. (Eds.), *Handbook for ship-board sedimentologists*. ODP Tech. Note, 8:45–67. [doi:10.2973/odp.tn.8.1988](https://doi.org/10.2973/odp.tn.8.1988)
- Munsell Color Company, Inc., 1991. *Munsell Rock Color Charts*: Baltimore, MD (Munsell).
- Munsell Color Company, Inc., 1992. *Munsell Soil Color Charts*: Baltimore, MD (Kollmorgen Instruments).
- Musgrave, R.J., Delaney, M.L., Stax, R., and Tarduno, J.A., 1993. Magnetic diagenesis, organic input, interstitial water chemistry, and paleomagnetic record of the carbonate sequence on the Ontong Java Plateau. *In* Berger, W.H., Kroenke, L.W., Mayer, L.A., et al., *Proc. ODP, Sci. Results*, 130: College Station, TX (Ocean Drilling Program), 527–546. [doi:10.2973/odp.proc.sr.130.035.1993](https://doi.org/10.2973/odp.proc.sr.130.035.1993)
- Rider, M.H., 1996. *The Geological Interpretation of Well Logs* (2nd ed.): Caithness (Whittles Publ.).
- Schlumberger, 1989. *Log Interpretation Principles/Applications*: Houston (Schlumberger Educ. Services), SMP-7017.
- Schlumberger, 1994. *Log Interpretation Charts*: Sugarland, TX (Schlumberger Wireline and Testing), SMP-7006.
- Serra, O., 1984. *Fundamentals of Well-Log Interpretation* (Vol. 1): *The Acquisition of Logging Data*: Dev. Pet. Sci., 15A: Amsterdam (Elsevier).
- Serra, O., 1986. *Fundamentals of Well-Log Interpretation* (Vol. 2): *The Interpretation of Logging Data*. Dev. Pet. Sci., 15B: Amsterdam (Elsevier).
- Serra, O., 1989. *Formation MicroScanner Image Interpretation*: Houston (Schlumberger Educ. Services), SMP-7028.
- Stax, R., and Stein, R., 1993. Long-term changes in the accumulation of organic carbon in Neogene sediments, Ontong Java Plateau. *In* Berger, W.H., Kroenke, L.W., Mayer, L.A., et al., *Proc. ODP, Sci. Results*, 130: College Station, TX (Ocean Drilling Program), 573–584. [doi:10.2973/odp.proc.sr.130.039.1993](https://doi.org/10.2973/odp.proc.sr.130.039.1993)

Expedition 320T Preliminary Report

Table T1. Summary, Site U1330. (See table notes.)

Hole	Latitude	Longitude	Water depth (mbrf)	Core type	Number of cores	Depth (m)		Cored interval (m)	Core recovered (m)	Core recovered (%)	Total penetration (m)	Time on hole (days)
						Top	Bottom					
U1330A	3°36.3349'N	156°37.4478'E	2816	W	1	0	103.60	NA	0.07			
						103.6	122.81	19.10	16.09	84.24	553.8*	2.7
U1330B	3°36.3213'N	156°37.4467'E	2814.8	H	10	0	92.20	92.20	87.23	94.61	92.2	4.3

Notes: * = drilled without coring 122.81–553.8 mbsf. W = wash core, R = rotary core barrel core, H = advanced piston corer core.

Table T2. Core summary, Site U1330. (See table note.)

Hole	Core	Top (mbsf)	Length (m)		Recovery (%)	Date (Feb 2009)	Ship time (hr)	Comment
			Cored	Recovered				
U1330A	1W	0	103.6	0.07	0.07	15	0915	
	2R	103.6	9.6	6.48	67.50	15	1105	
	3R	113.2	9.5	9.61	101.16	15	1258	
U1330B	1H	0	6.7	6.7	100.00	19	1005	
	2H	6.7	9.5	9.61	101.16	19	1140	
	3H	16.2	9.5	9.77	102.84	19	1250	
	4H	25.7	9.5	2.27	23.89	19	1420	76% of material lost. Flapper core catcher stuck in open position.
	5H	35.2	9.5	9.78	102.95	19	1545	
	6H	44.7	9.5	9.78	102.95	19	1655	
	7H	54.2	9.5	9.81	103.26	19	1810	
	8H	63.7	9.5	10.01	105.37	19	1910	
	9H	73.2	9.5	9.68	101.89	19	2100	
	10H	82.7	9.5	9.82	103.37	19	2155	

Note: W = wash core, R = rotary core barrel core, H = advanced piston corer core.

Table T3. Measurements and specifications for wireline logging tools. (See table notes.)

Tool string*	Logging speed (m/hr)	Tool	Measurement	Tool length (m)	Sampling interval (cm)	Approximate vertical resolution (cm)	Maximum temperature (°C)
Triple combination	600	HNGS	Spectral gamma ray	2.59	15.24	51	260
		HLDS	Borehole diameter	7.03	15.24	NA	175
		GPIT	Acceleration	1.22	0.25 and 15.24	NA	175
		DIT-E	Resistivity	9.52	15.24	76, 150, 200	175
Formation MicroScanner (FMS)-sonic combination	600	HNGS	Spectral gamma ray	2.59	15.24	51	260
		GPIT	Tool orientation	(in FMS)	0.25 and 15.24	43	175
		FMS	Microresistivity	7.72	0.25	0.5	175
Magnetic Susceptibility Sonde (MSS) combination	300–600	HNGS	Spectral gamma ray	2.59	15.24	51	260
		HLDS	Borehole diameter	7.03	Continuous	NA	175
		GPIT	Acceleration	1.22	0.25 and 15.24	NA	175
		MSS	Magnetic susceptibility	5.88	0.25	10, 40	+50

Notes: * = all tool and tool string names are trademarks of Schlumberger. For additional information about tool physics and use, consult IODP-USIO Science Services, LDEO, at iodp.ldeo.columbia.edu/TOOLS_LABS/tools.html. NA = not applicable.

Table T4. Acronyms and units used for wireline logging tools. (See table notes.)

Tool*	Output	Tool name/Explanation of output	Unit
DIT-E		Dual Induction Tool	
	IDPH	Deep induction resistivity	Ω -m
	IMPH	Medium induction resistivity	Ω -m
	SFLU	Spherically focused resistivity	Ω -m
FMS		Formation MicroScanner	
	C1, C2	Orthogonal hole diameter	Inch
	P1AZ	Pad 1 azimuth Spatially oriented resistivity images of borehole wall	Degree
GPIT		General Purpose Inclinometer Tool	
	DEVI	Hole deviation	Degree
	HAZI	Hole azimuth	Degree
	F_x, F_y, F_z	Earth's magnetic field (three orthogonal components)	Oersted
	A_x, A_y, A_z	Acceleration (three orthogonal components)	m/s ²
HLDS		Hostile Environment Litho-Density Sonde	
	LCAL	Caliper (measure of borehole diameter)	Inch
HNGS		Hostile Environment Gamma Ray Sonde	
	HSGR	Standard (total) gamma ray	gAPI
	HCGR	Computed gamma ray (HSGR minus uranium contribution)	gAPI
	HFK	Potassium (K)	wt%
	HTHO	Thorium (Th)	ppm
	HURA	Uranium (U)	ppm
MSS		Magnetic Susceptibility Sonde	
	HSUS	High-resolution sensor susceptibility	SI
	LSUS	Low-resolution sensor susceptibility	SI
	LCON	Low-resolution sensor conductivity (under development)	S/m
	TEMP	Temperature of MSS electronics	$^{\circ}$ C
	ZACC	Tool acceleration	m/s/s

Notes: * = All tool and tool string names (except the MSS) are trademarks of Schlumberger. For the complete list of acronyms used in the IODP and for additional information about tool physics and use consult the IODP Tools and Laboratories section at www.iodp-usio.org/default.html.

Table T5. Compositional percentages estimated from smear slides. (See table note.)

Core, section, interval (cm)	Foraminifers	Nannofossils	Diatoms	Radiolarians	Siliceous sponge	Silico-flagellates/Ebridians	Fish remains	Other bioclasts (organic matter)	Pyrite	Lithology		
										Type	Name	Color
320T-U1330A-1W-CC, 4	14	85		1	tr	tr				Major	Nannofossil ooze with foraminifers	White
2R-1, 19	12	85		2	1					Major	Nannofossil ooze with foraminifers	White
2R-1, 37	12	85		2	1					Minor	Nannofossil ooze with foraminifers	Yellow band
2R-1, 46	10	90		tr	tr					Minor	Nannofossil ooze with foraminifers	Green band
2R-1, 90	10	70	tr	tr	tr	tr			20	Minor	Nannofossil ooze with foraminifers and disseminated pyrite	Black
3R-2, 112	20	72		3	2	2		1		Minor	Nannofossil ooze with foraminifers	Yellow mottle
3R-2, 114	20	80		tr	tr	tr				Minor	Nannofossil ooze with foraminifers	Green band
3R-2, 115	20	79		tr		tr				Minor	Nannofossil ooze with foraminifers	Purple band
3R-2, 120	35	59		2		2	tr	tr	2	Minor	Foraminifer nannofossil ooze	Black spot
3R-2, 125	15	82		1	1	1				Major	Nannofossil ooze with foraminifers	White
3R-4, 135	20	78		tr	tr	1	tr			Major	Nannofossil ooze with foraminifers	White
3R-6, 22	25	82		2	1	tr			*	Minor	Foraminifer nannofossil ooze Dark pigmentation = submicroscopic sulfides?	Black spot
320T-U1330B-1H-2, 63	18	80	tr	1	tr	tr		1	tr	Minor	Nannofossil ooze with foraminifers	Dark layer
1H-2, 85	25	75	tr	tr	tr	tr		tr		Major	Nannofossil ooze with foraminifers	Tan
1H-4, 50	29	70	tr	1	tr	tr		tr		Major	Nannofossil ooze with foraminifers	Tan
2H-6, 52	10	89				1				Major	Nannofossil ooze with foraminifers	White/Gray
3H-5, 70	40	59		1					tr	Major	Nannofossil ooze with foraminifers	White/Gray
4H-2, 37	35	65							tr	Major	Foraminifer nannofossil ooze	White/Gray
5H-1, 141	20	73	1	2	1	1	1	1		Minor	Nannofossil ooze with foraminifers	Brownish yellow mottle
5H-2, 82	15	83		2	tr	tr				Major	Nannofossil ooze with foraminifers	White
6H-4, 108	20	75		2	2	1				Major	Nannofossil ooze with foraminifers	White
7H-4, 100	20	80		tr	tr	tr				Major	Nannofossil ooze with foraminifers	White/Gray
7H-5, 109	19	80							1	Minor	Nannofossil ooze with foraminifers	Green band
7H-5, 111	25	75							tr	Minor	Nannofossil ooze with foraminifers	Blue band
7H-7, 76	20	80				1	tr	tr	tr	Minor	Nannofossil ooze with foraminifers	Yellow-brown mottle
8H-5, 10	15	85								Major	Nannofossil ooze with foraminifers	White/Gray
9H-4, 72	20	75	1	2	tr	2	tr			Major	Nannofossil ooze with foraminifers	White/Gray

Note: tr = trace.

Expedition 320T Preliminary Report

Table T6. Key planktonic foraminifer datums, Hole U1330B. (See table notes.)

Datum	Zone (base)	Core, section	Depth (m)			Age (Ma)
			Present	Absent	Interpolated	
320T-U1330B-						
LO <i>Globigerinoides fistulosus</i>	Pt1	4H-CC	27.97	25.96	26.8	1.88
FO <i>Globorotalia truncatulinoides</i>	N22	4H-CC	27.97	44.86	36.3	2.03
LO <i>Dentoglobigerina altispira</i>	P15	7H-CC	63.86	54.45	59.1	3.02
FO <i>Globorotalia tosaensis</i>	N21	6H-CC	54.45	63.86	59.1	3.35
LO <i>Globorotalia margaritae</i>	P13	7H-CC	63.86	54.45	59.1	3.85
LO <i>Sphaeroidinellopsis seminulina</i>	P14	8H-CC	73.39	63.86	68.5	3.18
LO <i>Globoturborotalita nepenthes</i>	P12	10H-CC	92.20	82.70	87.3	4.37

Notes: Datums used in age-depth plot (Fig. F8). Base of Zone N18–N19 and base of P11 not reached in this hole. All samples are from working half. FO = first occurrence, LO = last occurrence.

Table T7. Alaklinity and pH data of interstitial water samples, Site U1330.

Text ID	Core, section	Depth (m)	Alkalinity (mM)	pH
320T-U1330A-				
LIQ469881	2R-2	106.5	4.37	7.29
LIQ470241	2R-4	109.1	Analysis failed	
LIQ470231	3R-2	116.1	4.22	7.89
LIQ470281	3R-5	120.6	4.10	7.53
320T-U1330B-				
LIQ474131	1H-2	2.9	Analysis failed	
LIQ474071	2H-2	9.6	3.07	7.40
LIQ474431	3H-2	19.0	3.29	7.44
LIQ474601	4H-1	26.6	3.43	7.39
LIQ474931	5H-2	38.0	3.70	7.34
LIQ475251	6H-2	47.5	3.85	7.35
LIQ476051	7H-2	57.0	3.97	7.37
LIQ476371	8H-2	66.5	4.16	7.28
LIQ476691	9H-2	76.0	4.13	7.35
LIQ477041	10H-2	85.5	4.34	7.23

Table T8. Elemental concentrations in interstitial water samples, Site U1330.

Text ID	Core, section	Depth (m)	Major elements (mM)			
			Na	K	Mg	Ca
320T-U1330A-						
LIQ469881-1	2R-2	106.5	471	9.78	44.47	11.1
LIQ469891-1	2R-4	109.0	463	9.57	40.79	10.5
LIQ470221-1	3R-2	116.1	457	9.83	42.70	11.2
LIQ470271-1	3R-5	122.0	460	9.69	43.17	10.8
320T-U1330B-						
LIQ474121-1	1H-2	2.9	472	9.77	48.24	9.42
LIQ474081-1	2H-2	9.6	466	9.71	46.59	9.54
LIQ474421-1	3H-2	19.0	477	9.95	48.43	9.63
LIQ474611-1	4H-1	26.6	458	10.1	44.76	9.80
LIQ474921-1	5H-2	38.0	473	9.81	46.51	9.76
LIQ475241-1	6H-2	47.5	460	9.98	45.45	9.97
LIQ475711-1	7H-2	57.0	450	9.69	43.70	10.1
LIQ476361-1	8H-2	66.5	439	9.56	42.62	10.0
LIQ476681-1	9H-2	76.0	478	10.1	45.02	10.2
LIQ477031-1	10H-2	85.5	451	9.76	43.63	10.7

Table T9. Elemental concentrations in whole rock samples, Hole U1330A. (See table notes.)

Core, section, interval (cm)	Color band	Major element oxide (wt%)										Trace element (ppm)								
		SiO ₂	TiO ₂	Al ₂ O ₃	Fe ₂ O ₃	MnO	MgO	CaO	Na ₂ O	K ₂ O	P ₂ O ₅	Ni	Cr	Sc	Cu	Zn	Sr	Zr	Y	Ba
320T-U1330A-																				
3R-2, 115-116	Yellow	5.25	BD	0.48	0.60	BD	0.58	21.13	0.98	0.12	0.12	85.05	15.42	0.35	6.5	108.0	1462.0	28.3	9.27	714.2
3R-2, 125-126	Green	4.36	BD	0.38	0.45	BD	0.38	22.06	0.57	0.07	0.12	84.03	6.25	0.58	23.1	95.1	1343.9	21.6	11.64	732.9
3R-2, 117-118	Purple	4.30	BD	0.35	0.16	BD	0.42	21.48	0.72	0.08	0.13	115.74	7.83	0.89	54.5	89.9	1436.5	26.7	10.23	754.6
3R-2, 121-122	Black	4.31	0.01	0.32	BD	BD	BD	24.44	0.47	0.07	0.05	6.16	1.78	1.26	18.4	119.0	1319.2	23.0	10.13	710.9
3R-2, 113-114	White	5.27	0.01	0.36	BD	BD	BD	24.28	0.87	0.09	0.05	5.83	6.66	0.92	20.1	114.5	1550.6	26.7	13.81	874.2
3R-2, 42-43	White	4.14	0.01	0.31	BD	BD	BD	23.71	0.66	0.07	0.04	6.14	BD	2.24	16.6	115.4	1442.7	26.5	16.48	705.1

Notes: All samples are from working half. BD = below detection.

Expedition 320T Preliminary Report

Table T10. Methane concentrations in headspace gas samples, Site U1330.

Text ID	Core, section	Depth (m)	Methane (ppmv)
320T-U1330A-			
CYL469841	2R-2	106.6	10.11
CYL469851	2R-4	109.1	13.88
CYL470161	3R-2	116.2	12.26
CYL470151	3R-5	120.7	6.63
320T-U1330B-			
CYL473781	1H-2	3.0	1.61
CYL474031	2H-2	9.7	1.88
CYL474441	3H-2	19.1	1.82
CYL474561	4H-1	26.7	2.54
CYL474881	5H-2	38.1	3.74
CYL475201	6H-2	47.6	4.30
CYL475551	7H-2	57.1	2.17
CYL476321	8H-2	66.5	1.84
CYL476641	9H-2	76.1	1.97
CYL476991	10H-2	85.6	2.28

Table T11. Magnetic survey of the shielded room. (See table notes.)

Room coordinates (m)		Near ceiling (-2 m above the floor; mG)				Middle (1.0 m above the floor; mG)				Near the floor (mG)			
x-distance	y-distance	x	y	z	Total	x	y	z	Total	x	y	z	Total
0	0	264.00	-585.00	143.00	657.55	-362.00	-235.00	154.00	458.24	-364.00	-134.00	203.00	437.79
1	0	-545.00	11.00	68.00	549.34	-428.00	-138.00	121.00	465.69	-354.00	-82.00	100.00	376.88
2	0	-333.00	-180.00	141.00	403.94	-282.00	-144.00	200.00	374.51	-287.00	-60.00	-44.00	296.49
3	0	-357.00	-170.00	540.00	669.29	-324.00	-152.00	152.00	388.82	-121.00	-205.00	-54.00	244.09
4	0	-302.00	-38.00	185.00	356.19	-320.00	-90.00	124.00	354.79	-245.00	-160.00	-422.00	513.53
5	0	-545.00	214.00	400.00	709.10	-352.00	-60.00	109.00	373.34	-450.00	-200.00	-258.00	555.94
6	0	-409.00	-133.00	30.00	431.13	-364.00	-197.00	59.00	418.07	-81.00	-336.00	743.00	819.45
7	0	-270.00	-120.00	-380.00	481.35	-354.00	-164.00	71.00	396.55	-375.00	-222.00	-310.00	534.80
8	0	-188.00	176.00	292.00	389.34	-348.00	-98.00	25.00	362.40	-537.00	-266.00	220.00	638.38
0	1	-320.00	-232.00	447.00	596.69	-504.00	855.00	-124.00	1000.21	-277.00	-166.00	430.00	537.76
1	1	-90.00	-7.00	133.00	160.74	-34.00	-850.00	155.00	864.69	-458.50	-1.50	170.00	489.00
2	1	-390.00	-220.00	262.00	518.79	-350.00	-220.00	170.00	446.99	-640.00	163.00	-90.00	666.54
3	1	-262.00	-145.00	47.00	303.11	-286.00	-162.00	163.00	366.89	-472.00	-122.00	38.00	488.99
4	1	-380.00	-360.00	58.00	526.65	-437.00	-8.00	14.00	437.30	-506.00	-181.00	35.00	538.54
5	1	-400.00	-405.00	-80.00	574.83	-432.00	-50.00	65.00	439.71	-540.00	-240.00	32.00	591.80
6	1	-203.00	24.00	20.00	205.39	-285.00	45.00	37.00	290.89	-349.00	-417.00	-8.00	543.83
7	1	-288.00	-169.00	237.00	409.48	-302.00	-115.00	73.00	331.30	-681.00	-511.00	152.00	864.86
8	1	-485.00	-439.00	143.00	669.62	-324.00	-110.00	-5.00	342.20	-180.00	52.00	268.00	327.00
0	2	-214.00	-342.00	-157.00	432.91	-836.00	-287.00	359.00	954.02	-551.00	-62.00	96.00	562.73
1	2	-561.00	-278.00	299.00	693.83	-293.00	-880.00	309.00	977.61	-204.00	-463.00	-301.00	588.72
2	2	-334.00	-232.00	161.00	437.38	-201.00	-399.00	310.00	543.78	-252.00	-185.00	21.00	313.32
3	2	-280.00	-319.00	4.00	424.47	-160.00	-342.00	283.00	471.86	-451.00	-98.00	35.00	462.85
4	2	-304.00	-164.00	-240.00	420.61	-137.00	95.00	-23.00	168.29	-201.00	-245.00	445.00	546.31
5	2	-312.00	-107.00	79.00	339.17	-870.00	361.00	-260.00	977.15	-288.00	-260.00	854.00	938.01
6	2	-613.00	-204.00	98.00	653.44	-390.00	-50.00	21.00	393.75	-350.00	-55.00	404.00	537.35
7	2	-402.00	-190.00	-145.00	467.68	-341.00	-96.00	46.00	357.23	-391.00	152.00	844.00	942.51
8	2	-504.00	-130.00	-51.00	522.99	-386.00	-233.00	-30.00	451.87	-99.00	845.00	-883.00	1226.18
0	3	-350.00	-300.00	-240.00	519.71	-1000.00	40.00	-30.00	1001.25	-887.00	190.00	-160.00	921.12
1	3	-410.00	-90.00	330.00	533.95	-370.00	171.00	35.00	409.10	-804.00	-261.00	102.00	851.43
2	3	-233.00	-213.00	88.00	327.72	-224.00	90.00	70.00	251.35	-415.00	-381.00	-61.00	566.66
3	3	256.00	-220.00	20.00	338.14	-149.00	-6.00	40.00	154.39	274.00	189.00	-25.00	333.80
4	3	-170.00	-644.00	1090.00	1277.39	-183.00	-220.00	-13.00	286.46	-475.00	796.00	184.00	945.04
5	3	-495.00	-161.00	-25.00	521.12	-460.00	-303.00	11.00	550.94	-399.00	669.00	-73.00	782.36
6	3	-366.00	-122.00	-141.00	410.76	-364.00	-80.00	-14.00	372.95	-118.00	461.00	90.00	484.30
7	3	-183.00	-208.00	-11.00	277.26	-293.00	2.00	-95.00	308.02	-220.00	144.00	559.00	617.75
8	3	-1090.00	55.00	85.00	1094.69	-433.00	-129.00	36.00	453.24	-581.00	-245.00	-1.00	630.55

Notes: Survey conducted while at Site U1330. Room coordinate 0,0 = the front (bow) and port corner of the lab. Elevator is at x = 9.8 m and between y = 0 to 3. y = 0 line is along the passageway on the port side of the magnetometer. y = 4 line is along the passageway between the magnetometer and the core description station. Ceiling height = 2 m. 1 G = 1 Oe = 0.1 mT = 100 μT = 100,000 nT. 0.5 G = 500 mG = 0.05 mT = 50 μT = 50,000 nT. Highlighted text = interpolated data.

Table T12. Magnetic survey of the shield oven.

Distance (cm)	x (up) (mG)	y (starboard) (mG)	z (into magnetometer) (mG)	Total (mG)	Comment
0.0	138.00	-6.00	-4.00	138.19	Mouth of oven
5.0	110	10.00	-3	110.49	Heating chamber
10.0	48.00	4.00	-0.80	48.17	Heating chamber
15.0	17.90	1.10	-0.70	17.95	Heating chamber
20.0	6.40	0.70	-0.80	6.49	Heating chamber
25.0	2.20	0.20	-0.40	2.24	Heating chamber
30.0	1.30	0.13	-0.18	1.32	Heating chamber
35.0	1.29	0.14	-0.20	1.31	Heating chamber
40.0	1.82	0.33	-0.72	1.98	Heating chamber
45.0	3.05	0.77	-2.41	3.96	Heating chamber
50.0	4.68	2.22	-5.87	7.83	Heating chamber
55.0	4.51	2.68	-4.23	6.74	Heating chamber
60.0	7.80	1.24	-0.66	7.93	End of the heating chamber
65.0	3.15	0.02	-0.13	3.15	Cooling chamber
70.0	0.51	0.03	-0.09	0.52	Cooling chamber
75.0	0.13	0.05	-0.08	0.16	Cooling chamber
80.0	0.16	0.04	-0.06	0.18	Cooling chamber
85.0	0.18	0.02	-0.07	0.19	Cooling chamber
90.0	0.20	0.01	-0.07	0.21	Cooling chamber
95.0	0.23	0.00	-0.07	0.24	Cooling chamber
100.0	0.26	-0.01	0.07	0.27	Cooling chamber
105.0	0.47	-0.20	0.07	0.52	Cooling chamber
110.0	4.29	0.14	2.48	4.96	Cooling chamber
115.0	56.10	2.00	18.20	59.01	Cooling chamber (but beyond where samples holder resides during cooling)
120.0	198.00	7.00	37.00	201.55	Cooling chamber (but beyond where samples holder resides during cooling)
125.0	393.00	20.00	91.00	403.89	Cooling chamber (but beyond where samples holder resides during cooling)
130.0	764.00	50.00	231.00	799.72	Cooling chamber (but beyond where samples holder resides during cooling)
134.0	884.00	58.00	317.00	940.91	End of cooling chamber

Expedition 320T Preliminary Report

Table T13. Magnetic survey of the superconducting rock magnetometer (SRM). (See table notes.)

Distance (cm)	x (long axis) (mG)	y (port side) (mG)	z (up) (mG)	Total (mG)	Total (nT)	Total (μT)	Comment
0.0	-17.00	33.00	327.00	329.10	32,910.0	32.91	At the home switch
10.5	-11	38	355	357.20	35,719.7	35.72	
21.0	2	22	375	375.65	37,565.0	37.57	
31.5	4	23	405	405.67	40,567.2	40.57	
42.0	-3	19	437	437.42	43,742.3	43.74	
52.5	0	10	493	493.10	49,310.1	49.31	
63.0	-4	9	557	557.09	55,708.7	55.71	
73.5	-28	-5	653	653.62	65,361.9	65.36	
84.0	-87	-20	790	795.03	79,502.8	79.50	
94.5	-213	-77	979	1,004.86	100,485.8	100.49	
105.0	-744	-163	1,253	1,466.33	146,632.7	146.63	
115.5	-1,357	20	1,116	1,757.07	175,707.3	175.71	
126.0	-1,054	143	624	1,233.18	123,318.3	123.32	
136.5	-580	159	550	814.97	81,497.3	81.50	
147.0	-108	35	569	580.22	58,021.5	58.02	
157.0	3.8	1	51.5	51.65	5,165.0	5.16	In the magnetometer
167.0	-3.2	-2	2.2	4.37	436.8	0.44	
177.0	-4	-2.4	1.2	4.82	481.7	0.48	
187.0	-5.2	-2.3	-1.9	5.99	599.5	0.60	
197.0	-3.7	-1.4	-1.2	4.13	413.4	0.41	
207.0	-2.5	-0.9	-1	2.84	283.9	0.28	
217.0	-1.7	-0.5	-0.9	1.99	198.7	0.20	
227.0	-1	-0.3	-0.7	1.26	125.7	0.13	
237.0	-0.54	-0.1	-0.36	0.66	65.7	0.07	
247.0	-0.23	-0.05	-0.08	0.25	24.9	0.02	
257.0	-0.018	0.03	-0.063	0.07	7.2	0.01	At sensor
267.0	0.092	0.017	-0.153	0.18	17.9	0.02	
277.0	0.091	-0.001	-0.397	0.41	40.7	0.04	
287.0	0.02	0.005	-0.795	0.80	79.5	0.08	
296.0	-0.067	0.001	-1.213	1.21	121.5	0.12	
305.0	-0.093	-0.054	-1.78	1.78	178.3	0.18	
314.0	-0.07	-0.15	-2.43	2.44	243.6	0.24	
323.0	0.06	-0.19	-3.15	3.16	315.6	0.32	
332.0	0.32	-0.23	-3.52	3.54	354.2	0.35	
341.0	1.9	-0.3	4.8	5.17	517.1	0.52	
350.0	13.4	-1.1	47.3	49.17	4,917.4	4.92	
360.0	-19.3	-5	138.4	139.83	13,982.9	13.98	Shield break
369.0	-2.9	-0.7	29.5	29.65	2,965.0	2.97	
378.0	-0.5	-0.2	5.6	5.63	562.6	0.56	
387.0	-0.1	-0.1	1.9	1.91	190.5	0.19	
396.0	0.08	-0.06	1.53	1.53	153.3	0.15	
405.0	0.28	-0.07	2.63	2.65	264.6	0.26	
414.0	0.2	-0.2	2.5	2.52	251.6	0.25	
423.0	1.1	-0.3	7.6	7.69	768.5	0.77	
432.0	3	-1.3	32.5	32.66	3,266.4	3.27	Shield break
442.0	0.9	3.8	14.6	15.11	1,511.3	1.51	
451.0	0.7	0.5	6.4	6.46	645.8	0.65	
460.0	-0.1	0.3	4	4.01	401.2	0.40	
469.0	-0.01	0.3	3.8	3.81	381.2	0.38	
478.0	-0.4	0.1	3.6	3.62	362.4	0.36	
487.0	-0.1	0.1	3.6	3.60	360.3	0.36	
496.0	0	-0.2	3.8	3.81	380.5	0.38	
505.0	-0.1	-0.1	3	3.00	300.3	0.30	~1 m from end

Notes: Measured in transit after magnetometer was reconfigured. Date = 24 February 2009, location = Pacific Ocean (~300 km northeast of the Marshall Islands), latitude = 8.55, longitude = 175.167, heading = N61°E. Coordinate system used is same as SRM (Table T10).

Table T14. Magnetic survey of the superconducting rock magnetometer (SRM) in Guam, 8 February 2009. (See table note.)

Distance (cm)	Field (nT)	Comment
179.0	776.9	
189.0	538.7	
199.0	358.1	
209.0	239.8	
219.0	163.2	
229.0	100.1	
239.0	51.6	
249.0	16.4	
257.0	1.4	At sensor
268.0	22.0	
278.0	50.3	
288.0	93.3	
298.0	139.6	
308.0	196.6	
318.0	269.3	
328.0	339.1	
336.0	421.1	
345.0	967.7	
352.0	5050.6	Shield break
370.0	2461.9	Shield break
381.0	450.4	
388.0	237.8	
408.0	228.0	
416.0	474.5	
426.0	1040.0	
431.0	2143.6	Shield break
441.0	1499.3	
451.0	603.1	
461.0	405.5	
471.0	358.1	
481.0	353.2	
491.0	339.7	
501.0	311.5	
511.0	265.5	
521.0	221.2	
531.0	196.5	

Note: Measured with ship oriented ~N85°E.

Figure F1. Map of the ~6400 nmi voyage of Expedition 320T (Sea Trials and Assessment Readiness Transit) from Singapore to Guam to Honolulu.

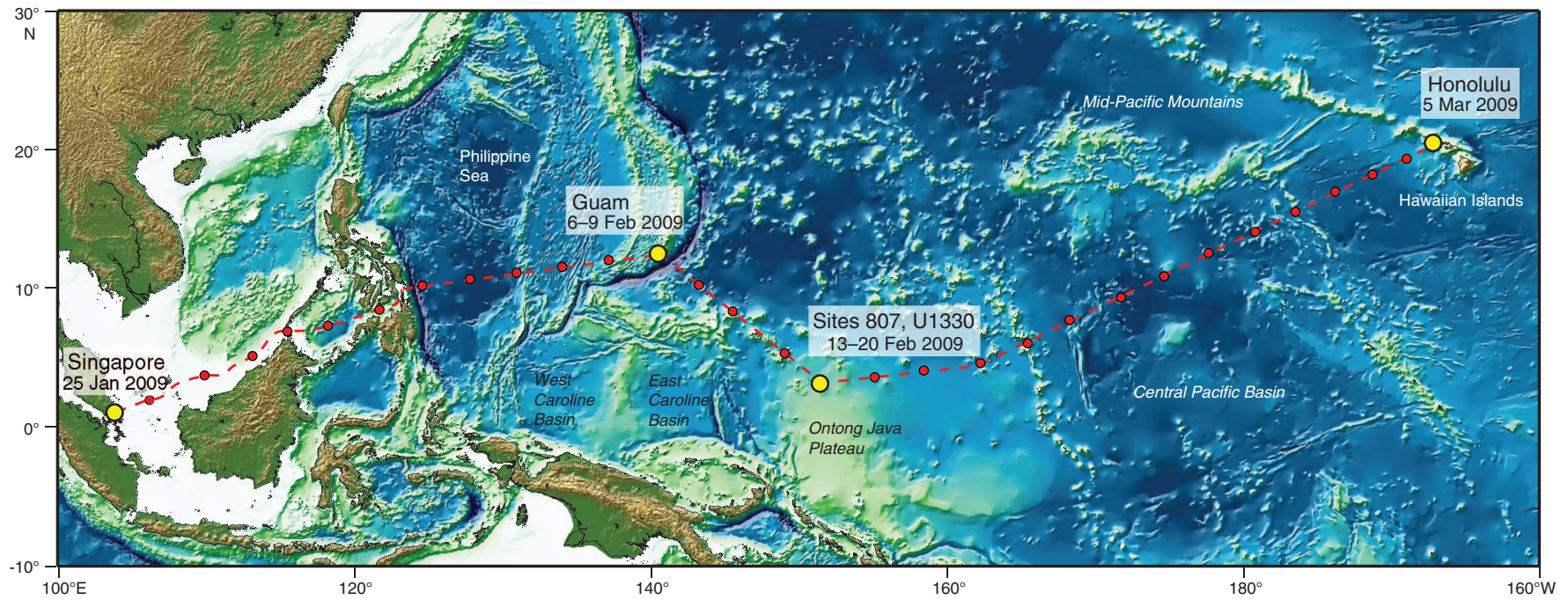


Figure F2. Location map of ODP Leg 130 sites and IODP Site U1330 on the Ontong Java Plateau, southwest Pacific Ocean.

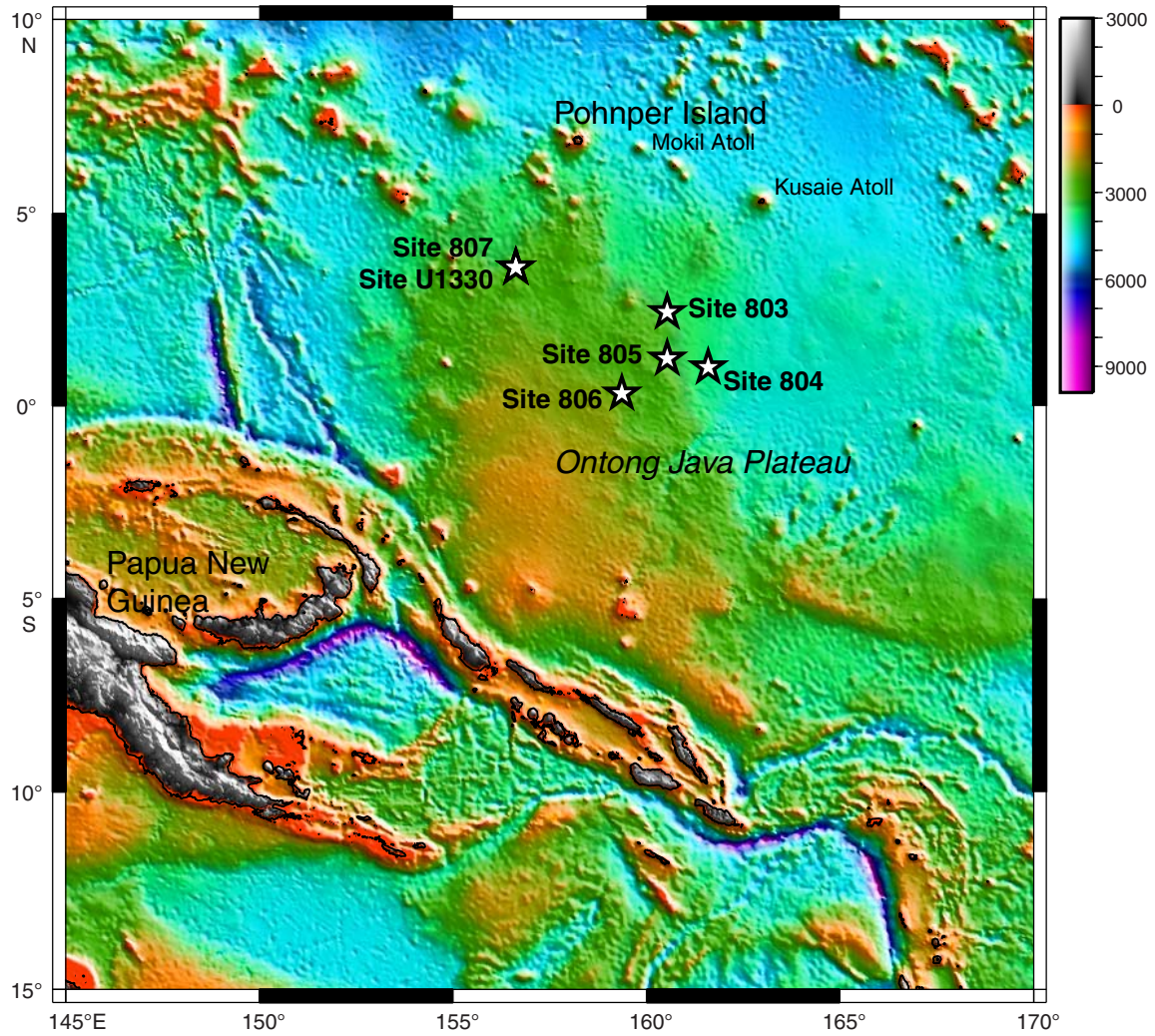


Figure F3. Screen capture of the Expedition 320T core description template.

The screenshot displays the 'Tabular DeskLogik' application window. At the top, there is a toolbar with icons for 'New', 'Save', 'Save as', 'Open', 'Save', 'Select Sample', 'Columns Hide/Unhide', 'Columns Dynamic', 'Export Excel', 'Upload', 'Download', and 'Lims Transfer'. A 'Filter Downloaded Results by:' dropdown is set to 'Template', and a 'Clear Sheet' button is visible.

Below the toolbar is the 'Current Sample' section, which contains input fields for 'Sample 1', 'Top Offset' (in cm), 'Sample 2', and 'Bottom Offset' (in cm). To the right of these fields is a 'Sample Image' area.

The main data table is titled 'Lithology02' and has several tabs: 'Contacts & Strata', 'Bioturbation & Fossils', 'Diagenetic Features', 'Drilling Disturbance', 'Stratigraphic Unit', and 'Summary Description'. The table has the following columns: 'Sample 1', 'Top', 'Sample 2', 'Bottom', 'Top Depth', 'Bottom Depth', 'LITHOLOGY (Principal Name)', 'LITHOLOGY Classification', 'LITHOLOGY (PREFIX)', 'LITHOLOGY (SUFFIX)', and 'LITHOLOGY MAX'. The rows are numbered 1 through 10.

At the bottom of the window, the status bar shows 'Username: geldmacher', 'Template: 320T Core Description Template', 'Workspace: none', and a 'Save On Sample Type' dropdown menu.

Figure F4. Screen capture of the Expedition 320T smear slide description template.

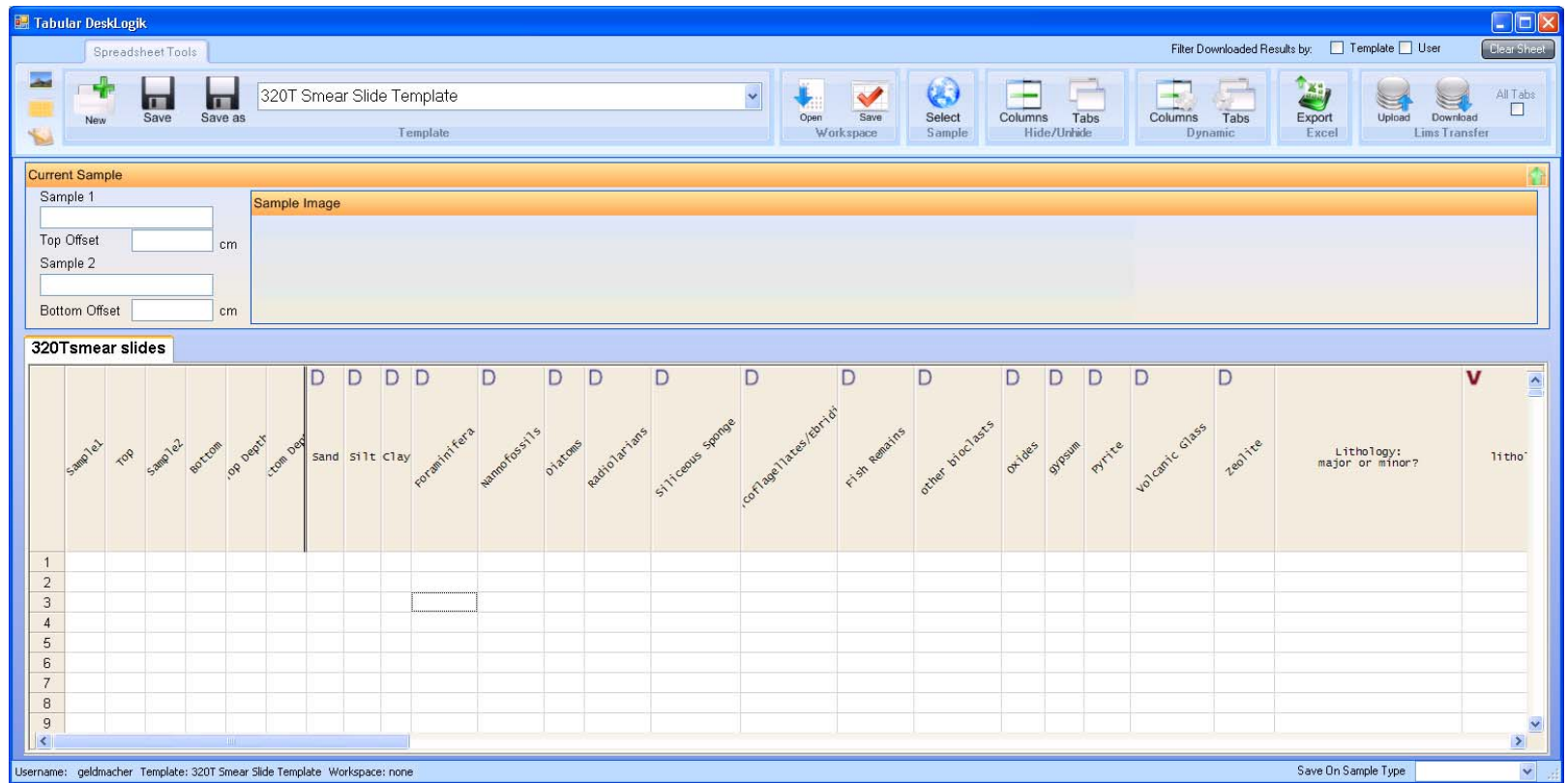


Figure F5. Legend for core description as depicted in core summary (barrel) sheets.



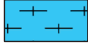












Lithology:		Drilling disturbance	
	Nannofossil ooze with foraminifers		Biscuit
	Foraminifer nannofossil ooze		Slight
Sedimentary structure			Moderate
	Color banding		Mousseliike
	Alteration halo		Very disturbed
	Disseminated fine black minerals		Soupy
	Mottling		Fractured
Bioturbation		Shipboard analysis	
	Moderate	SS	Smear slide
	Slight		

Figure F6. Schematic of wireline tool string configurations. See Tables T3 and T4 for tool specifications and measurements. FMS = Formation MicroScanner, ELIC = enhanced fast transfer bus (LDEO interface cartridge), MSS = Magnetic Susceptibility Sonde.

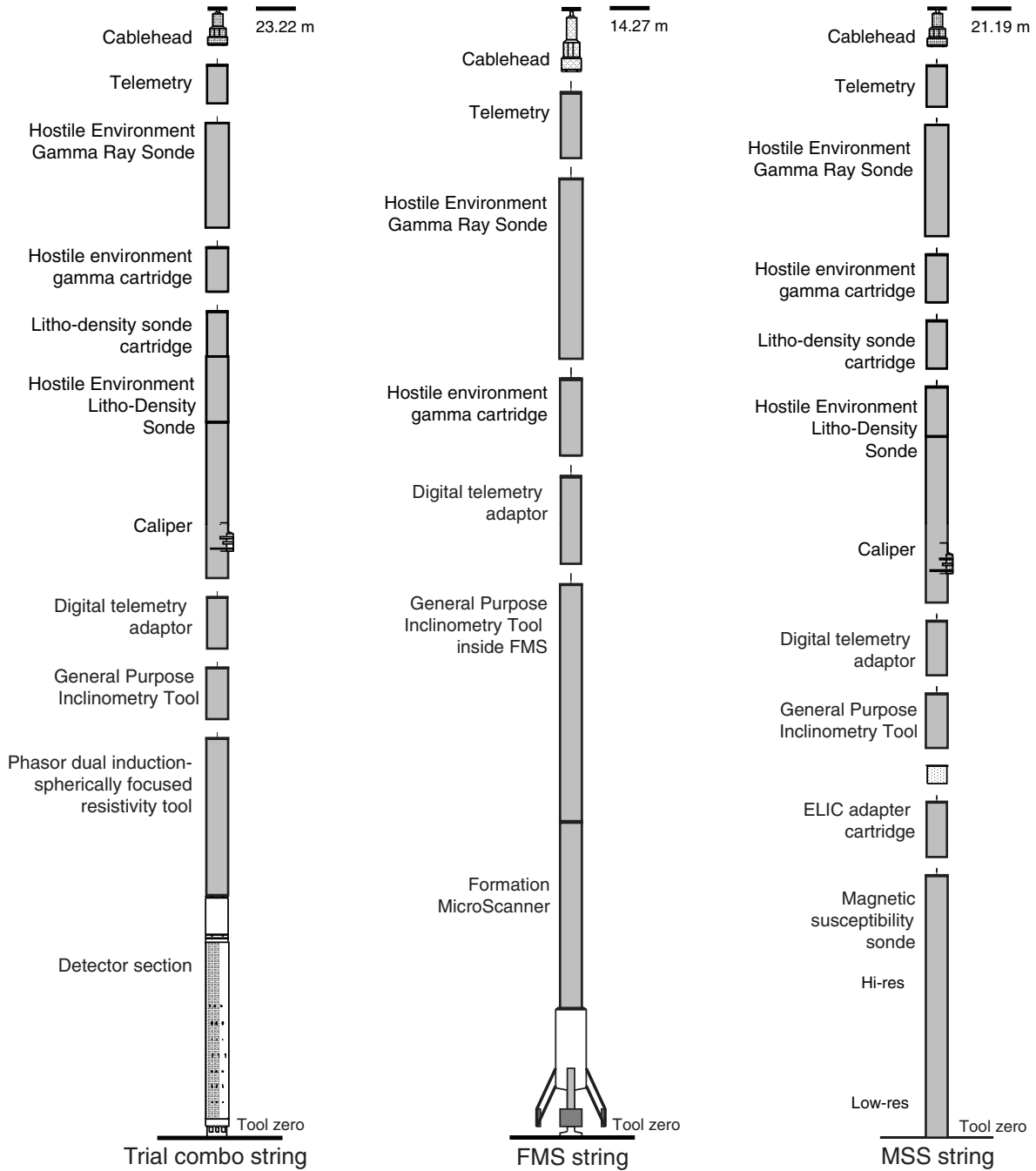


Figure F7. Summary stratigraphy, Site U1330. A = Hole U1330A, B = Hole U1330B.

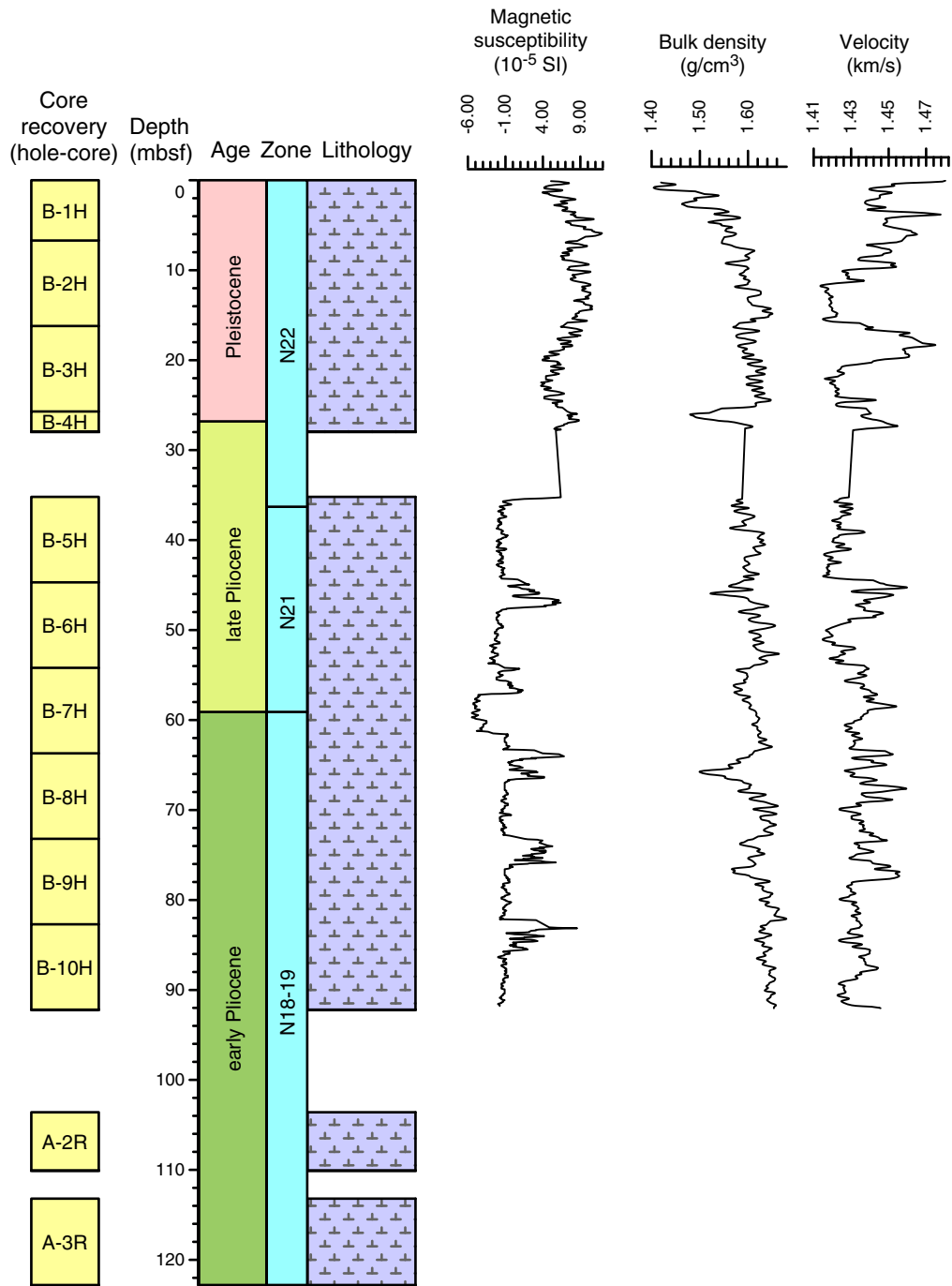


Figure F8. Age-depth plot and relative sedimentation rate estimates through the Pliocene–Pleistocene interval, Hole U1330B. Key planktonic foraminifer datums are labeled. FO = first occurrence, LO = last occurrence.

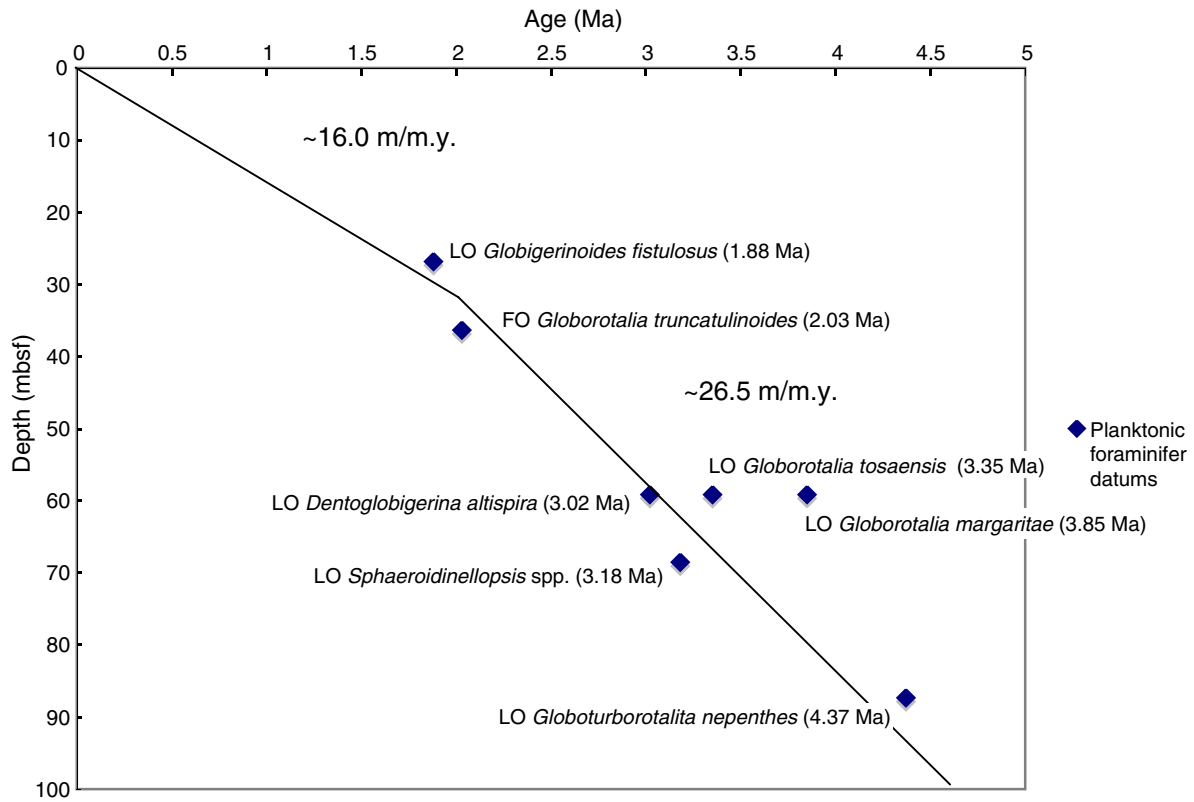


Figure F9. Plots of interstitial water alkalinity and pH, Holes U1330A and U1330B.

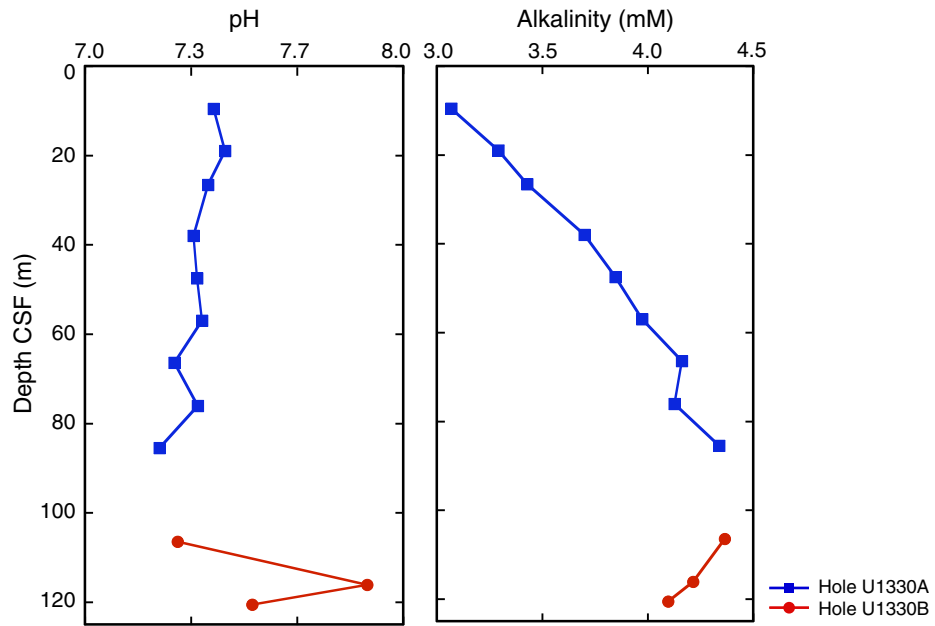


Figure F10. Plots of interstitial water major element concentrations, Holes U1330A and U1330B.

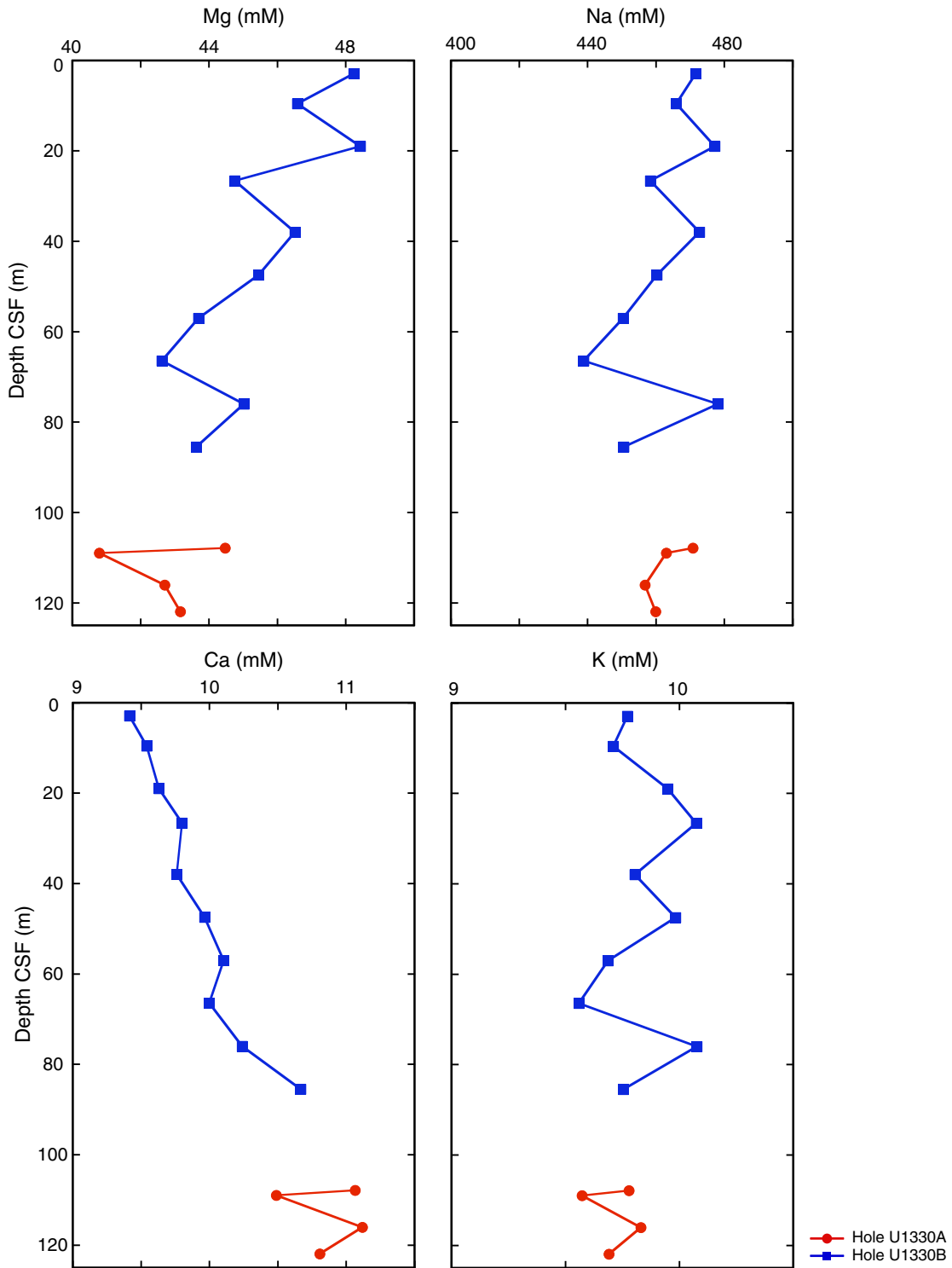


Figure F11. Close-up image of color banding in Section 320T-U1330A-3R-2. ICP-AES = inductively coupled plasma-atomic emission spectroscopy.

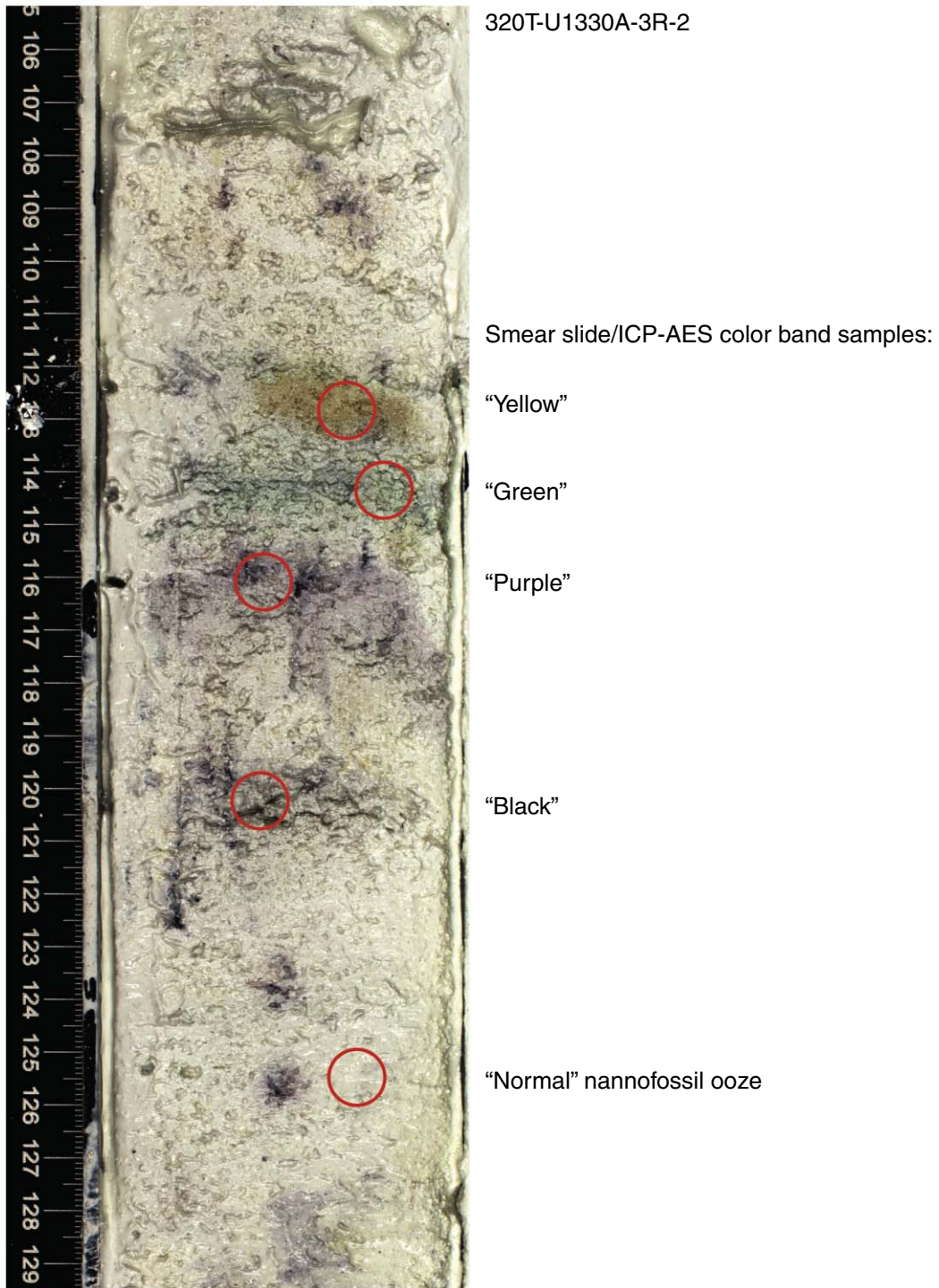


Figure F12. Methane concentration plots from headspace gas analysis, Holes U1330A and U1330B.

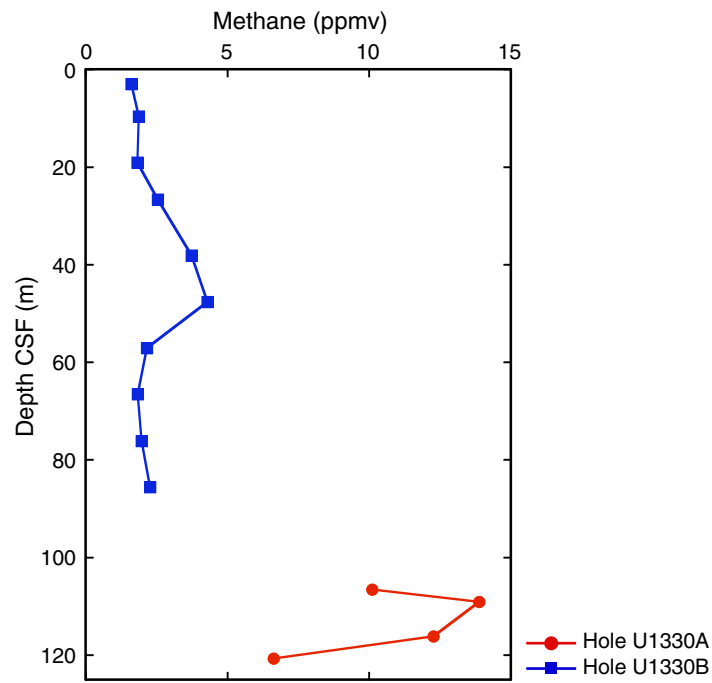


Figure F13. Bulk density and compressional wave velocity profiles, Hole U1330B. WRMSL = whole round multisensor logger.

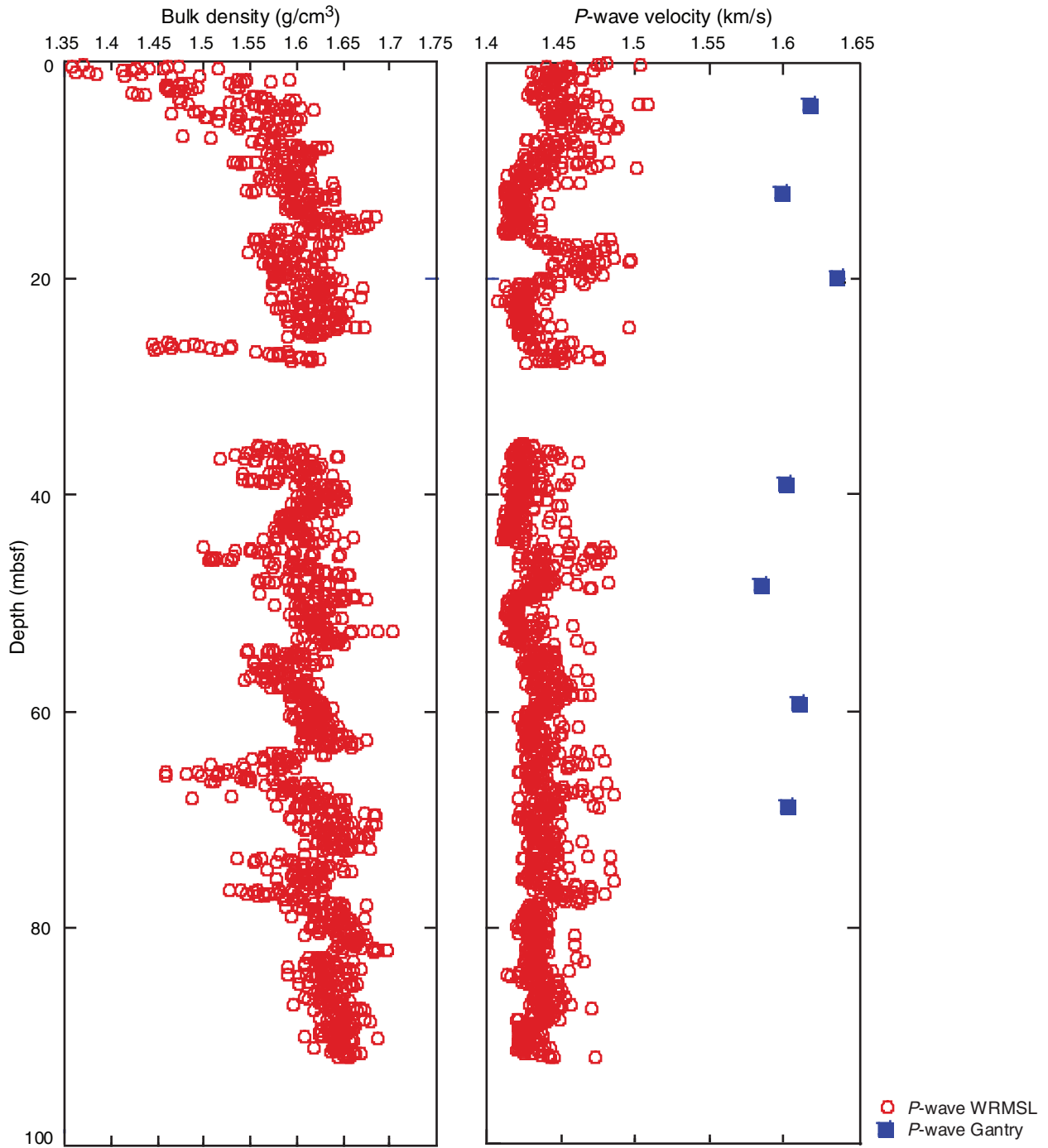


Figure F14. Bulk density, grain density, and porosity profiles, Hole U1330B.

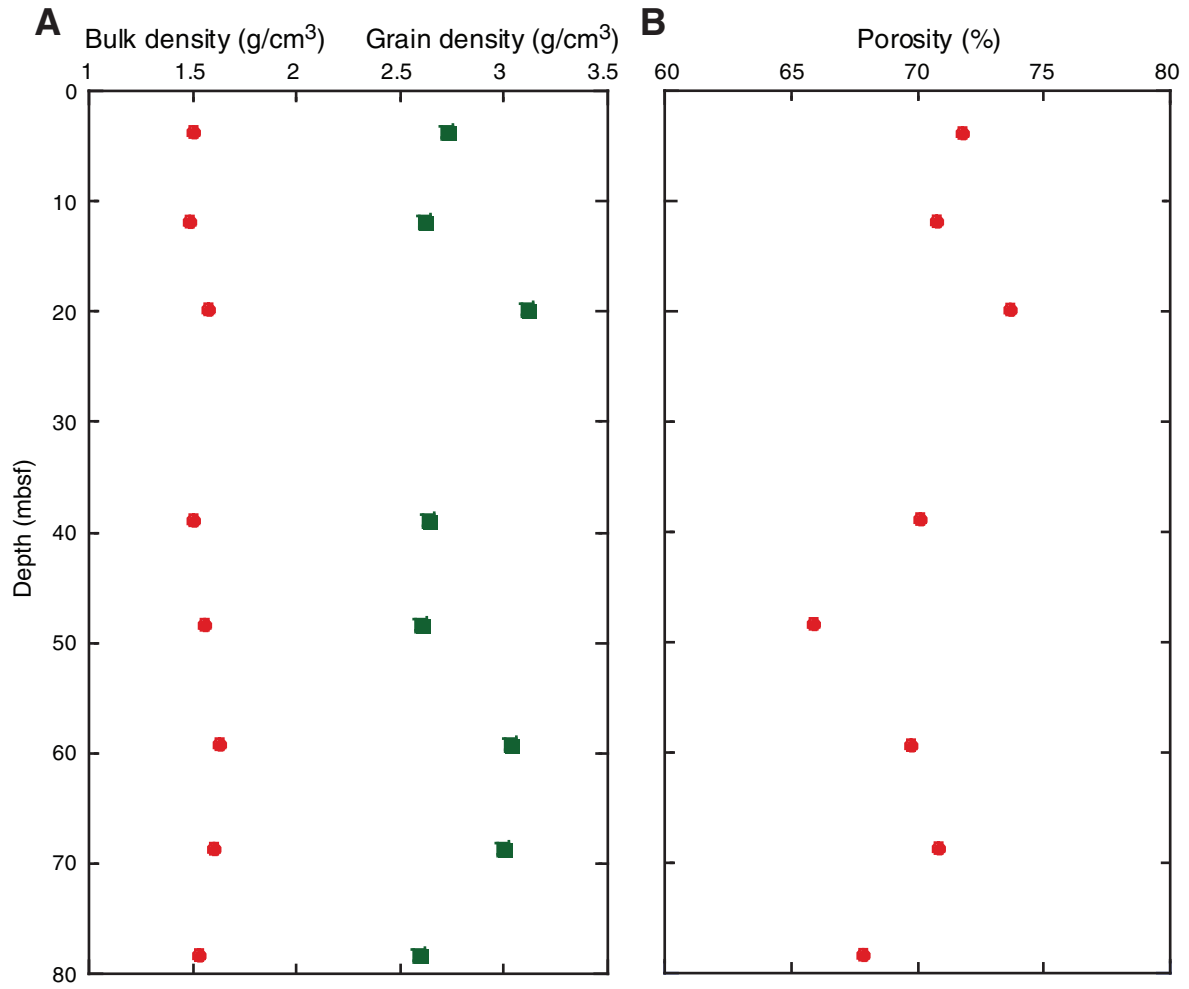


Figure F15. Natural gamma ray activity plot, Sections 320T-U1330B-1H through 3H.

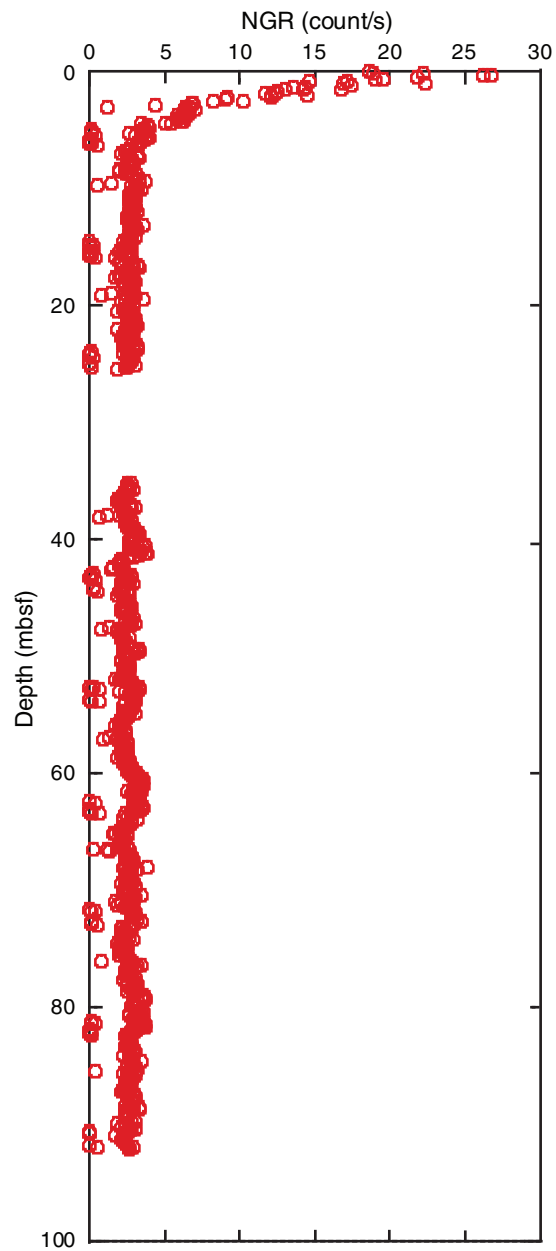


Figure F16. Temperature vs. time profiles for three deployments of the APCT-3: upper panel is from measurement at ~45 mbsf, middle panel from measurement at ~64 mbsf, and lower panel from measurement at ~83 mbsf.

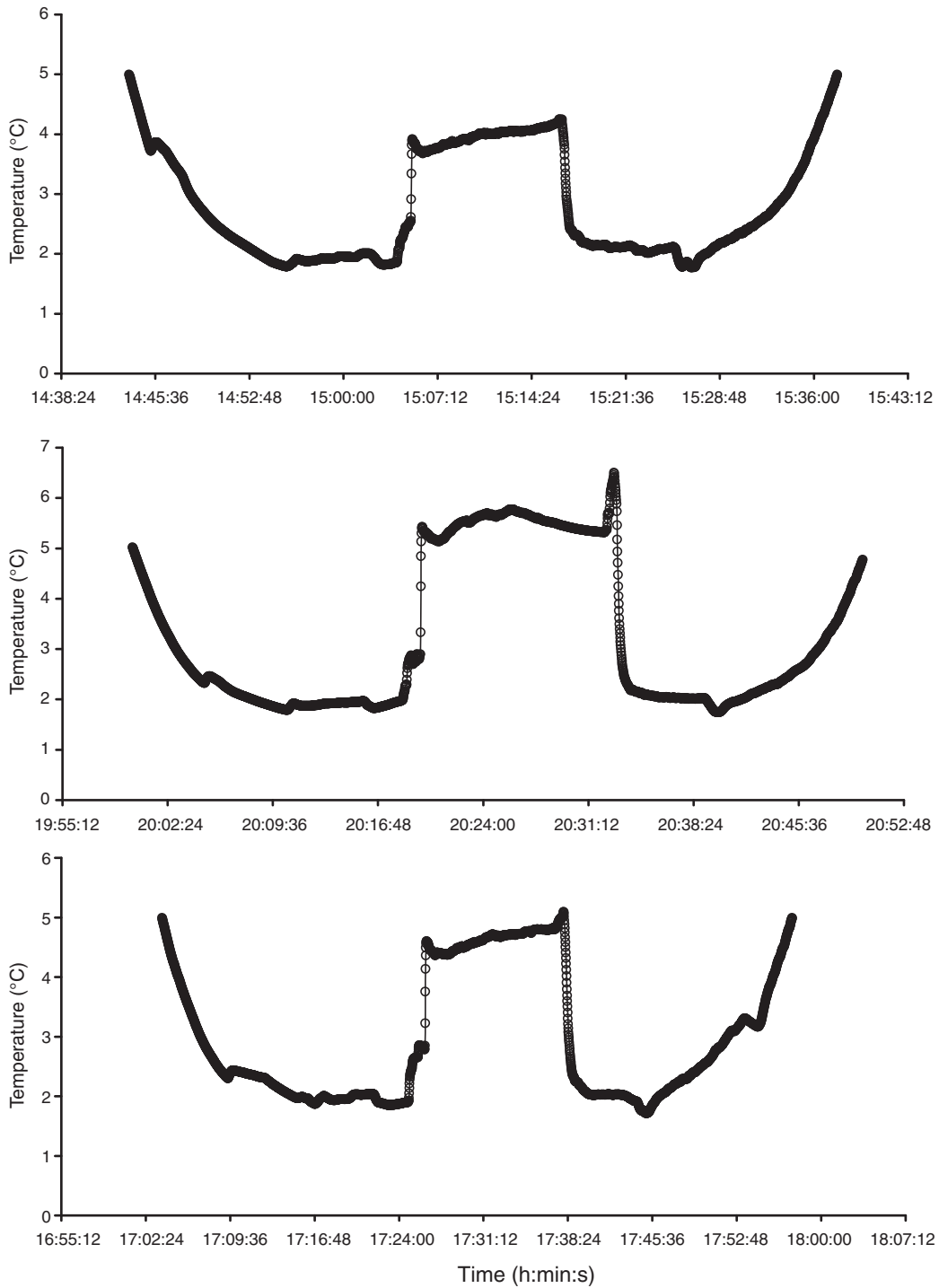


Figure F17. Plot of temperatures vs. depth, Hole U1330B.

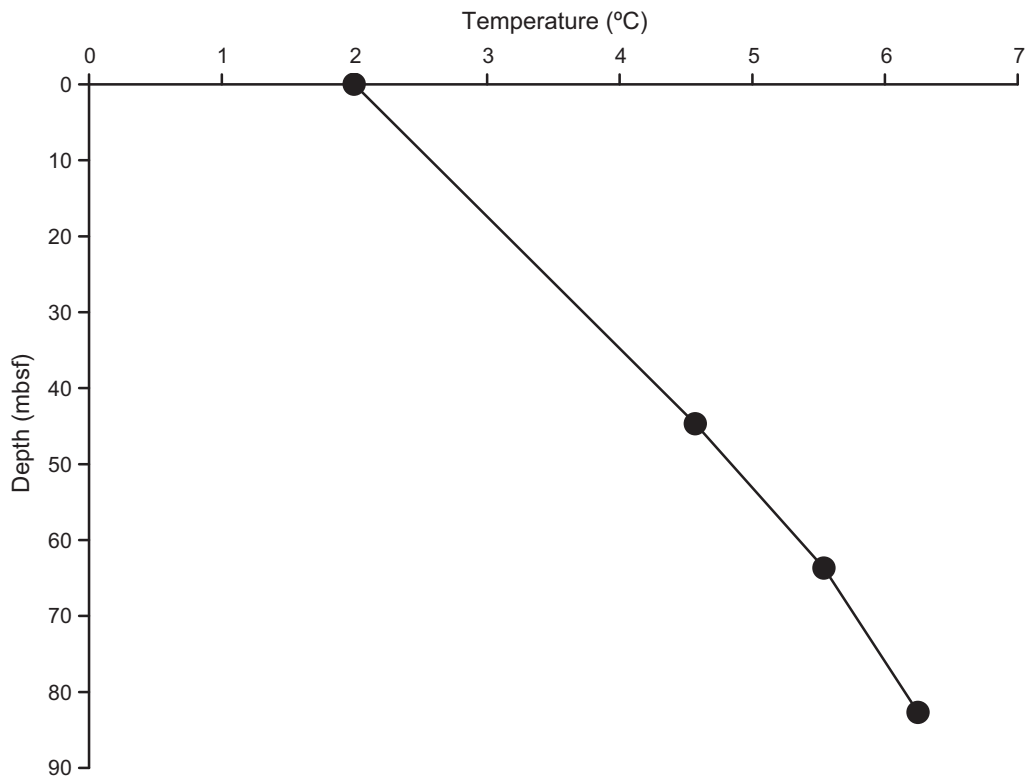


Figure F18. Comparison between main logs recorded in Hole U1330A (blue) and data recorded in Hole 807A (green). **A.** Hole diameter is measured by the arm of the density sonde. **B.** Gamma ray log is a measure of the natural radioactivity of the formation. **C.** Resistivity measured deep in the formation by the Dual Induction Tool. **D.** Logging units. WMSF = wireline log matched depth (below seafloor).

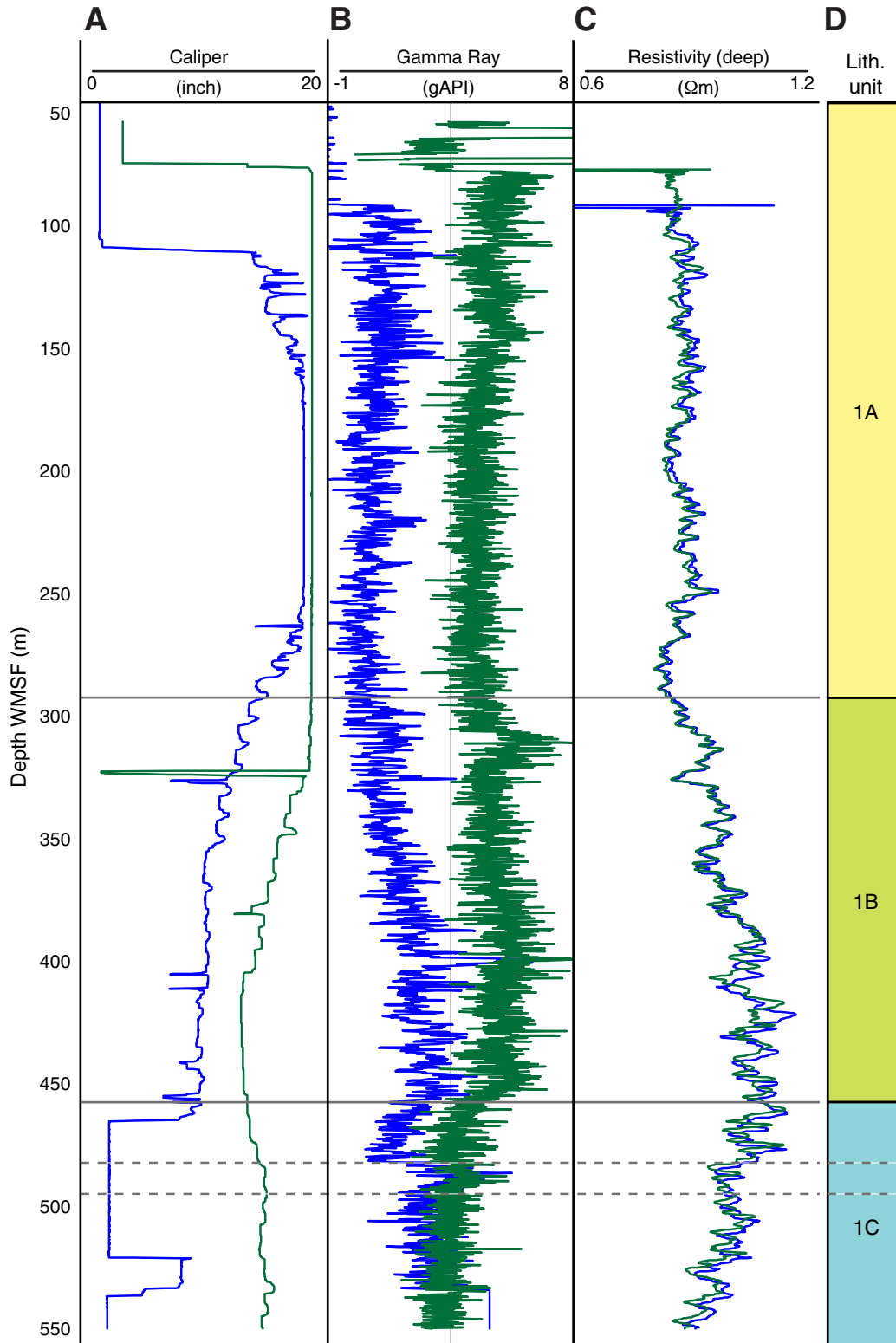


Figure F19. Logging data, Hole U1330. **A.** HLDS caliper measurement from first pass. **B.** Caliper data collected on Formation MicroScanner (FMS) tool string. Measurements taken simultaneously by the two sets of FMS arms in orthogonal directions. **C.** Gamma ray measured by FMS tool string. **D.** Orientation of Pad 1, which corresponds to Caliper 1 on the FMS tool string. All FMS data collected on second pass. WMSF = wireline log matched depth (below seafloor).

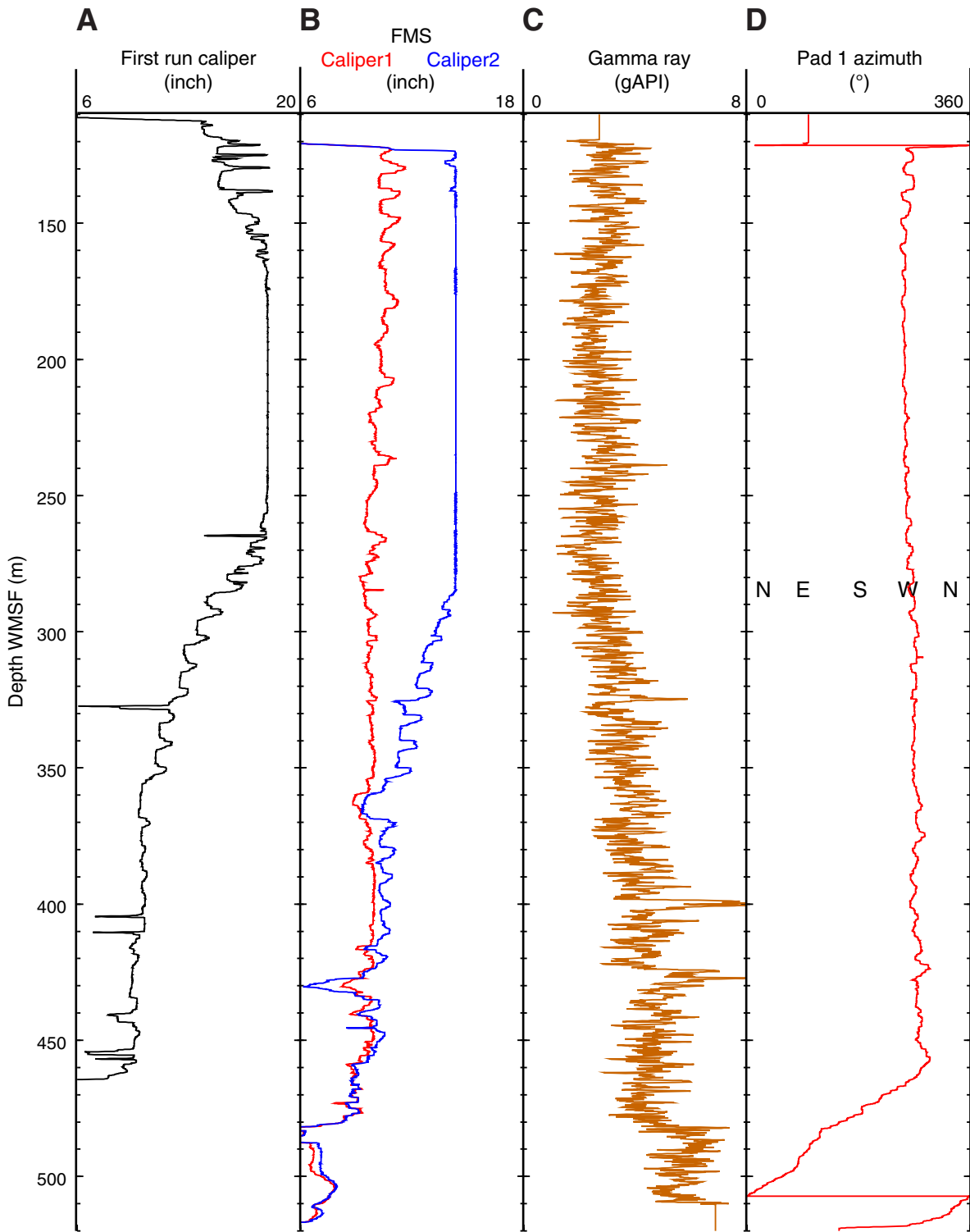


Figure F20. Formation MicroScanner (FMS) composite images. **A.** 2.5 m section of FMS showing examples of sinusoidal features (dashed lines) in the formation at ~425.75 and ~ 426.80 WSF. 1 = dipping north, 2 = dipping northeast. **B.** 2.5 m section of FMS highlighting the layered nature of the formation (bar summary to the right of image). Arrows = locations of very conductive small rounded and elongate structures that probably relate to bioturbation and associated iron mineralization (e.g., pyrite). **C.** 2.5 m section of FMS illustrating how braided “flaser” bands of more compressed material are represented by highly resistive bands in the image. Arrows = strongly resistive layers indicating the presence of “wispy” structures, as observed in Hole 807A core.

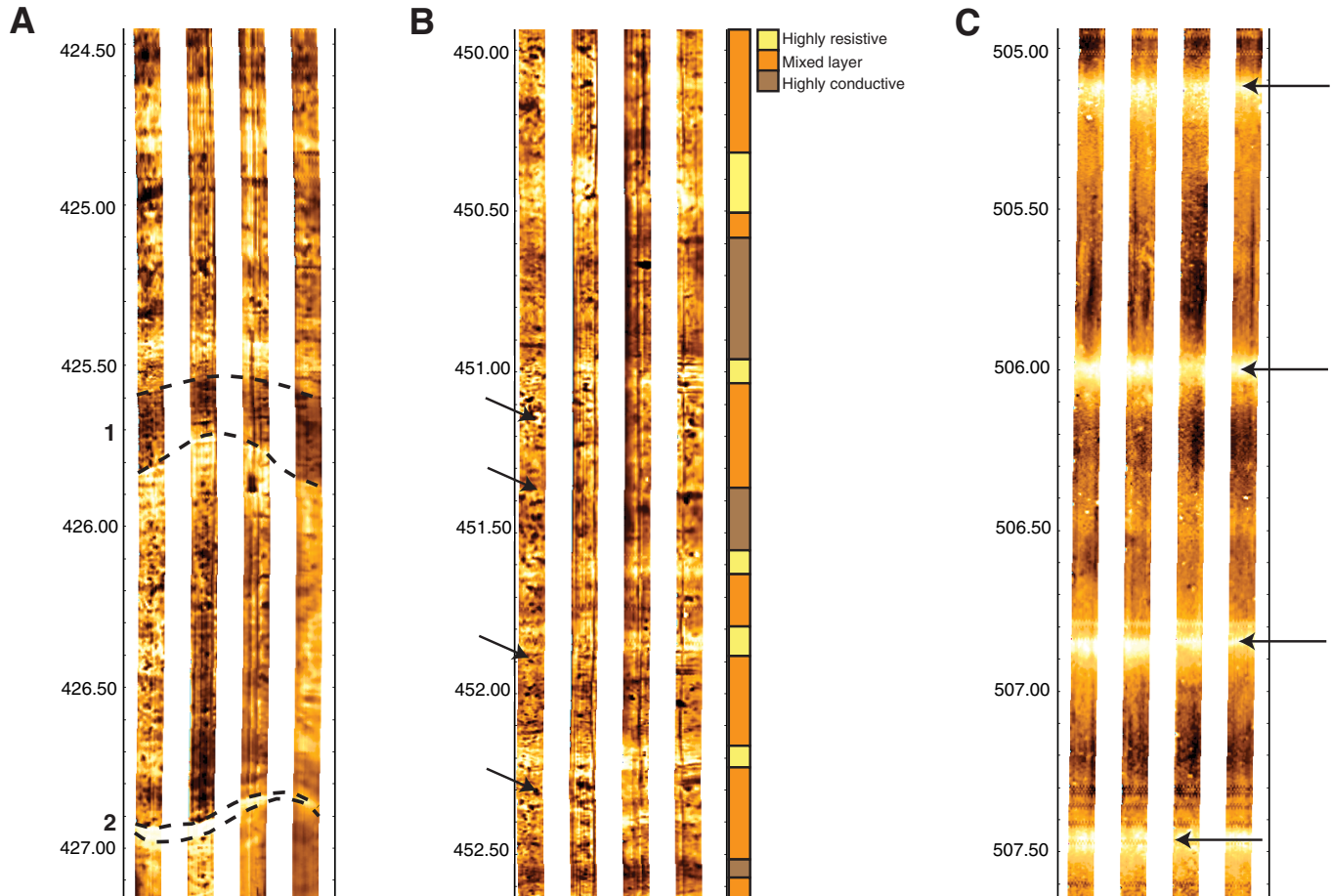


Figure F21. Plots of paleomagnetic results, Section 320T-U1330B-8H-7. A. Intensity of magnetization. B. Declination. C. Inclination.

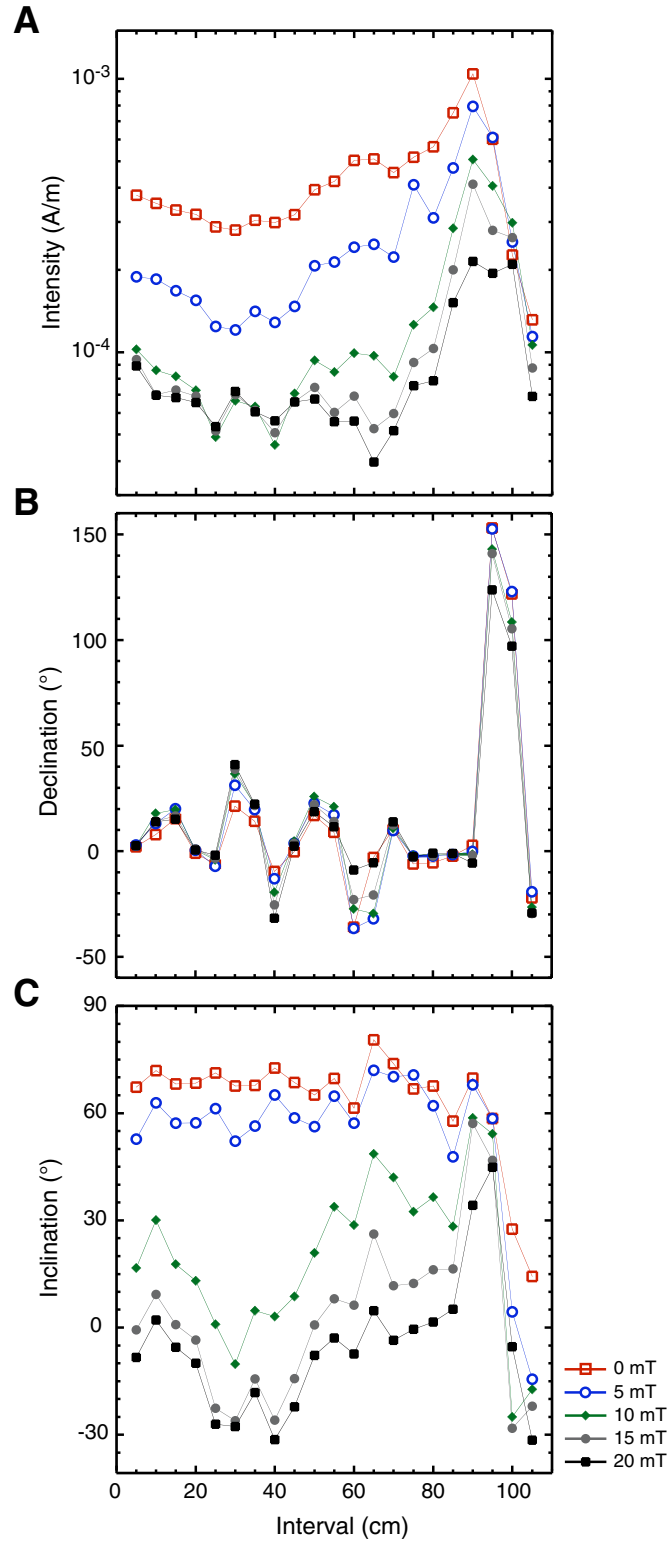


Figure F22. Split-core paleomagnetic data, Section 320T-U1330B-8H-7, 85 cm. **A.** Decrease in magnetization as sample is demagnetized. **B.** Orthogonal vector diagram of change in direction. **C.** Stereonet of change in direction.

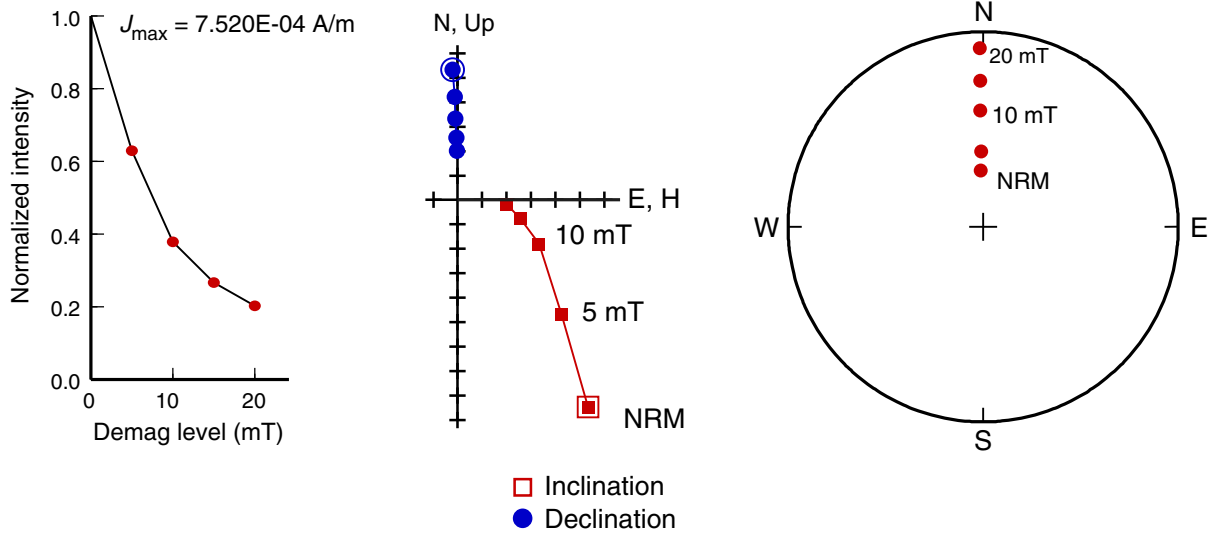


Figure F23. The Brunhes/Matuyama reversal recorded in split-core data, Section 320T-U1330B-2H-4, 80 cm (11.95 m depth).

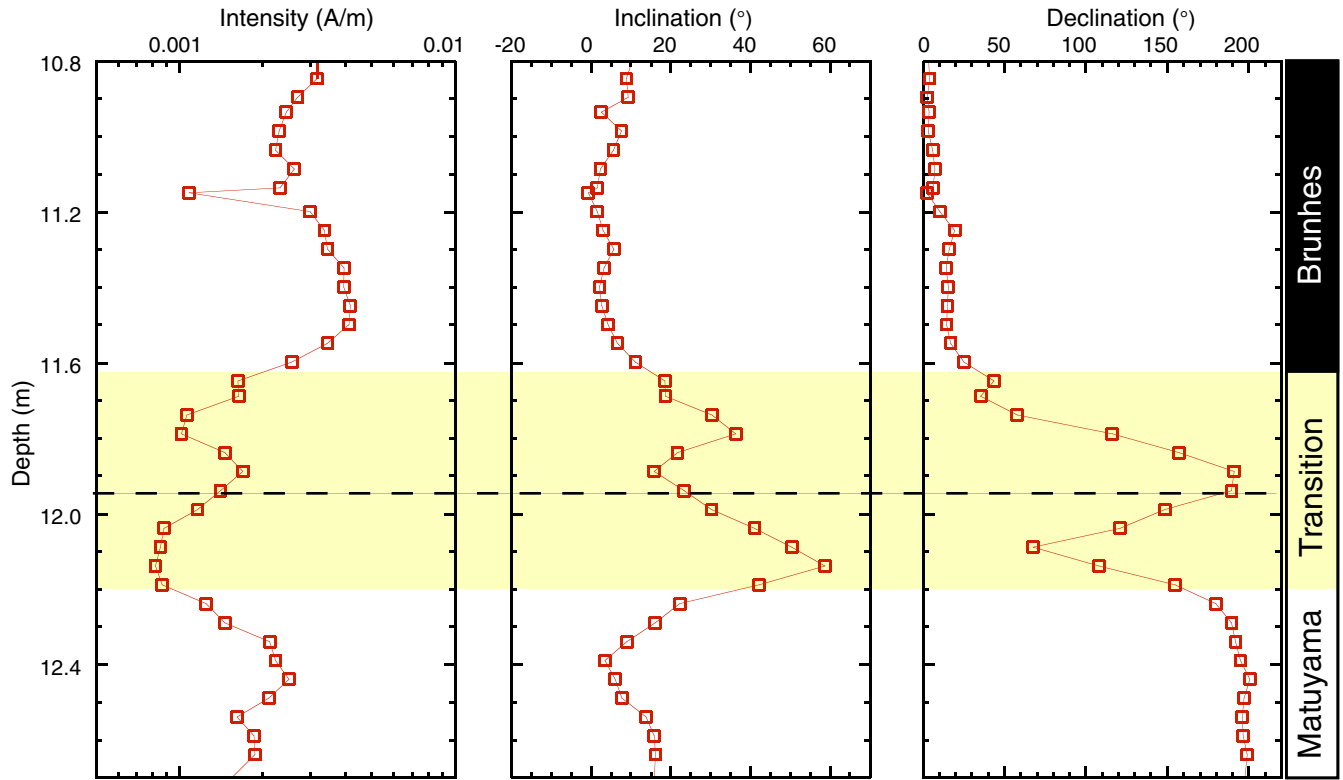


Figure F24. Susceptibility data from the three track systems, Site U1330. Disagreement between tracks and spikes in data are artifacts discussed in text.

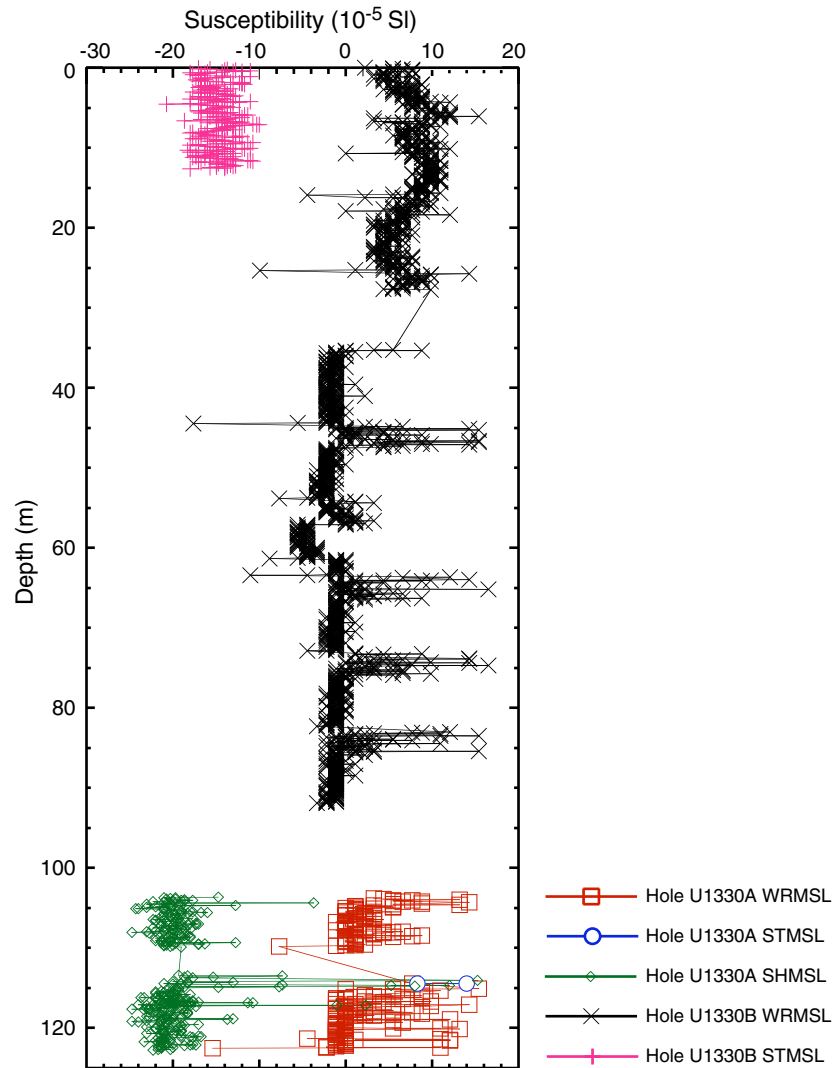


Figure F25. Comparison of the susceptibility data collected on the whole-round multisensor logger (WRMSL) and the section-half multisensor logger (SHMSL).

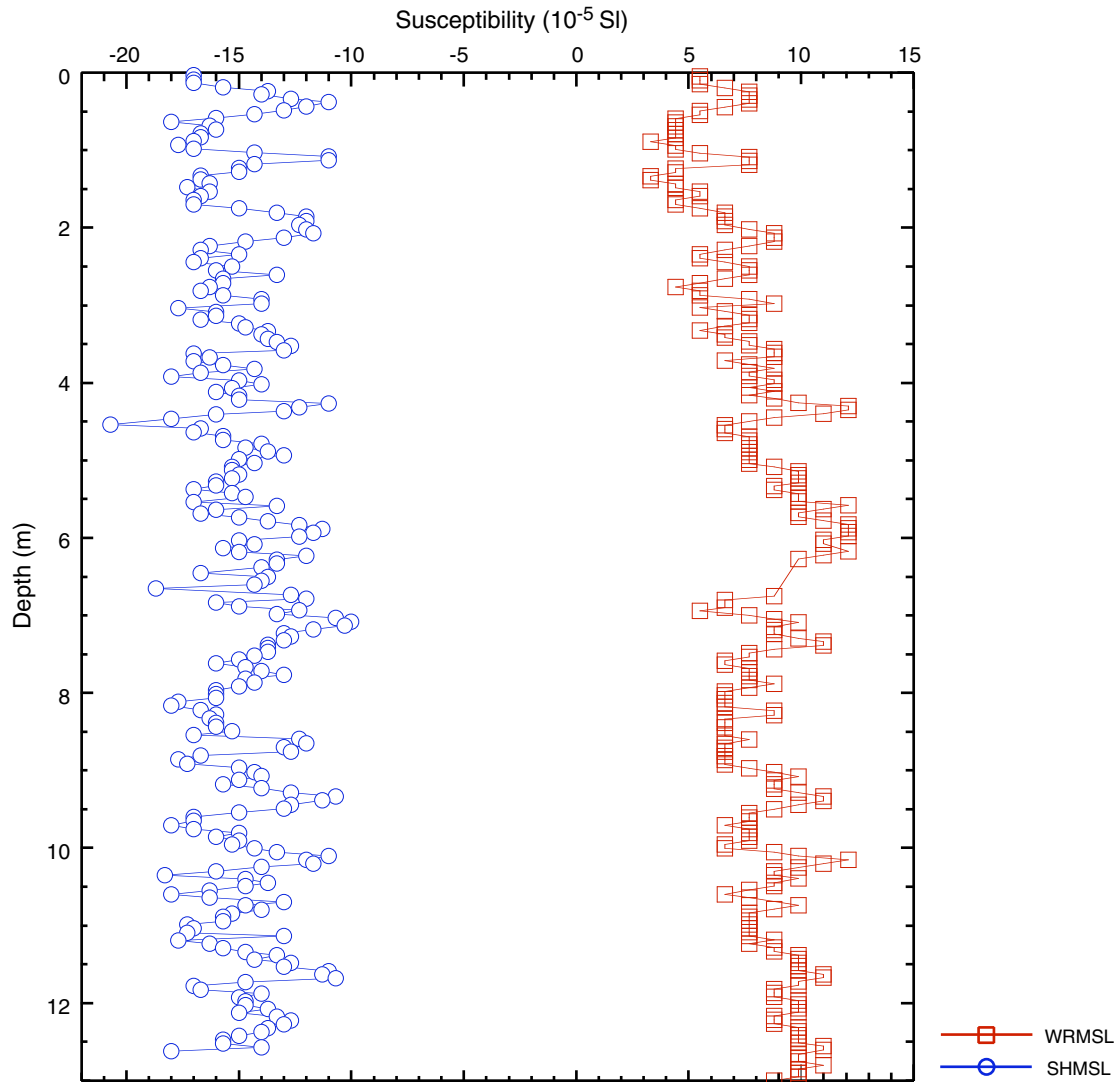


Figure F26. Site U1330 susceptibility data after filtering out artifacts and smoothing data with a 5 point box filter.

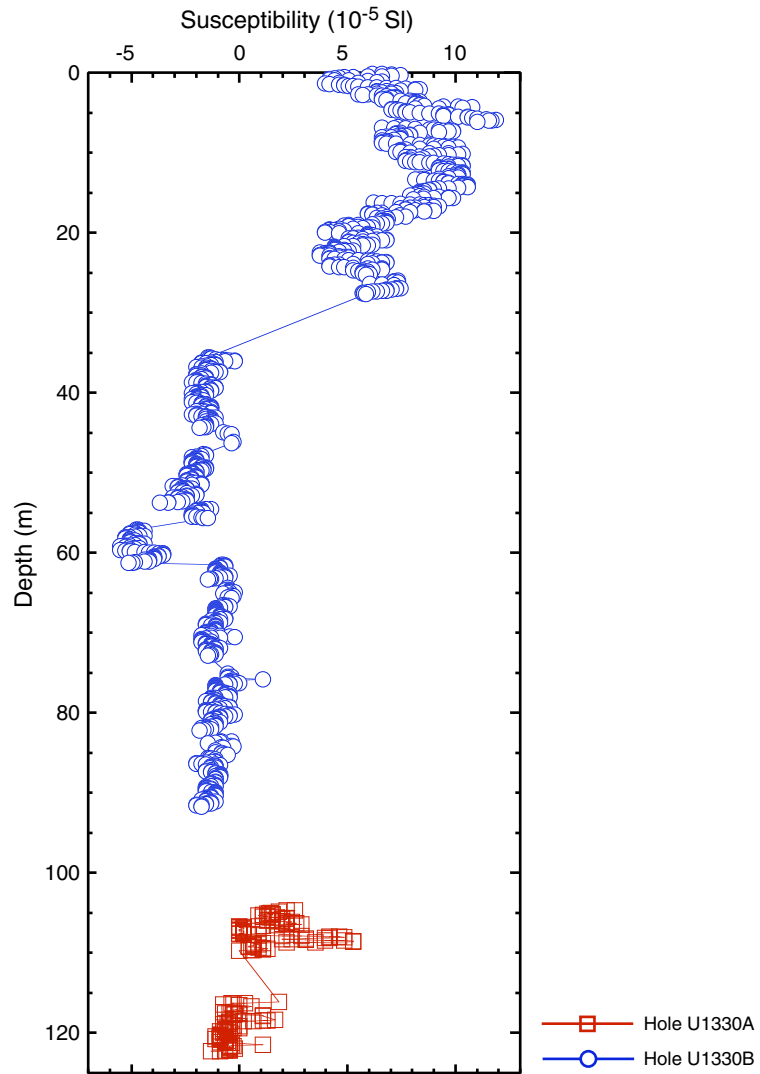


Figure F27. Magnetic survey of the shipboard Paleomagnetism Laboratory.

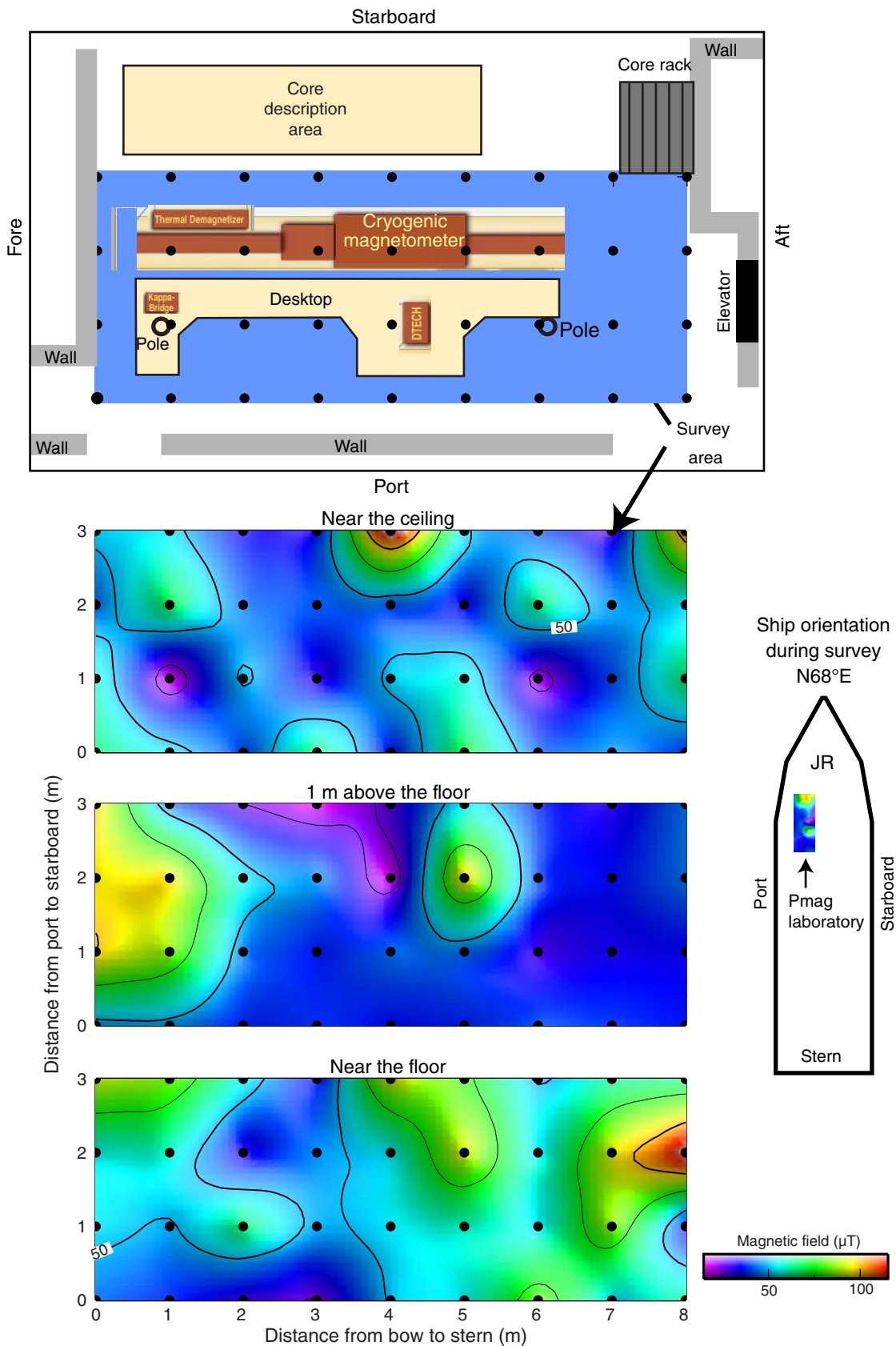


Figure F28. Magnetic survey along the track of the Super-Conducting Rock Magnetometer (SRM).

